AFRPL-TR-71-63

Prepared by
HERCULES INCORPORATED
ALLEGANY BALLISTICS LABORATORY
CUMBERLAND, MARYLAND

DEVELOPMENT OF A ROCKET MOTOR BURN RATE MEASUREMENT SYSTEM

W.C. Schuemann
L.S. Zajdel
J.H. Rice

October 1971

Prepared for
Rocket Propulsion Laboratory
Air Force Flight Test Center
Edwards Air Force Base
Edwards, California

SPECIAL NOTICES

U. S. Government agencies may obtain copies of this report from the Defense Documentation Center. Other qualified DDC users will request through the Air Force Rocket Propulsion Laboratory.

Foreign announcement and dissemination by the Defense Documentation Center is not authorized.

When U. S. Government drawings, specifications, or other data are used for any purpose other than a definitely related Government procurement operation, the Government thereby incurs no responsibility nor any obligation whatsoever and the fact that the Government may have formulated, furnished, or in any way supplied the said drawings, specifications, or other data, is not to be regarded by implication or otherwise, or in any manner licensing the holder or any other person or corporation or conveying any rights or permission to manufacture, use or sell any patented invention that may in any way be related thereto.

Do not return this copy. When not needed, destroy in accordance with pertinent security regulations.

Unclassified

Security Classification

DOCUMENT CONTROL DATA - R & D

(Security classification of title, body of abstract and indexing annotation must be entered when the overall report is classified)

1. ORIGINATING ACTIVITY *(Corporate author)*

Hercules Incorporated/Allegany Ballistics Laboratory

2a. REPORT SECURITY CLASSIFICATION

Unclassified

2b. GROUP

3. REPORT TITLE

Development of a Rocket Motor Burn Rate Measurement System

4. DESCRIPTIVE NOTES *(Type of report and inclusive dates)*

Final Report (Work Period July 15, 1970 through April 14, 1971)

5. AUTHOR(S) *(First name, middle initial, last name)*

W. C. Schuemann, L. S. Zajdel, J. H. Rice

6. REPORT DATE	7a. TOTAL NO. OF PAGES	7b. NO. OF REFS
April 1971	98	4

8a. CONTRACT OR GRANT NO.	9a. ORIGINATOR'S REPORT NUMBER(S)
F04611-70-C-0085	ABL-TR-71-8
b. PROJECT NO.	
c.	9b. OTHER REPORT NO(S) *(Any other numbers that may be assigned this report)*
d.	AFRPL-TR-71-63

10. DISTRIBUTION STATEMENT

In addition to security requirements which must be met, this document is subject to special export controls and each transmittal to foreign governments or foreign nationals may be made only with prior approval of AFRPL (RPPR/STINFO), Edwards, California 93523

11. SUPPLEMENTARY NOTES

12. SPONSORING MILITARY ACTIVITY

Rocket Propulsion Laboratory
Air Force Flight Test Center
Edwards Air Force Base, Edwards, Calif.

13. ABSTRACT

The technique chosen to develop into a microwave burn rate sensor was that of the microwave interferometer. Microwave energy is beamed through a "window" in the rocket motor case and into the propellant. At the burning propellant surface, this microwave energy is reflected and beamed back through the "window" to a detector system. At this detector system, the combination of transmitted and reflected energy produces a standing wave of energy which is monitored by the detectors. As the burning surface moves, the standing wave will also move a proportional amount. Thus, by monitoring the motion of the standing wave, the motion of the burning surface is obtained. Three microwave interferometers were proposed and "breadboarded." Extensive testing was done on these systems using a burning surface simulator to determine which system offered the best performance. This system was then developed into a rugged compact unit suitable for test firings. A high pressure microwave window was developed and fabricated providing an effective pressure seal between the rocket motor and microwave equipment while passing microwave energy without distortion. The factors which could affect the microwave burn rate sensor performance such as temperature, bulk modulus, and dark zone were investigated. A computer program was written to process the detector system outputs into burn rate and burn distance information. Twenty-two test firings were conducted yielding excellent burn distance information and fair burn rate information.

DD FORM 1 NOV 65 1473

Unclassified

Security Classification

14. KEY WORDS	LINK A		LINK B		LINK C	
	ROLE	WT	ROLE	WT	ROLE	WT
Sensor						
Burning Rate						
Microwave						
Solid Propellant						

HERCULES INCORPORATED
ALLEGANY BALLISTICS LABORATORY, P. O. BOX 210 • CUMBERLAND, MARYLAND 21502
TELEPHONE RIDGELEY, WEST VIRGINIA AREA CODE 304-726-4500

April 6, 1972

ERRATA SHEET

for

AFRPL-TR-71-63

DEVELOPMENT OF A ROCKET MOTOR BURN RATE MEASUREMENT SYSTEM

October 1971

1. The report number, AFRPL-TR-71-63, should appear on the left side of the front cover rather than on the right side.

2. The notice on the cover page should read:

Prepared for
Air Force Rocket Propulsion Laboratory
Edwards AFB, California

3. The following statement should appear on the front of the cover page, replace the last paragraph on the inside of the front cover, and replace the distribution statement used in paragraph 10 of Form DD-1473:

"Approved for public release; distribution unlimited."

4. Delete References 3 and 4 on page 94.

ABL-TR-71-8

AFRPL-TR-71-63

DEVELOPMENT OF A ROCKET MOTOR BURN RATE MEASUREMENT SYSTEM

Final Report

Work Period: July 15, 1970 - October 1, 1971

Contract F04611-70-C-0085

W. C. Schuemann
L. S. Zajdel
J. H. Rice

FOREWORD

This is the final report for Contract F04611-70-C-0085. The primary objective of this contract was to develop and deliver a system for the measurement of solid propellant burn rate and distance in medium size rocket motors. The purpose of this report is to trace the development and testing of the microwave burn rate sensor and to present all data necessary to successfully utilize the microwave burn rate sensor. This work was carried out by Hercules Incorporated, Allegany Ballistics Laboratory, Cumberland, Maryland.

Publication of this report does not constitute Air Force approval of the report's findings or conclusions. It is published only for the exchange and stimulation of ideas.

Mr. Charles Beckman, MKPA
AFRPL Project Engineer

ABSTRACT

The technique chosen to develop into a microwave burn rate sensor was that of the microwave interferometer. Microwave energy is beamed through a "window" in the rocket motor case and into the propellant. At the burning propellant surface, this microwave energy is reflected and beamed back through the "window" to a detector system. At this detector system, the combination of transmitted and reflected energy produces a standing wave of energy which is monitored by the detectors. As the burning surface moves, the standing wave will also move a proportional amount. Thus, by monitoring the motion of the standing wave, the motion of the burning surface is obtained. Three microwave interferometers were proposed and "breadboarded." Extensive testing was done on these systems using a burning surface simulator to determine which system offered the best performance. This system was then developed into a rugged compact unit suitable for test firings. A high pressure microwave window was developed and fabricated providing an effective pressure seal between the rocket motor and microwave equipment while passing microwave energy without distortion. The factors which could affect the microwave burn rate sensor performance such as temperature, bulk modulus, and dark zone were investigated. A computer program was written to process the detector system outputs into burn rate and burn distance information. Twenty-two test firings were conducted yielding excellent burn distance information and fair burn rate information. The vacuum tube type klystron microwave oscillator was then replaced with a solid state microwave oscillator. This resulted in a more compact and reliable system. Three test firings were accomplished utilizing the solid state oscillator yielding burn rate and burn distance data superior to that of the klystron oscillator.

TABLE OF CONTENTS

LIST OF ILLUSTRATIONS

List of Abbreviations and Symbols

α	propellant attenuation constant
β	propellant phase constant
$\frac{dx}{dt}$	burn rate
db	decibel
ϵ_r	propellant dielectric constant
E	electric field
F.M.	frequency modulation
H	magnetic field
VSWR or SWR	voltages standing wave ratio
X	burn distance
ϕ	phase angle between the reference and reflected signal
λ	microwave wavelength in waveguide
λ_P	microwave wavelength in sample

I

BACKGROUND

Allegany Ballistics Laboratory has been operated by Hercules since 1946. The primary mission of the laboratory has been to develop solid rocket motors and related technology. The formulation, testing and use of propellants with particular burning rates have always been a vital portion of this effort.

The importance of accurate burn rate data in the initial design and in the subsequent production of reliable rocket motors is well understood.

Hercules recognizes that burning rate is a dynamic phenomenon influenced by acceleration, bulk propellant temperature, acoustic resonance in the chamber cavity, erosive effects of high-velocity gases, abrupt and gradual changes in chamber pressure, radiant heat flux and anomalies in grain structure such as cracks, non-homogeneity, and insulator delaminations. One or more of the above influences may be present in a motor to an unknown extent and for an unknown duration requiring many tests to approximately determine and finally adjust the operation of the rocket.

The average burn rate determined by propellant thickness consumed from ignition through end of burning will not describe the instantaneous burning rate of a pulse solid motor which, in addition to wide and rapid pressure changes, may have several of the other rate influences of the preceding paragraph.

Cineradiography, microwave, ultrasonics and embedded linear resistors have been used to determine burn rate and/or propellant thickness at ABL.

Cineradiography requires an expensive facility for equipment and shielding, test operations are costly, and time resolutions are inadequate. Burning rate by cineradiograph was measured at ABL in 1963. The time resolution frame rate was 10 per second. Linear resolution was about 1/4 inch. Hercules' experience in the development of an ultrasonic NDT method for determining case bond integrity in A3 Polaris Second-Stage motors[1] did not encourage the use of 2.5 mc ultrasonics as a technique of in-depth examination of propellant as required in burning rate. Subsequent work with low-frequency ultrasonics (100 Kc) on Sprint NDT problems did not show appreciably better depth penetration. Embedded linear resistors are used

---

(1) R. O. Forthman, "Development of Ultrasonic NDT Method for Determining Case Bond Integrity in A3 Polaris Second-Stage Motors," 32nd Meeting Polaris/Minuteman/Pershing NDT Committee, United Technology Center, Sunnyvale, California, October 7-8, 1964.

at this facility to measure rates of 35,000 ft/sec.[2] Embedded resistors require modification of the rocket propellant configuration to be tested, a requirement that destroys their practical usefulness in most applications. Hercules, therefore, chose microwaves as the medium to measure burning rate.

Microwave flame front detector electronic packages which were designed and developed by Hercules have been successfully utilized on static firings of full-scale rocket motors for a period of five years. As a result of experience in the testing of solid propellant rocket motors, it was possible to design the detectors for ease of installation, setup and operation under actual test conditions which are basic requirements inherently present in all test operations. The units were designed to be completely self-contained and therefore could be utilized at any test facility with minimal effort. The microwave detectors have been successfully utilized on motors developing in excess of 30,000 lbs. thrust and with action times exceeding 40 seconds.

The microwave detectors were utilized on 15 full-scale static firings of Polaris second-stage motors conducted at the Naval Weapons Center, China Lake, California. The test motors contained case bond-to-propellant separations which could cause a malfunction due to increased burning surface generated when the normal burning front reached the separated areas. The detectors were positioned around the expected anomalies on the motors to provide data defining the position of the flame front. The microwave energy was transmitted through the fiberglass motor case to the burning surface. Data were subsequently used to study rocket failure modes. Similar work has been done recently in the Poseidon Program. The microwave system developed for this contract was a further development of this earlier work.

The principle employed for burn rate measurement was that of a microwave interferometer. Microwave energy is transmitted through a "window" in the rocket motor case and into the propellant. The microwave energy passes through the propellant and is reflected back to transmitter by the burning propellant surface. When the transmitted and reflected microwave energy meet, a standing wave of microwave energy is formed. As the flame front and thus reflected signal move, they cause the standing wave pattern to move a proportional amount. Hence by monitoring the movement of the standing wave pattern with microwave detectors, information about the burning surface movement is obtained. The microwave detector outputs were recorded on a digital recording system and processed by a simple digital computer program yielding printouts and plots of burn rate and burn distance versus time.

---

[2] Research Progress Report, Hercules Incorporated, Allegany Ballistics Laboratory, January 10, 1967.

II

FACTORS AFFECTING SYSTEM PERFORMANCE

The five principal propellant parameters which could affect the accuracy of the burn rate system are (1) microwave attenuation, (2) dielectric constant, (3) bulk modulus, (4) thermal expansion, and (5) propellant dark zone. The properties were investigated for three propellant types: FMA, a composite modified double base propellant; KAA-114, an ammonium-perchlorate-oxidized aluminum-fueled propellant; and a fluoro-carbon propellant.

1. Microwave Attenuation

As the microwave signal travels through the propellant, its strength diminishes due to the attenuation of the propellant. The signal reflected by the burning surface must travel back through the propellant to reach the detectors, thus the effective propellant path length for the reflected signal is twice the propellant length. Figure 1 shows a graph of microwave power received by the detectors as a function of propellant length and propellant attenuation. The graph thus sets the limit on propellant thickness as a function of attenuation. Best results are obtained when the received signal strength is greater than 1% of the transmitted. For the three propellants used in this investigation, attenuation ranged from 1-4 db/inch.

The technique used to determine propellant attenuation is known as the substitution method. This method consists of inserting the sample in the microwave line and then taking a power measurement. The sample is then removed and a precision variable attenuator is substituted for the sample. Attenuation is dialed in on the attenuator until the power level noted with the sample is reached. The attenuation level present on the variable attenuator is then the measurement of the sample. The accuracy of this system is dependent on the attenuator accuracy. Accuracy of the Hewlett-Packard model X382A attenuator used for this measurement is $\pm 2\%$ of the reading or .1 db, whichever is greater.

2. Dielectric Constant

Dielectric constant is defined as the ratio of the permittivity of a substance to the permittivity of a vacuum. The dielectric constant is the most important propellant parameter. The dielectric constant contains information relating to the wavelength of the microwave energy in the propellant. Accurate knowledge of this wavelength is necessary to calibrate the measurement system. The microwave wavelength in an air-filled waveguide and in a propellant sample are quite different. Figure 2 shows this phenomenon more clearly. The microwave energy is transmitted at a given frequency and wavelength through the waveguide to the propellant. As the energy enters the propellant, the wavelength shortens due to the density change. When the flame front moves one shortened wavelength, the detectors see one normal

wavelength movement. Thus, data gathered from the detectors must be normalized by the wavelength in the propellant to get true burn rate and distance information.

Extensive experimentation was done on determination of the dielectric constant and the effects of voltage standing wave ratio (VSWR) and microwave window presence on dielectric constant measurement. It was originally planned to perfect a dielectric constant measurement method using a well known sample and then apply the method to the propellant samples. The method used in determining the dielectric constant was the two point transcendental method outlined in Reference 1. Polyethylene was chosen as the experimental material because its dielectric constant is well known. The experimental setups used for dielectric constant determination and VSWR tuning are shown in Figure 3 and the experimental results in Figure 4.

The experimental technique in case 1 is to place the sample directly in the end of the slotted line and cover it with a short circuit (flat plate). Positions of the null on the standing wave in the slotted waveguide are measured with and without the sample present. The null shift, along with the wave length and the sample length, are then used to mathematically determine the dielectric constant. It was expected that case 1 would provide the most accurate measurement.

The technique used in case 2 was to place the sample in a short length of waveguide with the waveguide shorted as in case 1. The waveguide was then attached to the slotted line. Measurements were then made as in case 1. Case 2 was expected to add small reflections due to the joints and extra waveguide.

In case 3a, b, and c an E-H tuner was inserted in the system between the slotted line and the length of waveguide which was discussed in case 2. Before the actual dielectric constant measurements were made, the short was temporarily replaced with a termination. In case 3a the E-H tuner was adjusted to give a VSWR of 1.01. The termination was then removed, the sample inserted into the waveguide and the short replaced. Measurements were then made as in case 1. Cases 3a, b, and c differ only in that the E-H stub tuner has been adjusted for different VSWR levels. When comparing the results of the measurements in 3a, b, and c, the importance of being able to tune out reflections caused by mismatch in system components is seen.

In case 4 the microwave window adapter was inserted in the system between the E-H tuner and the length of waveguide into which thesample is to be installed. The short was replaced with a termination. The E-H tuner was adjusted until the VSWR was 1.01. Again the sample and short were installed and measurements taken as in case 1. The presentation of case 4 in Figure 4 illustrates the disturbance caused by the microwave window in the configuration of Figure 10 even though VSWR was at 1.01 before the sample was introduced. This meant redesigning the microwave window would be necessary. Case 3a yielded excellent results and was chosen for the propellant measurements. This method, however, did not work well with

propellant samples. The two point transcendental method is most accurate for low loss (low attenuation) samples. Polyethylene has a very small value of attenuation and thus worked well with this method. The propellant samples having attenuation greater than 1 db/inch however did not produce consistent results.

Another method was then found which was vastly superior to the two point method. This new method consists of placing the sample into the slotted line assembly and measuring the voltage standing wave pattern in the sample. This method is superior because it measures directly the desired quantity, wavelength in the sample. Calculation of the dielectric constant is actually unnecessary since sample wavelength is known, however dielectric constant was found for validation of the method. The microwave setup is shown in Figure 5. The depth of the probe is adjusted so that it just rides above the sample surface. Using this method we obtained values of dielectric constants of 3.65 for FMA and 5.42 for KAA-114. Measurements of polyethylene samples with this method yielded a value of dielectric constant of 2.21 which is within 1.3% of the value determined by the two point transcendental method.

3. Bulk Modulus

Bulk modulus is defined as a change in length of a substance with respect to pressure. Propellant thickness will be a function of chamber pressure. This will necessitate a data correction over the pressure range of 0-3000 psi. Figure 6 shows the effects of bulk modulus as a function of initial thickness and pressure. The accuracy of these figures are approximately $\pm$5%. These graphs show that the corrections required are small except for large pressure excursions. The data and equations used for the bulk modulus calculations are given in Table I and Table II, respectively.

4. Thermal Expansion

Thermal expansion relates the change in length of propellant as a function of temperature. Figure 7 graphs the change in propellant thickness as a function of temperature. The plots indicate that the correction required for thermal expansion will be quite small, in the order of 1%.

5. Dark Zone

The dark zone is a region which exists between the unburned propellant and the flame front. The dark zone is not present in all propellants. Propellants containing significant amounts of ammonium perchlorate oxidizer do not exhibit the dark zone phenomenon. It is expected that the microwave signal will pass through the dark zone and be reflected from the highly ionized luminous region. The thickness of the dark zone is dependent on the chamber pressure and could be a source of error in the determination of flame front position, especially at low pressures. Figure 8 shows a graph of dark zone thickness vs. pressure. This plot is for FMA, one of the propellants involved in this program. Figure 9 shows a graph of burn rate error which

could be caused by changes in the dark zone thickness. The data presented in Figure 9 were obtained from the data in Figure 8 which represent a series of static measurements. For rapid pressure transients or oscillatory burning, the relationship between pressure, pressure rate, and dark zone thickness is more complicated. In propellants with ammonium perchlorate oxidizers generally 30% or more AP will eliminate the dark zone. The effects of other oxidizers on dark zone is extremely complicated and depends on parameters like pressure and propellant formulation. In our test firings dark zone did not appear to cause any problems.

Another factor in the design of a microwave system is frequency. The frequency of the klystron system was approximately 9.64 G. Hz. The frequency of the solid state system is 10.525 G. Hz. Both of these frequencies are in the X-band range of 8.2 to 12.4 G. Hz. Realistically, there were only two possible choices of frequency bands for design of the burn rate sensor: X-band and K-band. K-band frequencies range in the area of 35 G. Hz. This would have the advantage of providing more standing waves per unit length of sample than X-band, and also would be about one half the size of an X-band system. These advantages however were overshadowed by the high cost of K-band components. An X-band system was thus chosen.

III

MICROWAVE WINDOW

One of the most critical factors affecting system performance is the microwave window. The function of the microwave window is to provide an effective pressure seal between the rocket motor and microwave equipment, but pass all microwave energy without affecting the measurement of the burning surface. A total of three microwave windows were built for this project.

The first window to be constructed was a dummy high-pressure window as shown in Figure 10. This window was used solely for investigation of the microwave characteristics encountered when transmitting through a window and not for any high-pressure work. All dielectric measurements were made through this window. As shown in Figure 4, case 4, even by tuning for a minimum VSWR, the effects of this window could not be completely eliminated.

A second window was then designed and fabricated and is shown in Figure 11. This window was designed to operate at high pressures on the T-burner firings. A pressure test of the window verified the pressure strength of the design. Analysis of the microwave characteristics of the window proved better than the first window, but not good enough to be used on the T-burner firings. The internal chamber of the window assembly which held the glass was determined as the critical factor. Depending on the size of this chamber, it can act as a resonant cavity causing a high VSWR and destroying the system accuracy.

A third and final microwave window was designed and fabricated which corrected the faults of the previous designs. This window is shown in Figure 12. The window chamber was reduced to approximately the same size as the internal dimensions of the waveguide. This eliminated the resonant cavity effect and greatly reduced the VSWR produced by the window. A linearity check using a simulated flame front produced excellent results.

The necessity of a good microwave window cannot be over-emphasized. Windows 1 and 2 caused microwave reflections which could periodically add to and subtract from the flame front reflections. Window 1 produced burn distance errors as high as 50%. Window 2 produced errors in the area of 25% in burn distance. Window 3, by reducing its inner cavity to waveguide dimensions, produced errors of only 2% or less.

IV

PROPOSED SYSTEMS

The burning rate measurement system is based on the principle of a microwave interferometer. Microwave energy is beamed into the motor through the propellant grain. The energy reflected from the burning surface is received by a detection system and the resulting signal suitably processed to provide burning rate and burning surface position data. The approaches to the design and fabrication of a microwave interferometer are numerous. Three different approaches were proposed, "breadboarded" and evaluated.

The first of these systems, called the Servo Driven Phase Shifter, is shown schematically in Figure 13. Microwave energy is generated by the klystron and transmitted through the ferrite isolator and level set attenuator to the first directional coupler where part of the microwave energy is coupled to one arm of the hybrid tee. This provides the reference signal for the detectors. The other part of the microwave energy is transmitted through the second directional coupler, the microwave window, and the attenuator and is reflected by the movable short. The reflected energy passes back through the attenuator and window and is passed through the servo-driven phase shifter and then the other arm of the hybrid tee. The detectors receive a signal which is a combination of both reference and reflected signals. At one detector the sum of the reference and reflected signal is received; at the other detector the difference between the signals is received. The detector outputs are fed to a servo amplifier which drives the phase shifting device. When the short circuit is moved, the phase of the reflected signal changes and this in turn changes the outputs of the detectors. This generates an error signal to the servo amplifier and it drives the phase shifter the same number of degrees the reflected signal moved through. Hence monitoring the phase shifter will yield burn rate information.

The second proposed system, designated the Twin Hybrid Tee System, is shown schematically in Figure 14. In this case the transmitted microwave energy is coupled to two hybrid tees providing the reference signal at each. The reflected microwave energy is also coupled to each of the hybrid tees but with one exception. At hybrid tee number two the reflected signal is first shifted 90 degrees in phase before it is fed to the hybrid tee. Thus the outputs of one hybrid tee are 90 degrees out of phase with respect to the outputs of the other hybrid tee. Since the output waveforms are sinusoidal in nature but differ in phase by 90 degrees, one can be called the sin (x) and the other the cos (x) where x is burn distance.

The third system, called the Twin Detector System, is shown in Figure 15. Its operating principle is identical to that of the Twin Hybrid Tee System except it eliminates two detectors and replaces the hybrid tees with less complicated E-Plane tees. Once again the phase shifter is used at a fixed 90 degree shift. The outputs are of the form A + sin (x) and A + cos (x) where A is some constant and x is burn distance.

The three proposed burn rate systems were "breadboarded" and evaluated. A sliding short and attenuator were used in each case to simulate the burning surface. Figures 16, 17, and 18 demonstrate graphically the results of these tests. Figure 16a, b, c, and d show the systems' performance with the microwave window present and Figures 17 and 18 show system performance without the window.

The Phase Shift System performance at 5 and 15 db levels is shown in Figures 16a and 16b. At the 5 db attenuation level, accuracy is about 2% of the reading, while at the 15 db level errors as large as 24% occur. This points out the disadvantage of the phase shift method, namely the inherent limited ability to handle low signal levels.

The accuracy of both the Hybrid Tee and Twin Detector Systems is within 2% at several signal levels and the performance was not seriously affected by the microwave window.

At this point the Hybrid Tee System appeared more desirable due to its theoretical ability to eliminate any D.C. offset of the output signals. It was felt if the hybrid tees were electrically symmetrical, two of the four detectors used in the Hybrid Tee System could serve to null or balance out the D.C. level on the other two detectors. Thus only changes in the signal levels would be recorded.

Investigation brought to light several problems concerning the hybrid tees. When considering the problems relative to use of the hybrid tee, it was apparent that a method would have to be developed to adjust the two microwave detectors on the hybrid tee for tracking with changing input signal level.

The first method tried and later rejected was to install a set of 1N23C detector diodes in a detector mount one at a time and to plot a voltage output curve for each one. Then the curves were compared. When two diodes were found to have the same output characteristic they were installed in a set of detector mounts and these were installed on the hybrid tee. Again the detector's output was plotted with a changing input signal to the hybrid tee. In every case the detector did not then track as their voltage output plots indicated they should. It was determined then that the hybrid tee was not balanced so that the input signal would be split equally.

Each diode output was then replotted with the diode installed in the detector mount on a hybrid tee, and were compared to find two diodes which had the same output characteristic when used in opposite ports on the hybrid tee. However when the two matching diodes were removed from their mounts and then reinstalled, the output at any given input level was found to have changed. It was apparent that the output characteristic of the diodes was greatly affected by the position of the diode in the mount and the amount of torque applied to the cap which holds the diode in place. The detector mounts were then modified so that the 1N23C diodes could be securely attached to the cap of the detector mount. The output of each

diode was monitored with a digital voltmeter as the diode and cap were screwed into the detector mount. The cap was turned in until the output from the detector was .700 volt with a standard level of input signal to the hybrid tee. Each diode was set up in exactly the same way before its output was plotted. When all the diodes had been checked in both detector mounts on a hybrid tee, diodes with matching characterisitcs were selected. In this way sets of diodes were found which had matching characteristics when mounted on the hybrid tee.

The above tests were conducted with an input into one port of the hybrid tee and the other input port terminated. When the two input ports were switched, the diodes became offset from each other because of the unbalance in the hybrid tee. The amount of unbalance was considerably larger than hoped for, though not much larger than the manufacturer's specifications.

Figure 19 is a graphic illustration of a typical test which was conducted on the hybrid tees. Note that with a standard signal to input port "B," the two detector outputs are for all practical purposes the same. However when the same signal was switched to port "A," the total signal level changed as well as the proportion of the total signal which each detector received.

Figures 20 and 21 illustrated a series of tests which were conducted on hybrid tees Numbers 1 and 2. Detectors Numbers 4 and 15 were installed on tee Number 1 and detectors Numbers 8 and 14 were installed on tee Number 2. Note the difference in tracking of the detectors on each tee when the signal input was changed from one input port to the other.

The inability to completely balance the hybrid tees removes the only advantage they have over simple detectors, namely the ability to operate around zero volts rather than at an offset voltage. The hybrid tees offer no accuracy advantage, are much more complex than ordinary detectors, and because of unbalance offer no data reduction advantage; therefore, they were not considered further in our development work. The Twin Detector System was then chosen to develop and fabricate.

V

DEVELOPMENT OF THE TWIN DETECTOR SYSTEM

The laboratory model of the Twin Detector System shown in Figure 15, while proving the concept, was too cumbersome to be used in actual test firings. Thus it was necessary to design a compact version of the Twin Detector System. Figure 22 shows a block diagram of a practical embodiment of the Twin Detector System. The two detectors, because of the 1/4 SWR wavelength separation, exhibit a 90 degree phase difference in their output signals. The detector outputs are of the form A + sin (x) and A + cos (x).

Figure 23a shows the first twin detector; built to demonstrate the feasibility of the system. It consists of two microwave detectors located 1/4 SWR wavelength apart located in a section of waveguide. The detector outputs are fed by BNC type connectors to the recording system.

Figure 23b shows the first in a series of improved two-diode detectors. This design used commercial diode mounts chosen because of their compactness and efficiency. Availability of these diode mounts proved poor, hence their use in a final system design was not feasible. Since the waveguide insertion depth of these diodes could be adjusted on this model, a method was devised for determining the optimum insertion of a probe into the waveguide. If the insertion depth is too large, reflections between the diodes cause a loss of measurement accuracy while too little insertion results in an unnecessary loss of signal. The system used for this adjustment is shown in Figure 24a. Both diode mounts were inserted to their maximum depth into the waveguide. The insertion distance was measured to make sure it was the same on each diode. The sliding short was then moved to cause a null at one detector and the position of the short was recorded. The short was then moved again to cause a null at the other detector and this position was recorded. The phase difference between the null positions was then calculated. As the probe depth of both detectors was changed incrementally, with the above procedure repeated for each increment, the phase difference between null positions changed until an insertion depth of 0.150 inch was reached. Further reductions in the insertion depth resulted in no further change in the phase shift between the detectors. A value of 0.100 inch was chosen as representing a suitable compromise between accuracy and signal level and was used in all subsequent detectors.

Figure 23c shows the third two-diode detector which was built and tested. This system used diode mounts fabricated at this facility and were designed to accept the common IN23C microwave diode. This model showed an improvement in signal level but because of a design deficiency in the diode mount, the output was found to be frequency sensitive and useful only for experimentation. However the design did allow us to devise a method for matching diodes. The system used is shown in Figure 24b. A variable attenuator was installed between the klystron and the detector. The other end of the detector was terminated. A diode was installed in both diode mounts.

VI

SOLID STATE MICROWAVE SOURCE

During the development of the burn rate sensor it became ovbious that the use of a solid state microwave source would greatly improve the total system.

The klystron is a tube type microwave source used throughout the development and most of the testing period. The disadvantages of the klystron are many. It is expensive, costing about $1000. A costly high voltage power supply is needed to operate it. The klystron must be tuned each time it is turned on after warmup. The klystron is rather fragile and produces enough heat to necessitate a cooling fan during operation. Its output was low and it was necessary to have amplifiers in the bay area to boost the detector output signal to a higher level. Also the power supply for the klystron was located in the bay.

The solid state microwave source has many advantages not possessed by the klystron. The solid state source is compact and rugged. Its power requirements are 12 vdc @ 300 ma. The solid state unit contains its own isolator of approximately 20 db. There is no oscillator tuning procedure necessary when using the solid state source and it produces very little heat. Replacement cost of the solid state unit is approximately one-fifth of that of the klystron. The output power of the solid state unit (50 mw) was great enough to eliminate signal amplifiers in the test bay area. In the Test Results section it is shown that the performance of the system is equal to or superior to the performance using the klystron.

VII

TEST FIRINGS

A total of twenty-five test firings were conducted using the microwave burn rate sensor. The small T-burner rocket motor system was utilized to fire the propellant. A sketch of the system is shown in Figure 26. The T-burner was pressurized to the desired firing pressure and the propellant sample was then ignited. Microwave energy, transmitted through the waveguide, window, and propellant was reflected by the burning surface. The reflected energy travels back through the propellant, window, and waveguide to be monitored by the detectors. The complete test plan is presented in this report iu Appendix A.

Two methods of data recording were used on the twenty-five test firings. The first eleven test firings were recorded on an F.M. tape recording system. The F.M. tape was then transcribed to a digital tape suitable for computer data analysis. This sequence of events proved to be a problem. Sixty hertz noise present on the original recording and noise introduced during transcription severely distorted burn rate data. The T-burner system was then moved to a location where direct digital recording of the detector outputs was accomplished. This move was not accomplished sooner because the transcription of F.M. tapes to digital was not started until several test firings were accomplished.

Test firings twelve through twenty-five were recorded directly in the digital format. This eliminated the transcription problems.

VIII

TEST RESULTS

Twenty-four of the twenty-five test firings were computer analyzed and reduced. Outputs of the computer reduction are burn distance and burn rate versus time. Due to computer program development only eleven test firing data reductions contain meaningful burn rate information, whereas all twenty-four computer printouts yielded burn distance data. Some of the test firing results are presented in this report in Figures 28 through 37. These figures demonstrate both the success and remaining problems of the system.

Noticeable on all burn distance plots is a sinusoidal distortion or gentle oscillation about the burn distance curve. This same distortion is shown greatly magnified in the burn rate curves. The burn rate being the first derivative of the burn distance is understandably more sensitive to fluctuations in the raw data. It was originally believed this was caused by a resonant phenomena between the flame front and microwave window. This is no longer a favorable argument. If a resonance existed between the propellant burning surface and window, its effect would grow larger as the firing progressed. This is due to the fact that as the propellant burned, less and less attenuation would separate the window and burning surface. This would cause the resonance to peak sharper and higher each time. This is not the case however. The data show the peaking to be approximately equal in magnitude and width. This demonstrates the peaking effect is not on the propellant side of the window but on the stub tuner-detector side. On this side all reflections are fixed and are not a function of propellant position. Since the peaking effect is not a function of burning position, it seems highly probable that it is due to a fixed reflection or a reflection from a stationary object. This fixed reflection then adds to and subtracts from the data reflection depending upon the phase relationship of each. At some points the data signal (signal reflected from the burning surface) will be in phase with the fixed reflection. At other times the data signal will be out of phase with the fixed reflection. The net effect of this is to cause the raw data to experience a zero offset. Unfortunately the zero offset is not a fixed level but is dependent on the phase of the fixed and flame reflected signals, and thus is constantly changing. If the zero offset were fixed, a new zero axis could be selected and the computer program could correct for it. However since the zero offset is sinusoidal in shape, no straight line can correct for it except at two points per cycle.

The reflections are believed due to either the tuners, detectors, microwave window, or some combination of these elements. The prime suspect is the detectors. The detector probe width and depth are of a magnitude which could easily be causing reflections. The use of very thin detector probes should help considerably. Figures 36 and 37 seem to show additional isolation is helpful in eliminating the peaking. All firings except that shown in Figures 36 and 37 used approximately 20 db of isolation between the microwave source and detector-tuner assembly. MBR-203 (Figures 36 and 37)

had about 40 db of isolation between the microwave generator and system. It is felt the peaking or zero shift can be effectively minimized by use of higher isolation and detector probes of small width and depth measurements.

Another problem which occurred on six occasions involved burning along the sides of the propellant samples. Since no inhibitor was used on the samples, this phenomena is easily understood. This often resulted in changes in the burn rate slope. This is shown in Figures 30 and 31. This is not to be confused with the indicated negative burn rate and distance shown in Figures 34-37. This resulted from simply interchanging channels A and B (diode A output, diode B output).

Figures 28-37 thus show some of the problems involved in the burn rate measurement and the successes also. Except for Figures 30 and 31 the burn distance curves are excellent. The effect of the fixed reflection is minor with respect to burn distance. The total burn distance is in excellent agreement with the measured lengths of the propellant samples. This is significant in that it verifies the propellant wavelength measurements and the system mathematics and computer program. It also demonstrates that the unwanted fixed reflection does not disturb the total burn distance measurement.

Figure 29 depicts a total burn distance of 1.03 inches compared to a sample length of 1.00 inches. Average burn rate, or slope of the burn distance curve is .293 inches/second compared to an expected rate of .290 inches/second. Although average burn rate is not a significant accomplishment in terms of program goals, it does demonstrate the validity of the system's measurement technique.

Figure 32 depicts a burn distance within 2% of the measured value. Average burn rate measured with the system is .30 inches/second compared to an expected value of .200 inches/second.

Figure 33 shows a burn distance curve within 1% of the expected value and an average burn rate within 2% of the predicted value.

Figures 35 and 37 compare favorably with results found with the klystron source. Accuracy of total burn distance is within 2% and average burn rate is .55 inches/second compared to an expected rate of .54 inches/second.

Figures 28, 28A, 34 and 36 represent burn rate data. Figures 28 and 28A are a test firing utilizing the klystron source and Figures 34 and 36 are test firings with the solid state source.

The effect of the fixed reflection is very pronounced in the burn rate plots. Figure 28 shows several peaks caused by this unwanted reflection. An expanded graph of Figure 28 between $t = .40$ and $t = .90$ second is shown in Figure 28A. This is between the peaks and shows the system capability with the unwanted reflection eliminated.

Figures 34 and 36 exhibit burn rate measurement made with the solid

state microwave source. In Figure 34, the peaking action is very regular in its period and magnitude. A line drawn equidistant between the high and low peaks would yield true burn rate data. This imaginary line would be at approximately .55-.60 inches/second. This compares favorably to the expected value of .54 inches/second. The larger spikes at the beginning and end of the data are caused by ignition and burnout respectively.

Figure 36 shows a much improved burn rate curve due to additional isolation provided between the solid state oscillator and the tuner-detector assembly. The solid state unit contains an internal isolator of approximately 20 db. This corresponds to the value used with the klystron during its use. An additional 20 db (total 40 db) was utilized during the test depicted in Figures 36 and 37. Notice in Figure 36 that a line drawn equidistant between the high and low peaks would be at approximately .55 inches/second. The largest peaks occur at ignition and burnout as expected. Figure 36 clearly demonstrates the capability for accurate burn rate measurement.

It is believed the additional isolation tends to aid the system accuracy by reducing the magnitude of the unwanted reflection. Any reflected energy entering the isolator is absorbed. It was well known at the outset of this program that isolation between the microwave source and the detector-tuner assembly would be necessary, however it was assumed 20-30 db would be adequate. It now appears isolation in excess of 30 db is further beneficial.

The basic design and accuracy of the system have been well demonstrated. The remaining problem of unwanted reflection seems solvable by further isolation and minimization of detector probe dimensions.

The addition of the solid state source has proved a successful venture. The system is more reliable, more rugged, less expensive, easier to set up, and produces results equal or better than that of the klystron.

IX

DATA REDUCTION COMPUTER PROGRAM

Introduction

The two detectors in the microwave burn rate sensor are located 1/4 wavelength apart. This causes one detector output to lead the other by 90 degrees and the detector outputs can be thought of as a sine and cosine function since the sin $(x + 90^{o}) = \cos x$. The outputs are much more complex than just sine x and cos x, but if the sine function output is divided by the cosine function output, all the terms cancel leaving tan ϕ where ϕ is the phase angle between the reference and reflected signal. The tan ϕ is then converted to ϕ by an arctan routine and ϕ is converted to burn distance by λp, the wavelength in the sample.

Detailed Description

The signals produced by the two-detector microwave burning rate system are of the form

$$A = f(x)\, e^{2\alpha x} \cos 2\beta x$$

$$B = f(x)\, e^{2\alpha x} \sin 2\beta x$$

Where: A and B are the in-phase and quadrature components of the signal reflected from the burning surface

- x is the distance to the burning surface
- α is the propellant attenuation constant
- β is the propellant phase constant
- $f(x)$ is a function of the microwave launching device considered as an antenna and includes the inverse square loss of signal due to the distance from the antenna to the burning surface
- $e^{2\alpha x}$ is the signal loss due to absorption of microwave energy in the propellant
- $2\beta x$ is the phase angle of the returned signals with respect to the reference signal.

The phase constant β of the microwave signal in the propellant in a rocket motor is related to the propellant dielectric constant by;

$$\beta = \frac{1}{\sqrt{\epsilon_r}} \frac{2\pi}{\lambda}$$

where λ is the free space wavelength. The dielectric constant and free space wavelength are available from laboratory measurements.

The approach to the data reduction is to eliminate the effects of the antenna pattern, inverse square loss, and the signal attenuation by absorption, and to use the phase of the return signal with respect to the reference signal to determine the flame front position. The flame front position is related to the return signal phase by;

$$x = \frac{1}{2\beta}\phi$$

where ϕ is the phase angle between the return signal and the reference signal.

Dividing signal B by signal A;

$$\frac{B}{A} = \frac{f(x)e^{\alpha x}\sin \beta x}{f(x)e^{\alpha x}\cos \beta x} - \tan \phi$$

$$\phi = \text{Arc tan } \frac{B}{A}$$

This phase angle is immediately recovered. However, the arc tan function is periodic and direct calculation as indicated above would cause the signal to be discontinuous every $\beta x = \pi$, resulting in ambiguous position data. To resolve these ambiguities a slightly more sophisticated approach is required.

By choosing the digital sampling rate sufficiently high so that the burning surface advances only a small fraction of a wavelength between samples, the computer program is made to track the burning surface position with no ambiguity. To accomplish this the phase angle at each sample time is calculated, not with respect to a fixed phase reference, but to the phase at the time of the previous digital sample. The calculated incremental angles are always small, being much less than 180°, and discontinuities are thereby eliminated. The total phase change and hence the burning front position is found by adding up the incremental changes throughout the firing.

Sampling Rate

Various sampling rates have been investigated for recording microwave burn rate sensor outputs. The optimum sampling rate depends on several factors. An example will point up this problem. Assume it is desired to record at 3000 samples/second a KAA-114 test firing on digital equipment with a 2000 count span. At a pressure of approximately 750 psi, about 4 cycles of data (detector output) can be expected. This will happen in about 2 seconds. Thus we have 2 cycles/second or a rise from a low peak to high peak in 1/4 second. About $\frac{3000}{4}$ or 750 samples will be taken during 1/4 second. The total span of 2000 counts will actually be reduced to about 1800 to prevent saturation. Also during the early part of the firing the propellant attenuation will reduce the detector output span to about 500 counts. It is thus conceivable that during a time interval where it is desired to

record 750 samples, only 500 counts are available. Clearly some successive samples will record the same count. At this same time when detector A is going from a low to high peak, detector B is on a part of its curve which changes less than the part detector A is on. Thus it is certain that several occasions will occur when channel A and B will register no digital count change for the same sample. This will correspond to no burn rate for that sample point. Also consider that the digital system may contain 1-2 counts of random noise. At a sampling rate of 3000 samples per second this would render any burn rate measurement useless. Thus a moderate sample rate will often yield far better results in burn rate measurement.

Sampling rate also affects resolution. In the above example with a sampling rate of only 300 samples per second we record 600 data points in the 2 second test. Since 1 inch of propellant burned we are asking for a resolution of $\frac{1}{600}$ or .00166 inches. It is likely that the burning surface of propellant which appears smooth on a 1 inch or even .1 inch scale would be very rough burning when viewed on a .001 inch scale.

Thus sampling rate and resolution can be monumental factors when considering burn rate since it is calculated and plotted for each point. Burn distance which is also calculated and plotted for each point, is not normalized to inch/second like burn rate. For instance, if between sample 3001 and 3002 an increase in burn distance is found to be .0010 inch when it should have been .0009 inch, the net effect on the burn distance curve will be only .0001. The effect on burn rate however will be .3 inch/second error for that point. The effects of sampling rate on burn rate is thus obvious. A sampling rate of 300 samples per second was used on all firings, however the program has the capability to reduce this at 100, 30, and 10 samples/second rates.

X

SUMMARY

The goal of this contract was to develop a solid propellant burn rate measurement system to be used with small rocket motors. This system was to measure propellant burn rate and supply reduced data routinely in the same manner as pressure and thrust measurements are handled. The system therefore, had to be small and rugged, inexpensive, accurate, use practical data reduction procedures, and able to be set up and adjusted by firing range personnel.

Many techniques have been employed to measure propellant burn rate. Of these techniques, the various microwave based approaches are the most suitable for this application. They range in complexity from simple interferometers to pulsed radars. The first step in this contract was to define the simplest types of microwave apparatus which would satisfy the above requirements. These various possible approaches were then breadboarded and tested. The most successful approach was developed into a practical measuring device and used to determine the burning rate of several types of propellant. The developed device is somewhat more complicated than the simplest possible microwave interferometer in that two detectors are employed instead of one. This change allows the use of a simple digital data reduction technique and provides continuous burn rate data. Fifteen successful firings were conducted using the device and associated data reduction techniques. Average burn rate and burn distance obtained from the microwave burn rate detector usually agreed with the expected values within a few percent. However, instantaneous burn rate information often differed substantially from the average rate. This was caused by unwanted reflections from internal waveguide parts (detector probes, tuner stubs, flange misalignment) combining with the reflection from the flame front. This would cause an oscillating zero shift in the data which affects burn rate more serious than burn distance.

The unwanted reflections however can be minimized. Reduction of the probe depth and width should aid in minimization of the unwanted reflections. Possibly the use of an E-H plane tuner instead of a double stub tuner would be helpful. Clearly the use of additional isolation is beneficial.

The addition of a solid state microwave source was implemented. Its fixed frequency, low voltage power supply and high output greatly simplify the test setup. The system operates without any amplification in the bay area and thus operates as a standard transducer with power in and signal out in a standard gage line.

The principle accomplishment of this contract was to develop a small, rugged, inexpensive device which demonstrated excellent burn distance data and the capability of producing excellent burn rate data.

Table I

Propellant Properties

	FMA	KAA-114	Fluorocarbon*
Thermal Expansion (in/in/^{o}F)	0.731×10^{-4} [3]	0.525×10^{-4} [3]	0.65×10^{-4} [3]
Bulk Modulus (psi	1×10^{6} [2]	1×10^{6} [2]	1×10^{6} [Est]
Dielectric Constant(1)	3.65	5.42	4.92
Attenuation (db/in)	4.3	3.9	1.0

* A fluorocarbon propellant similar to TP-F1004

(1) Frequency = 9.6 G Hz

At 10.52 G Hz Dielectric Constant Values would be slightly larger.

Table II

Phenolic thickness @ static	=	T_{ph}	(in.)
Phenolic bulk modulus	=	M_{ph}	(psi)
Phenolic thermal expansion coefficient	=	E_{ph}	(in/in/^{o}F)
Propellant thickness @ static	=	T_{pr}	(in.)
Propellant bulk modulus			
Propellant thermal expansion coefficient	=	E_{pr}	(in/in/^{o}F)
Propellant expended thickness	=	T_{xpr}	(in.)
Temperature static	=	T_s	(^{o}F)
Temperature test	=	T_t	(^{o}F)
Pressure static	=	P_s	(psi)
Pressure test	=	P_t	(psi)
Dark zone thickness	=	T_{DZ}	
Distance from case to burning surface	=	D_s	

$$D_s = T_{ph} - \left[\frac{(P_t-P_s)\cdot T_{ph}}{M_{ph}}\right] + \left[T_{ph}\cdot E_{ph}\,(T_t-T_s)\right] +$$

$$T_{pr} - T_{xpr} - \left[\frac{(P_t-P_s)(T_{pr}-T_{xpr})}{Mpr}\right] + \left[(T_{pr}-T_{xpr})\cdot E_{pr}(T_t-T_s) + T_{DZ}\right.$$

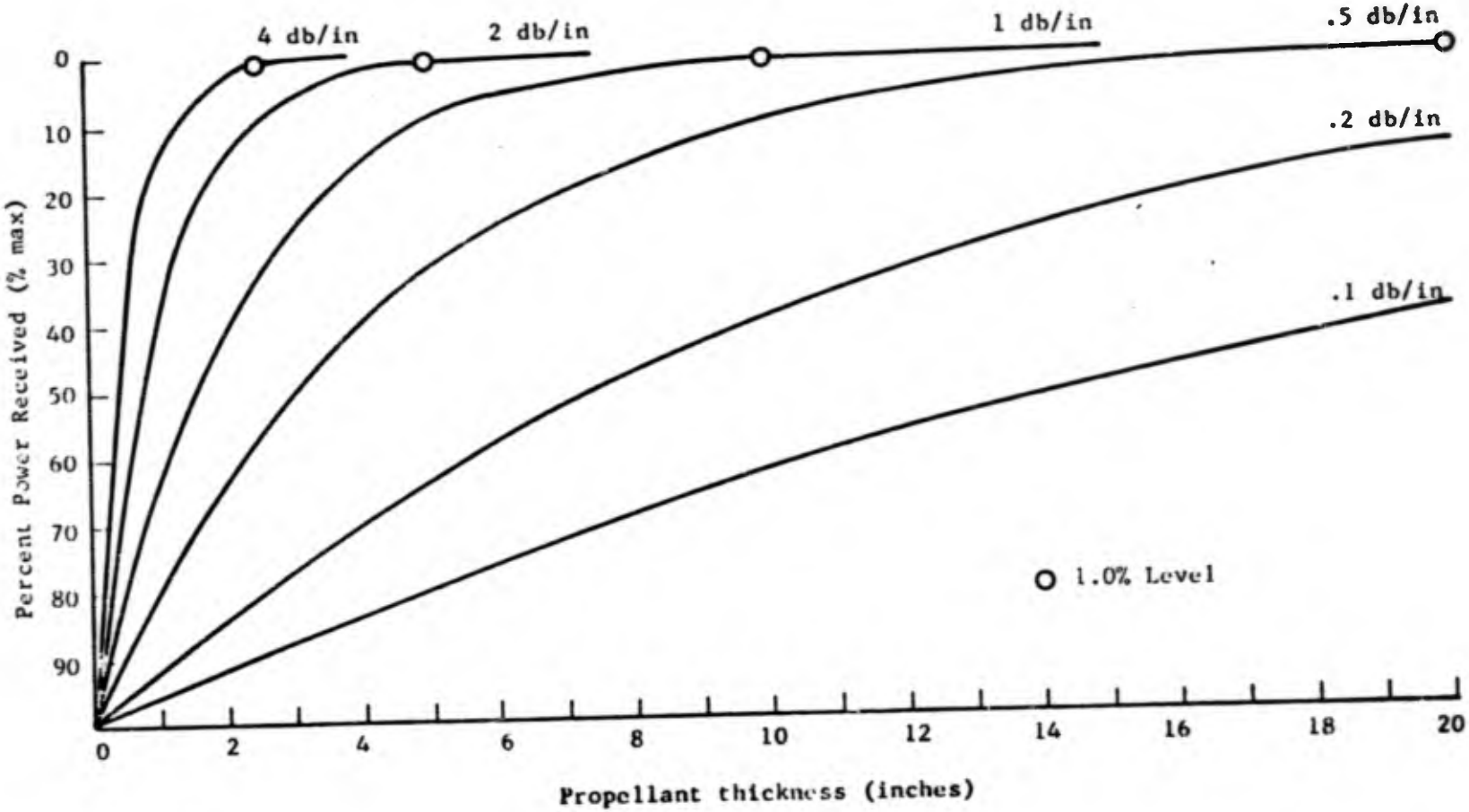

Figure 1. Microwave Attenuation Curves

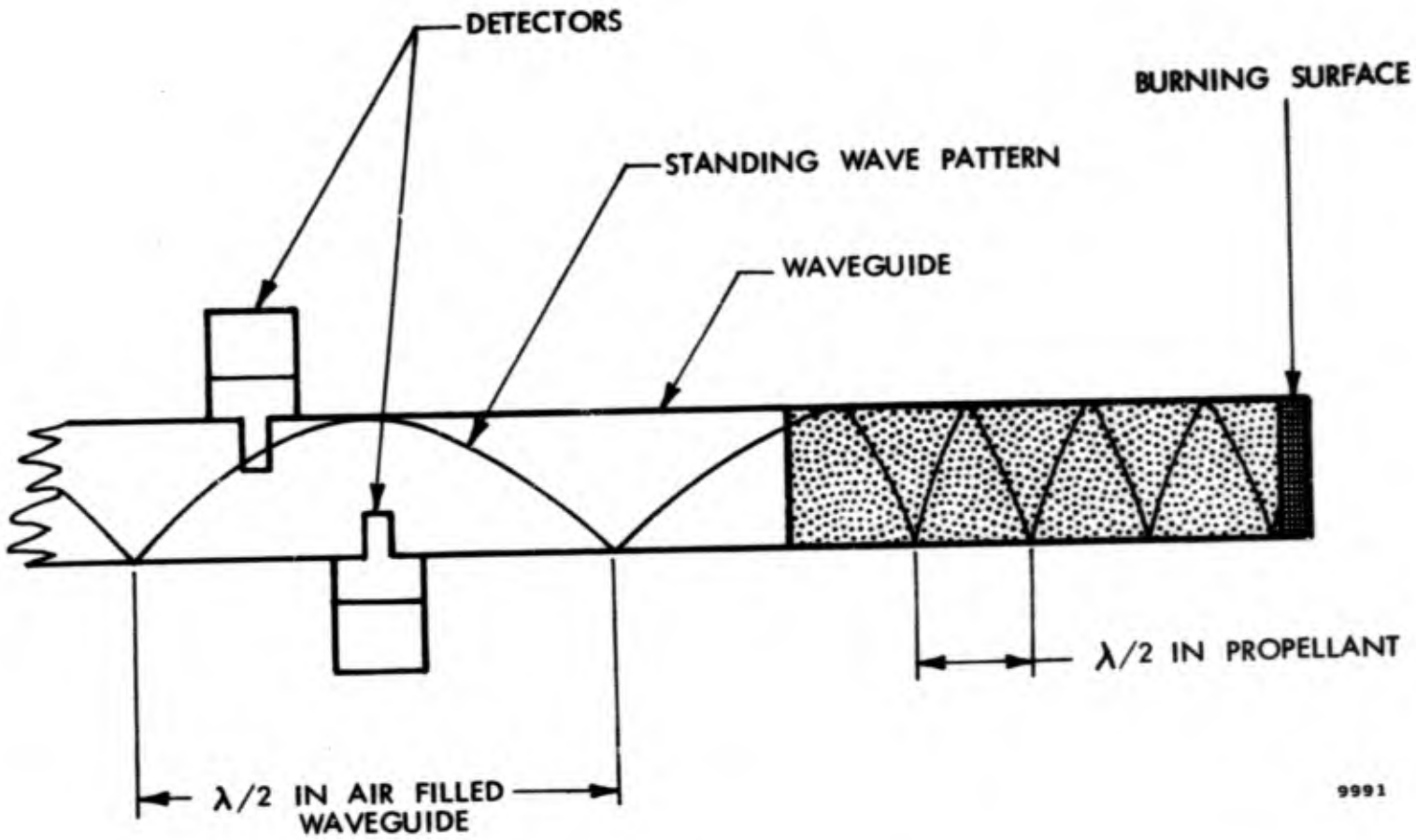

FIGURE 2
SWR Pattern in Waveguide and Propellant

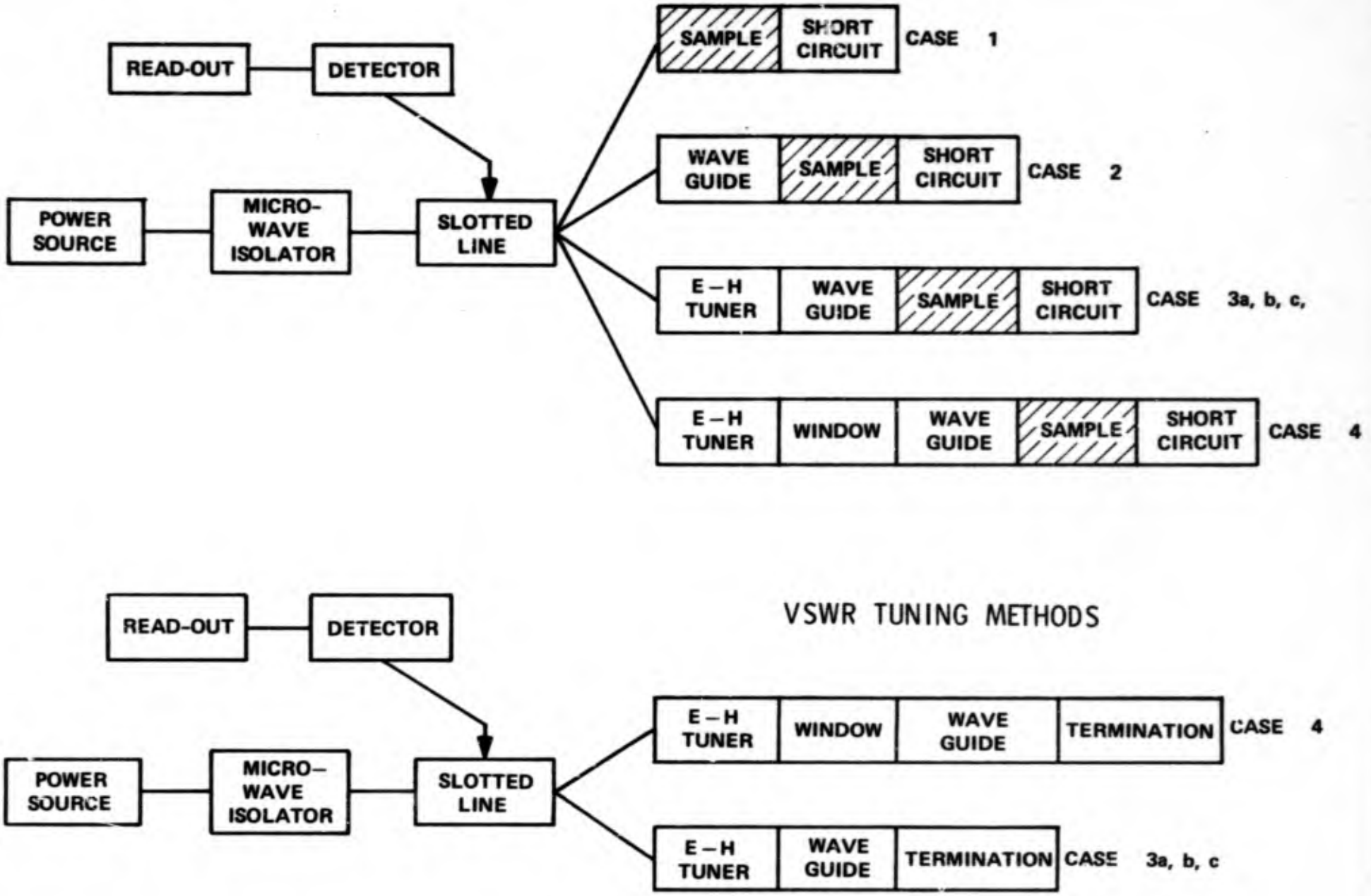

Figure 3. Dielectric Measurement Methods

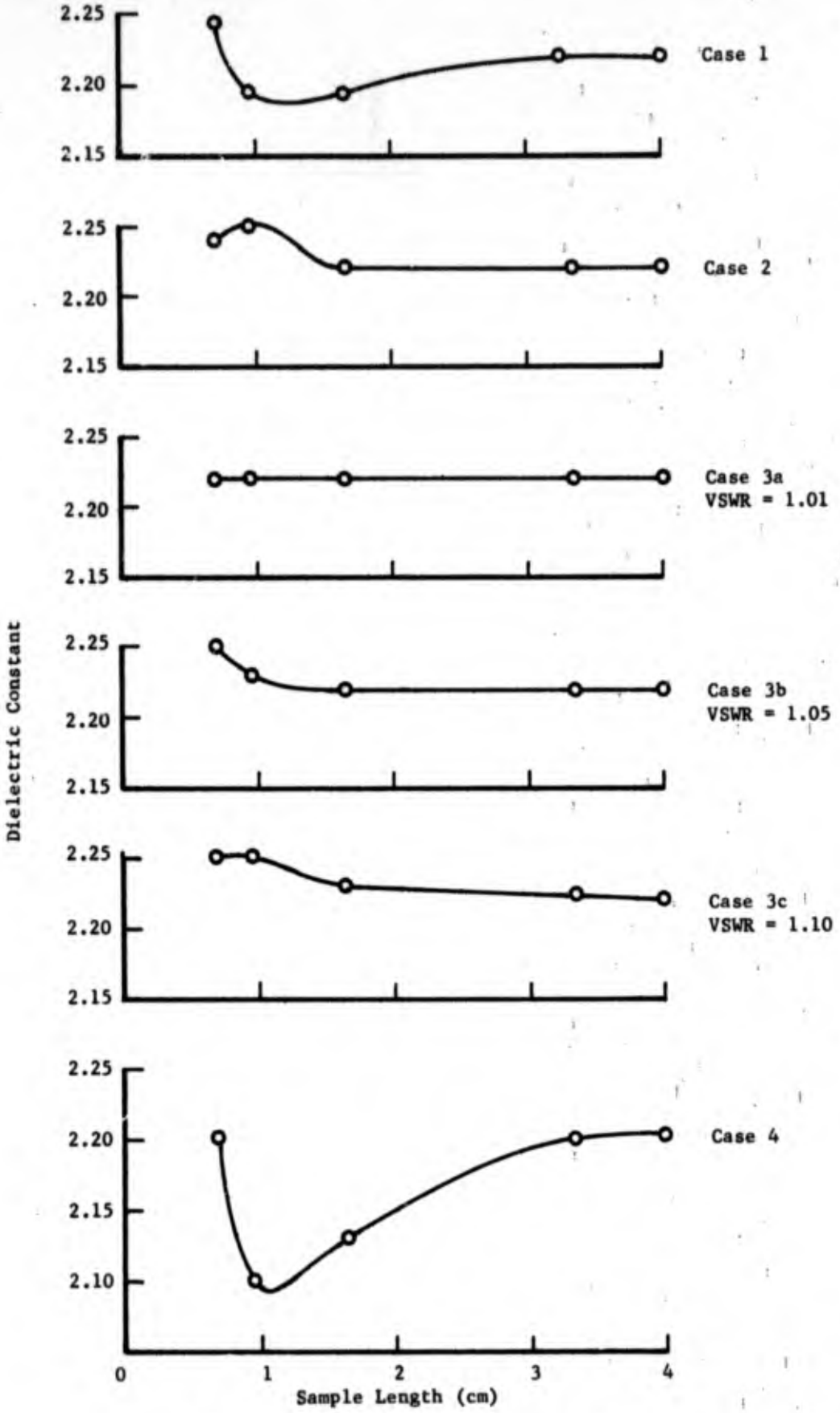

Figure 4. Results of Dielectric Constant Measurements

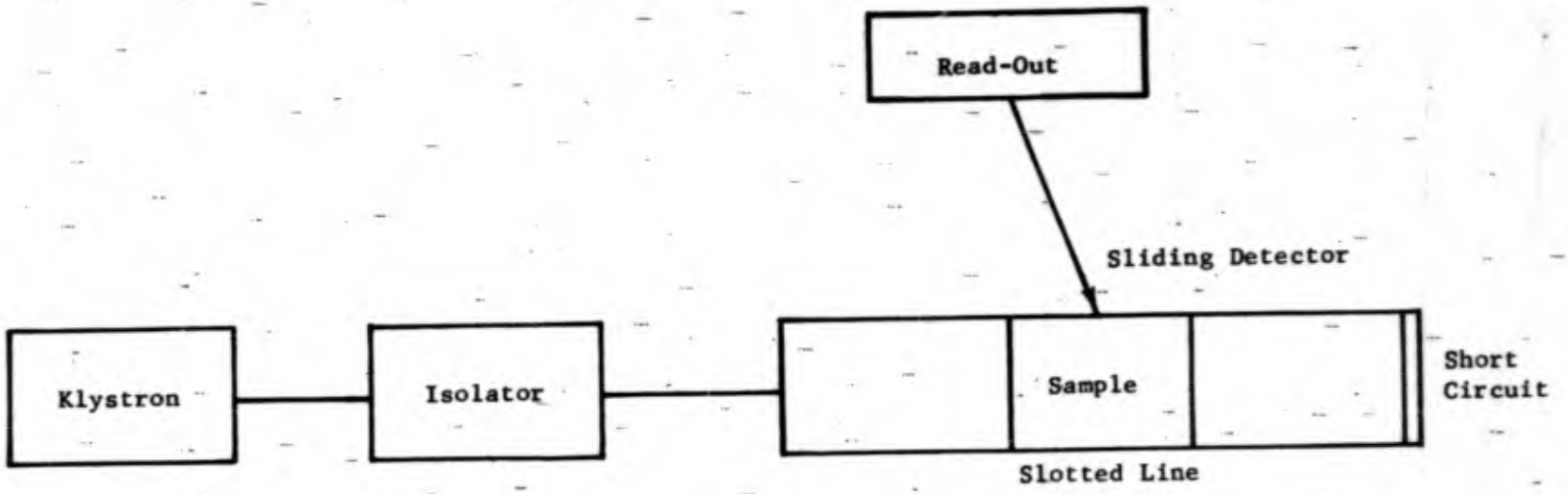

Figure 5. Dielectric Constant Measuring Apparatus

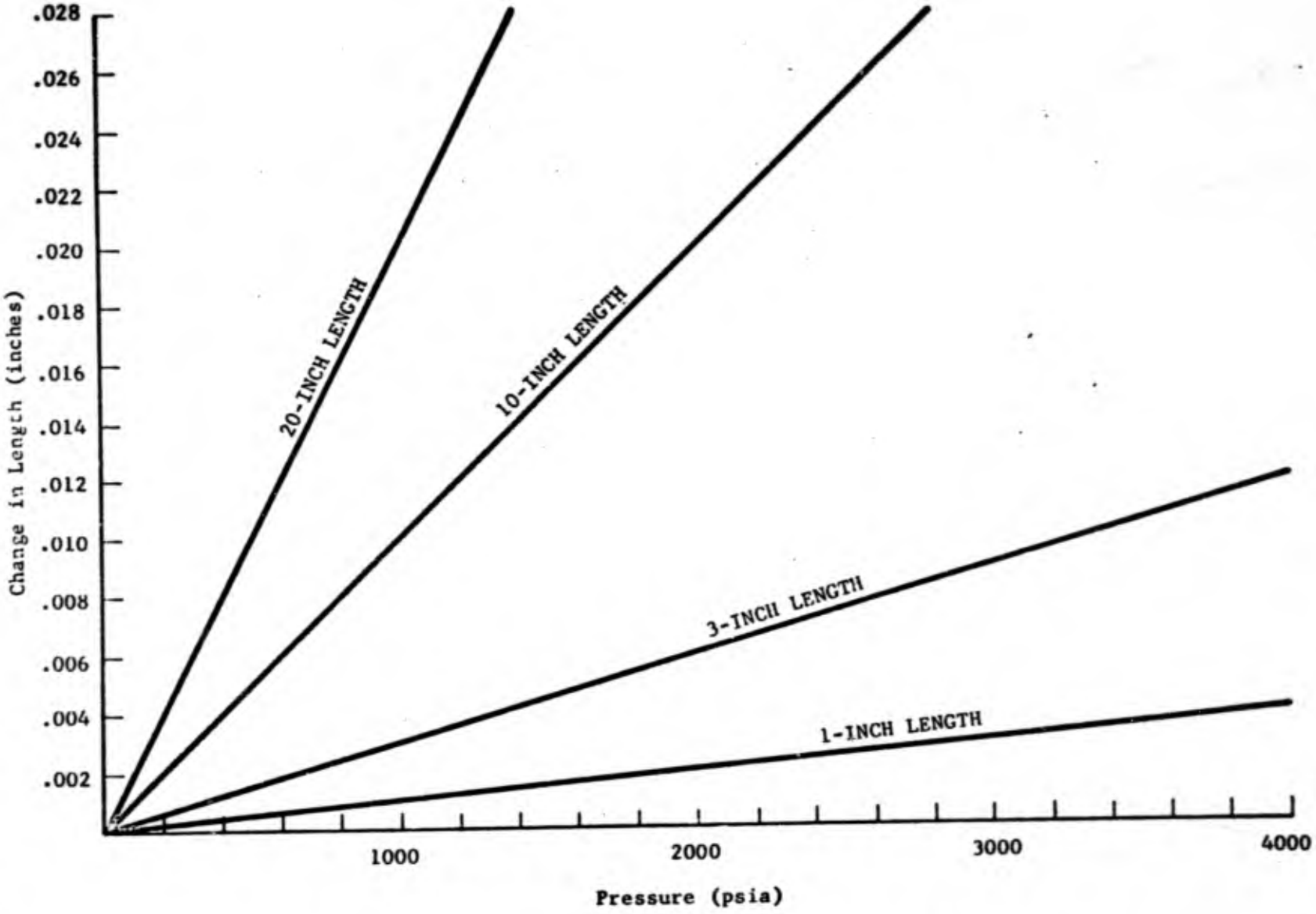

Figure 6. Propellant Bulk Modulus Pressure Effects

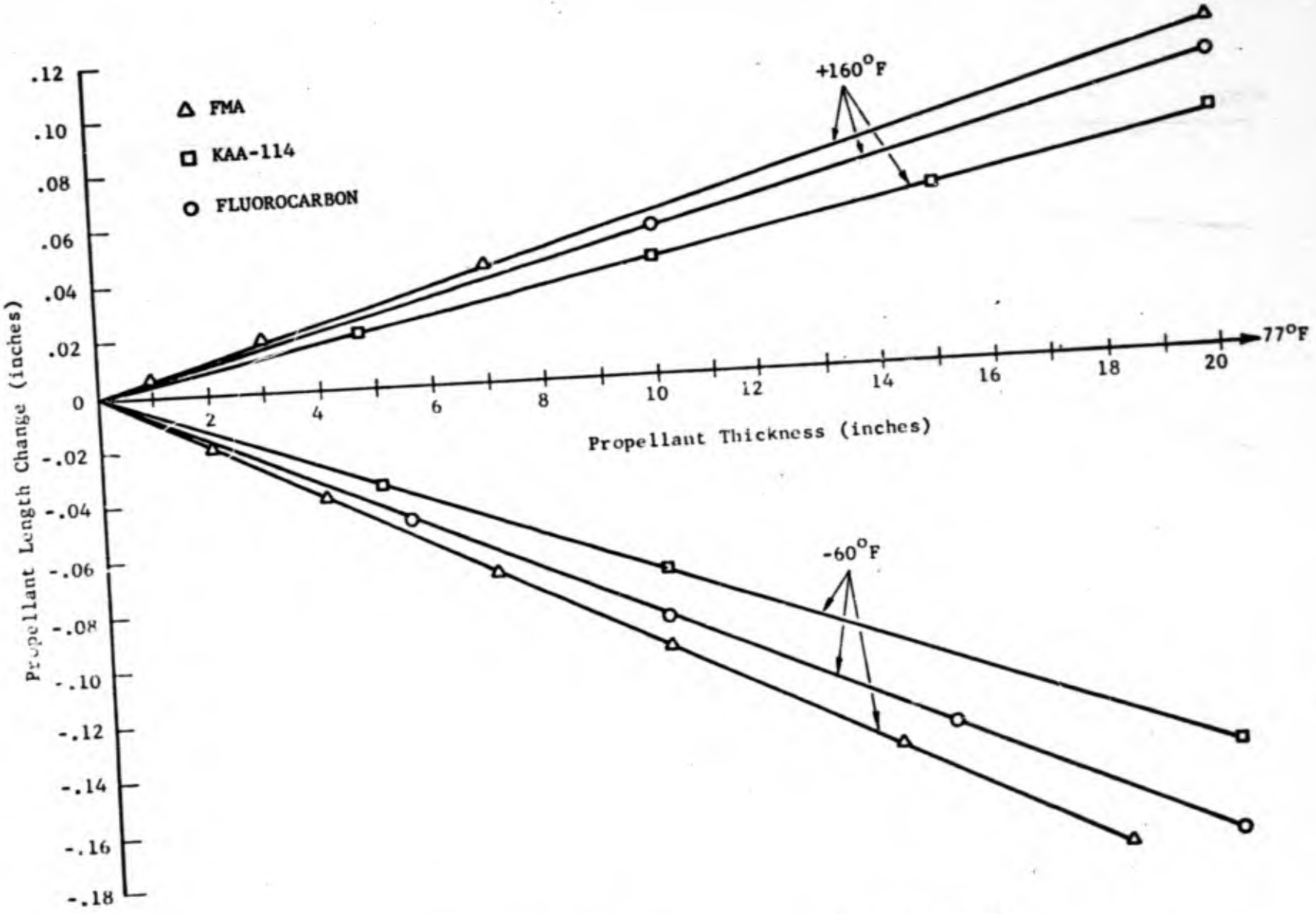

Figure 7. Propellant Thermal Expansion Characteristics

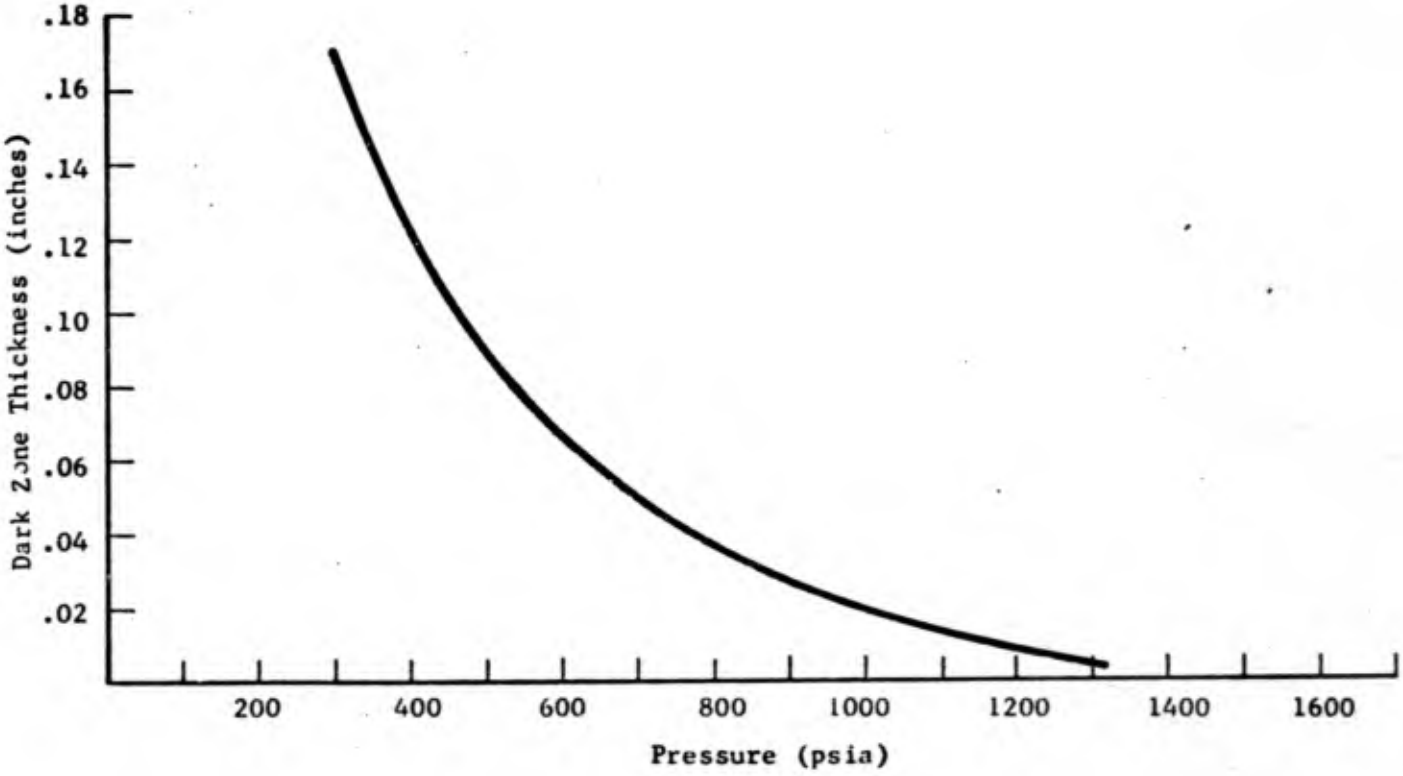

Figure 8. Dark Zone Pressure Dependance

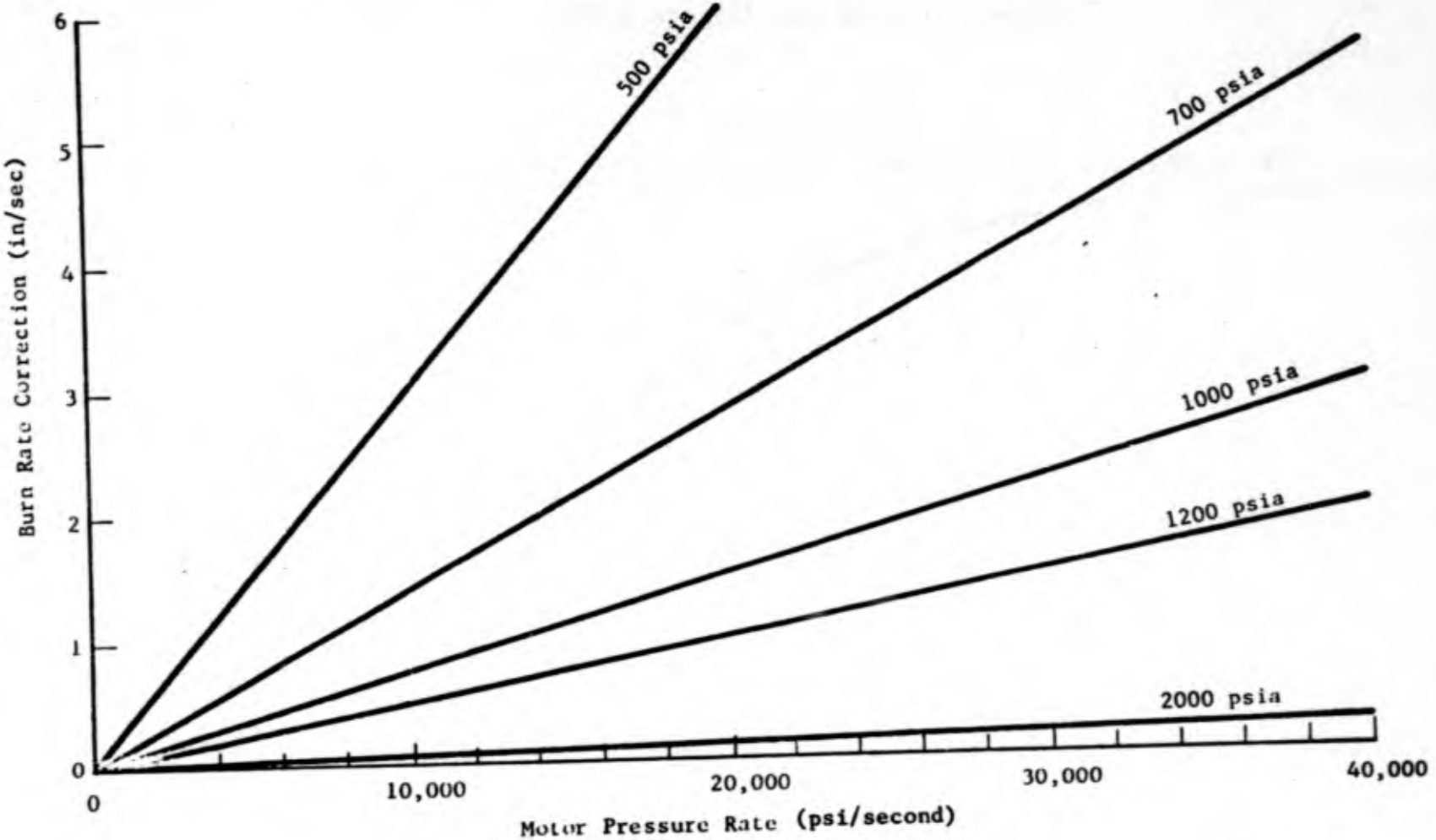

Figure 9. Dark Zone Burn Rate Correction

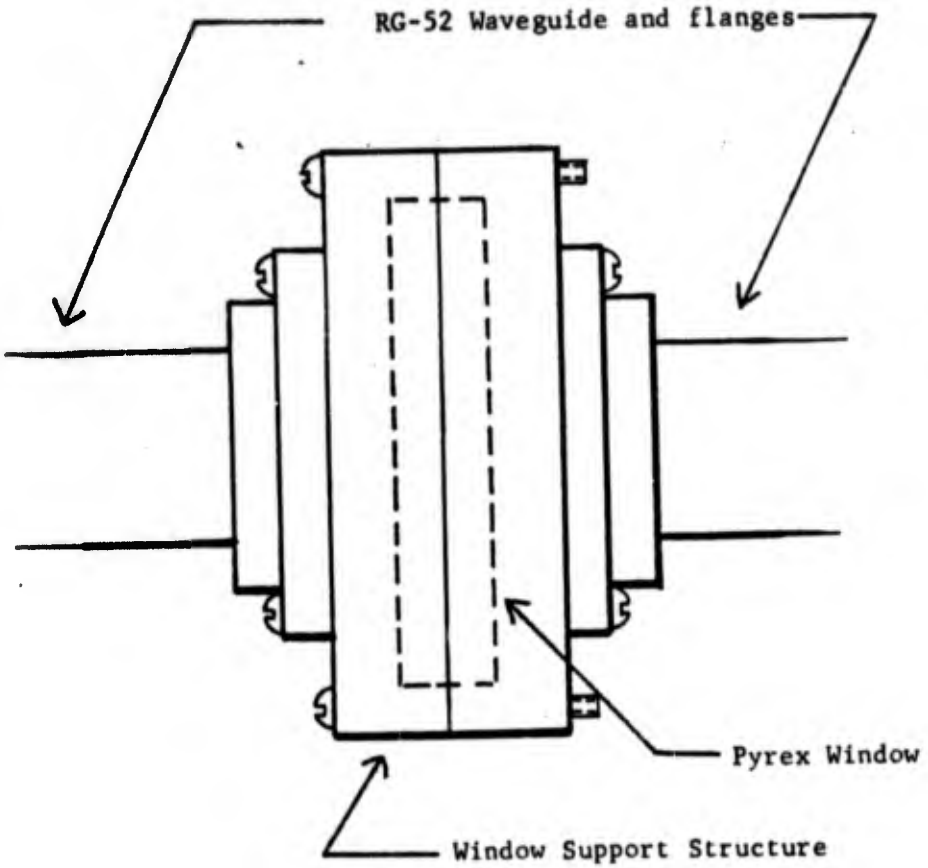

Figure 10. Dummy High Pressure Window used to Check Microwave Propagation Characteristics

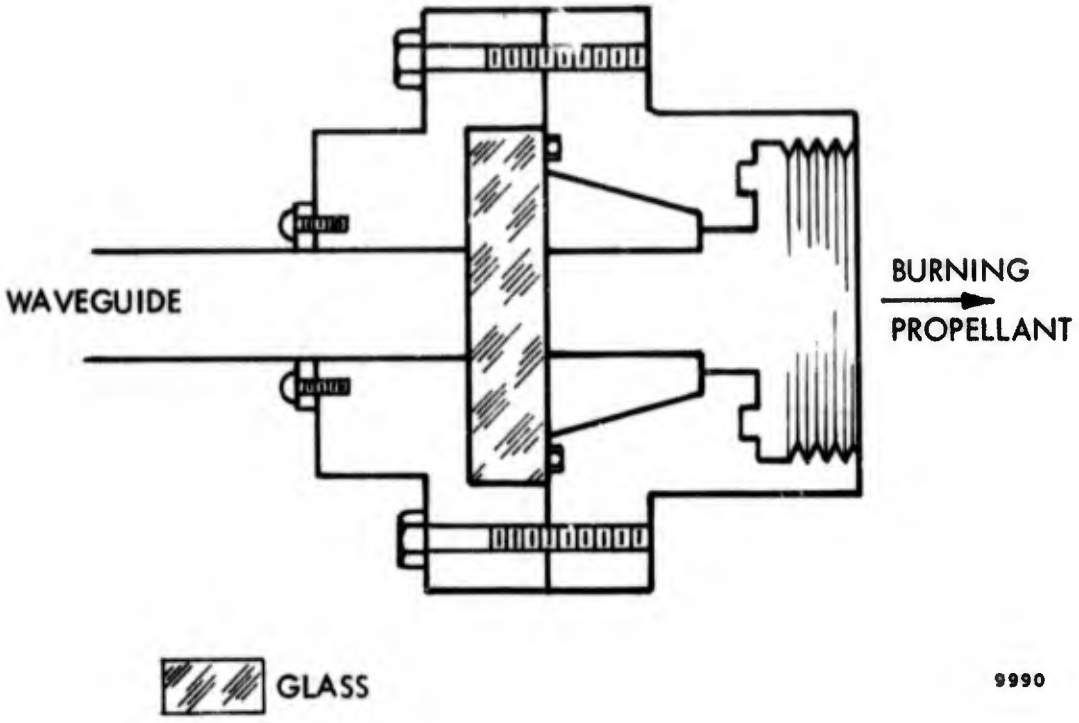

FIGURE 11
High Pressure Microwave Window

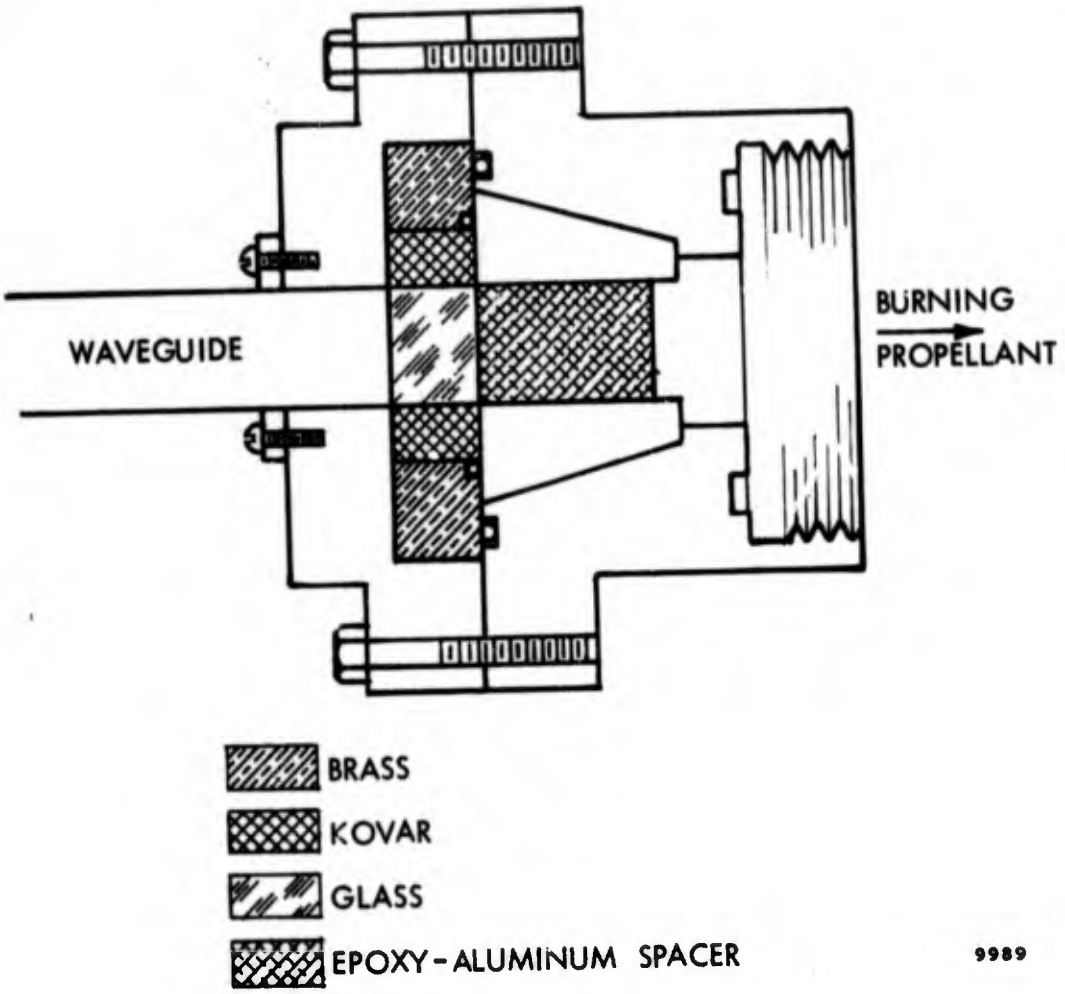

FIGURE 12
LowVSWR High Pressure Microwave Window

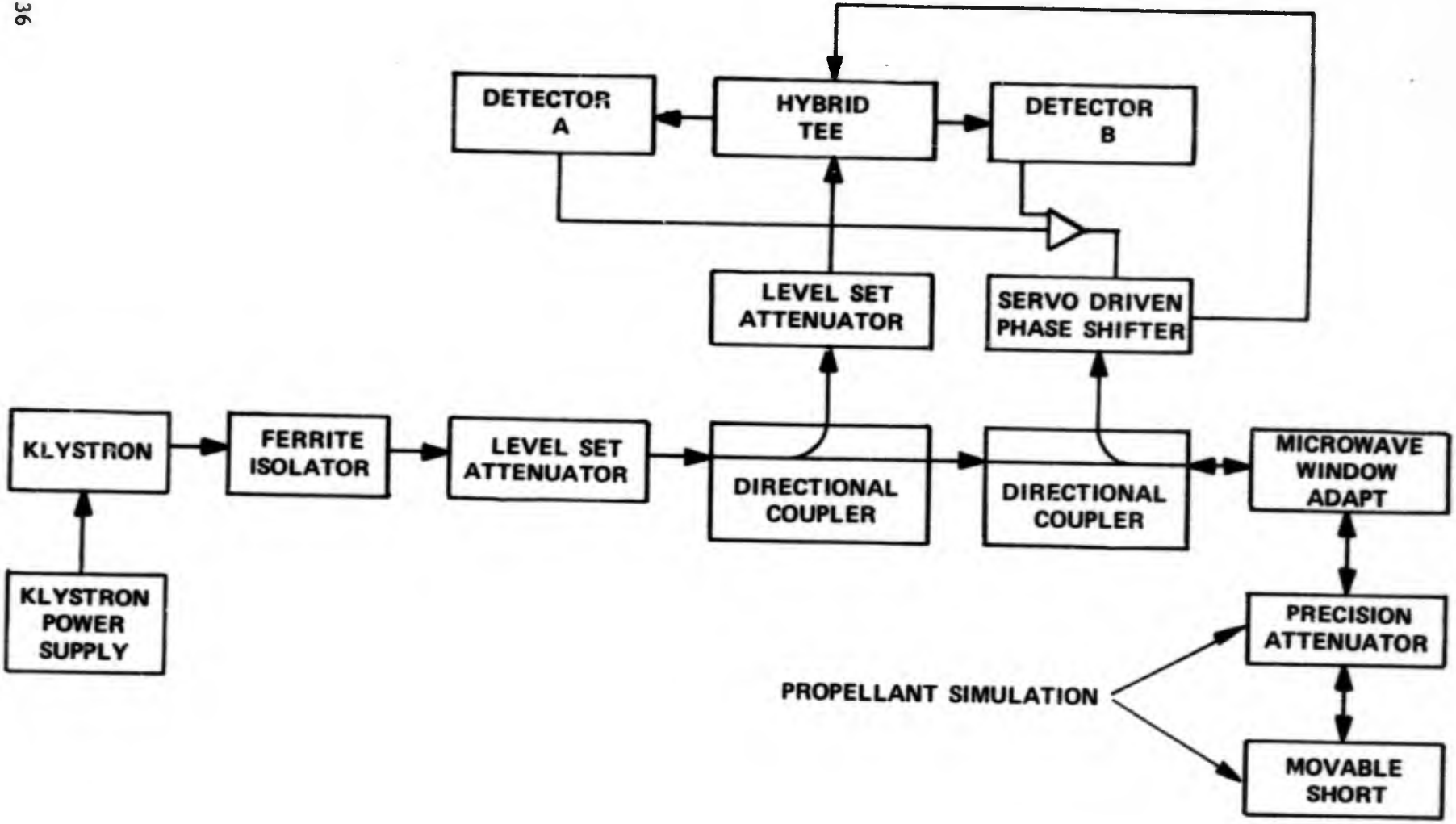

Figure 13. Servo Driven Phase Shifter Burn Rate Apparatus Schematic

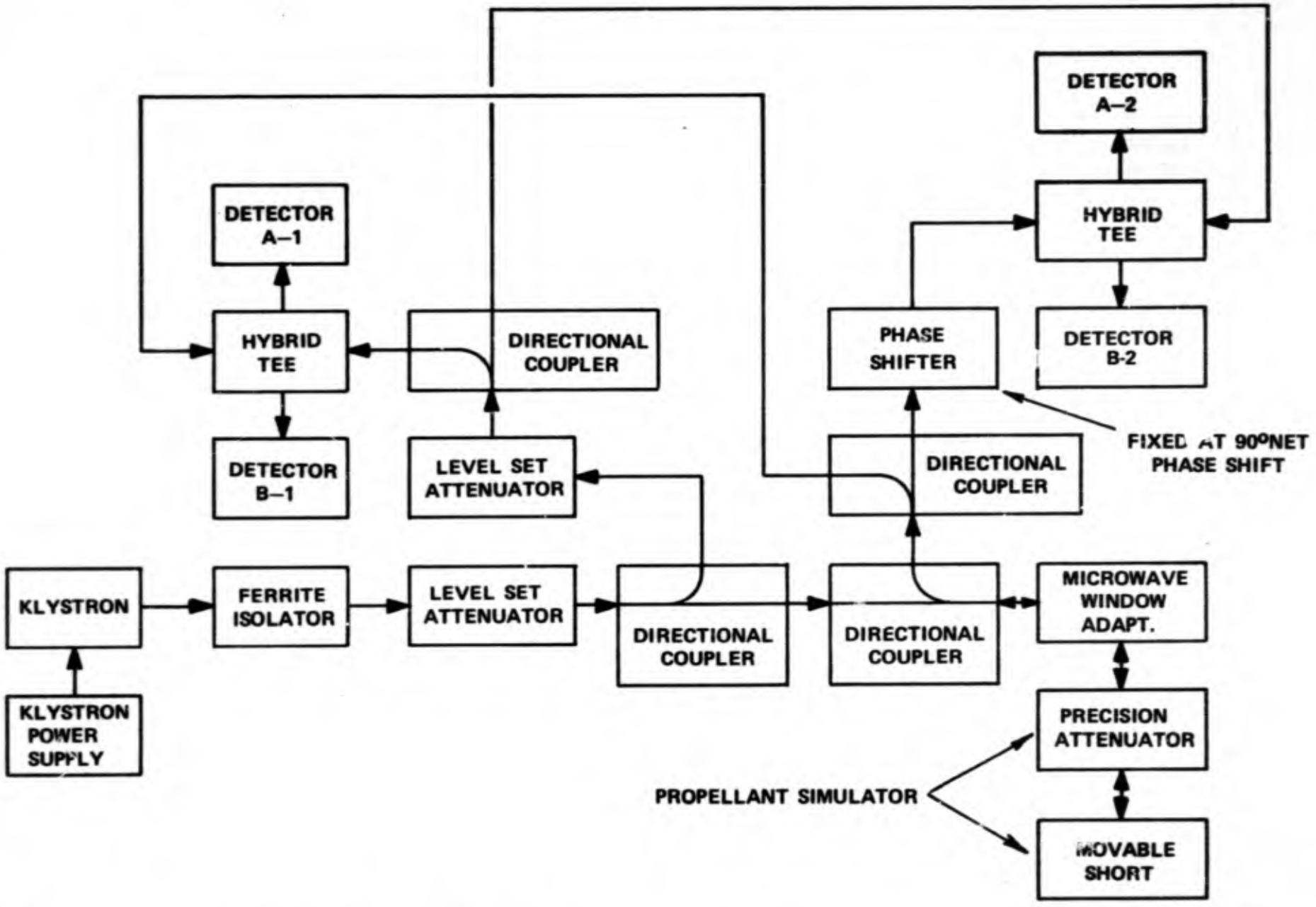

Figure 14. Twin Hybrid Tee Burn Rate Apparatus Schematic

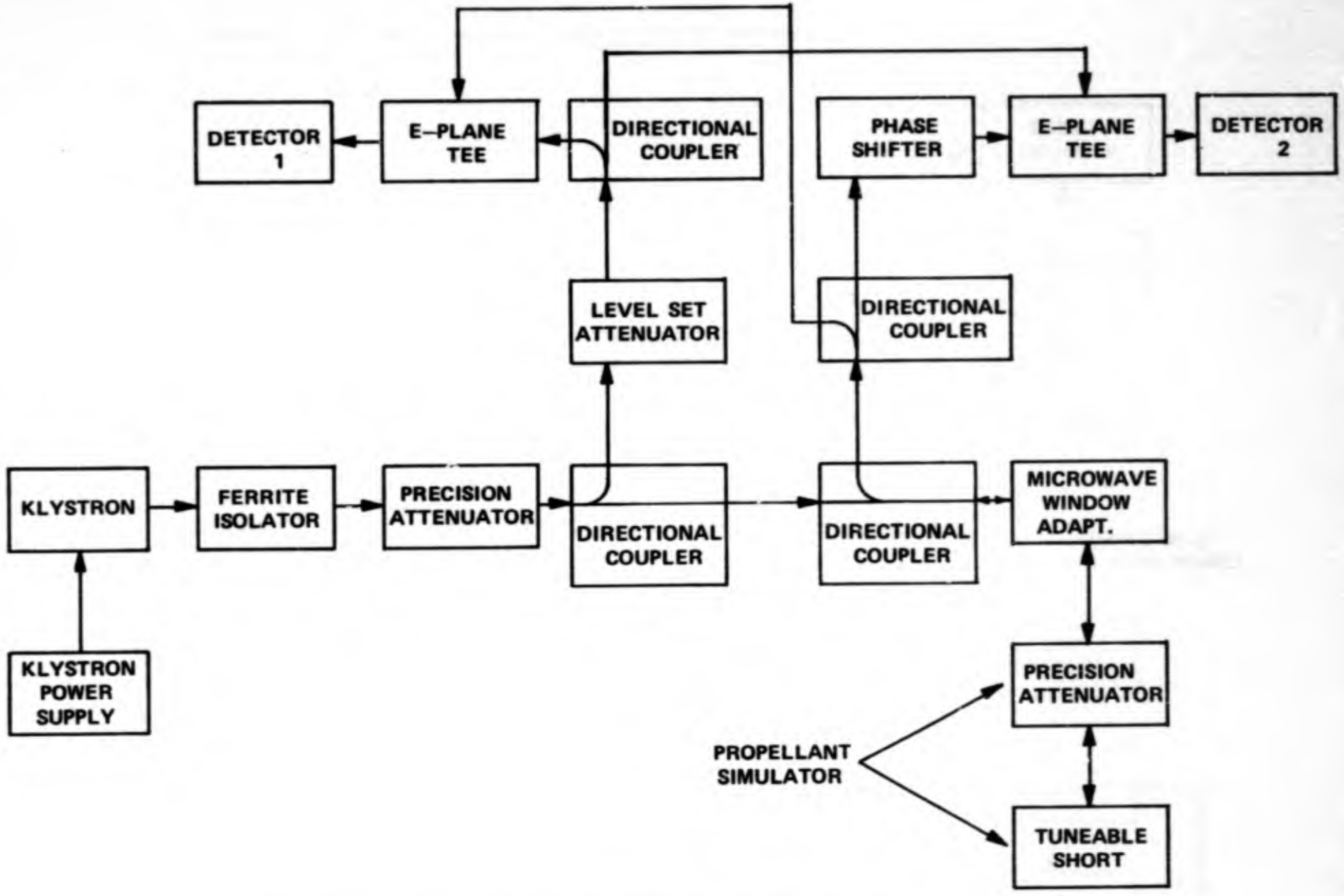

Figure 15. Twin Detector Burn Rate Apparatus Schematic

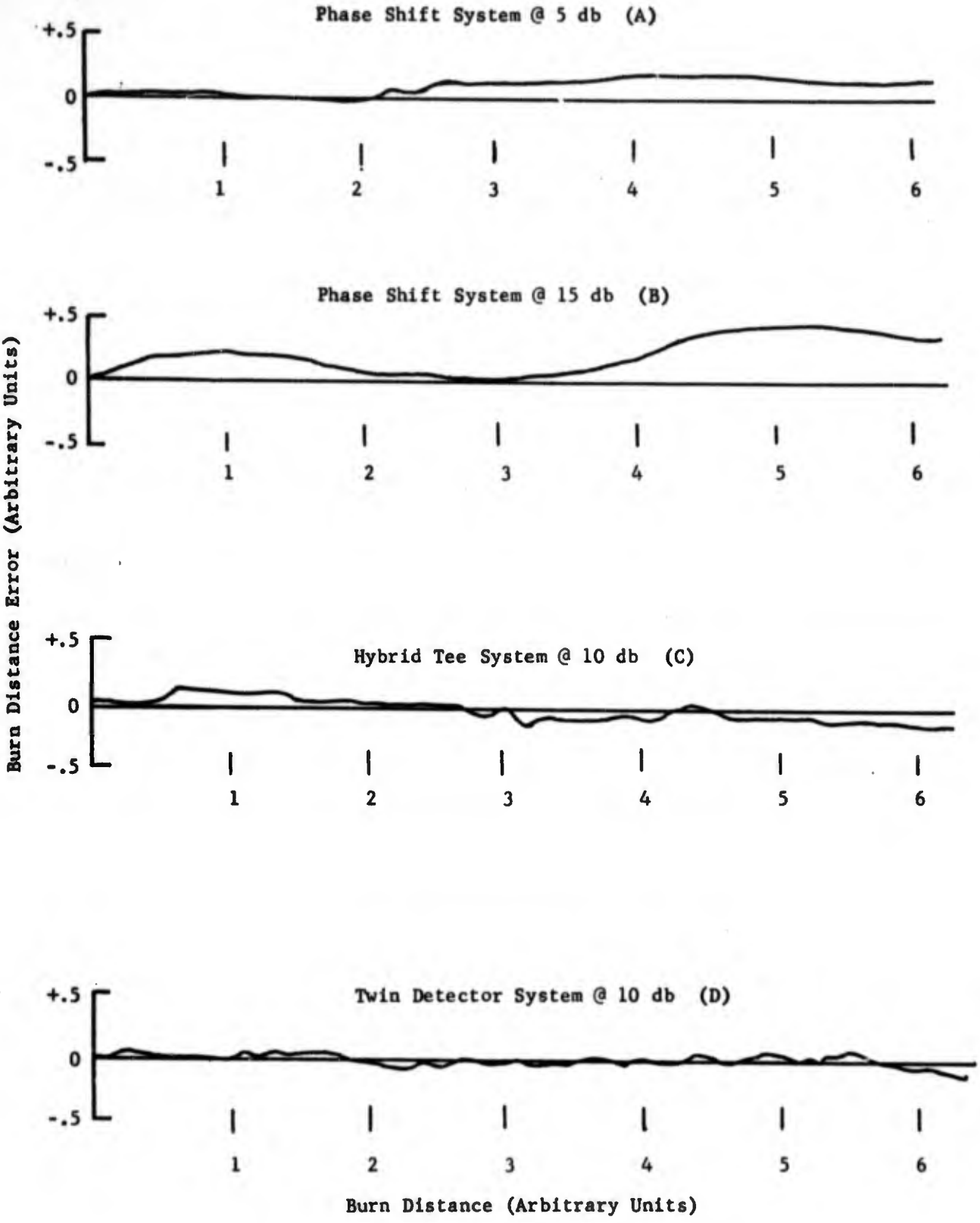

Figure 16a, b, c, d. Performance of Breadboard Microwave Burn Rate Systems with Microwave Window

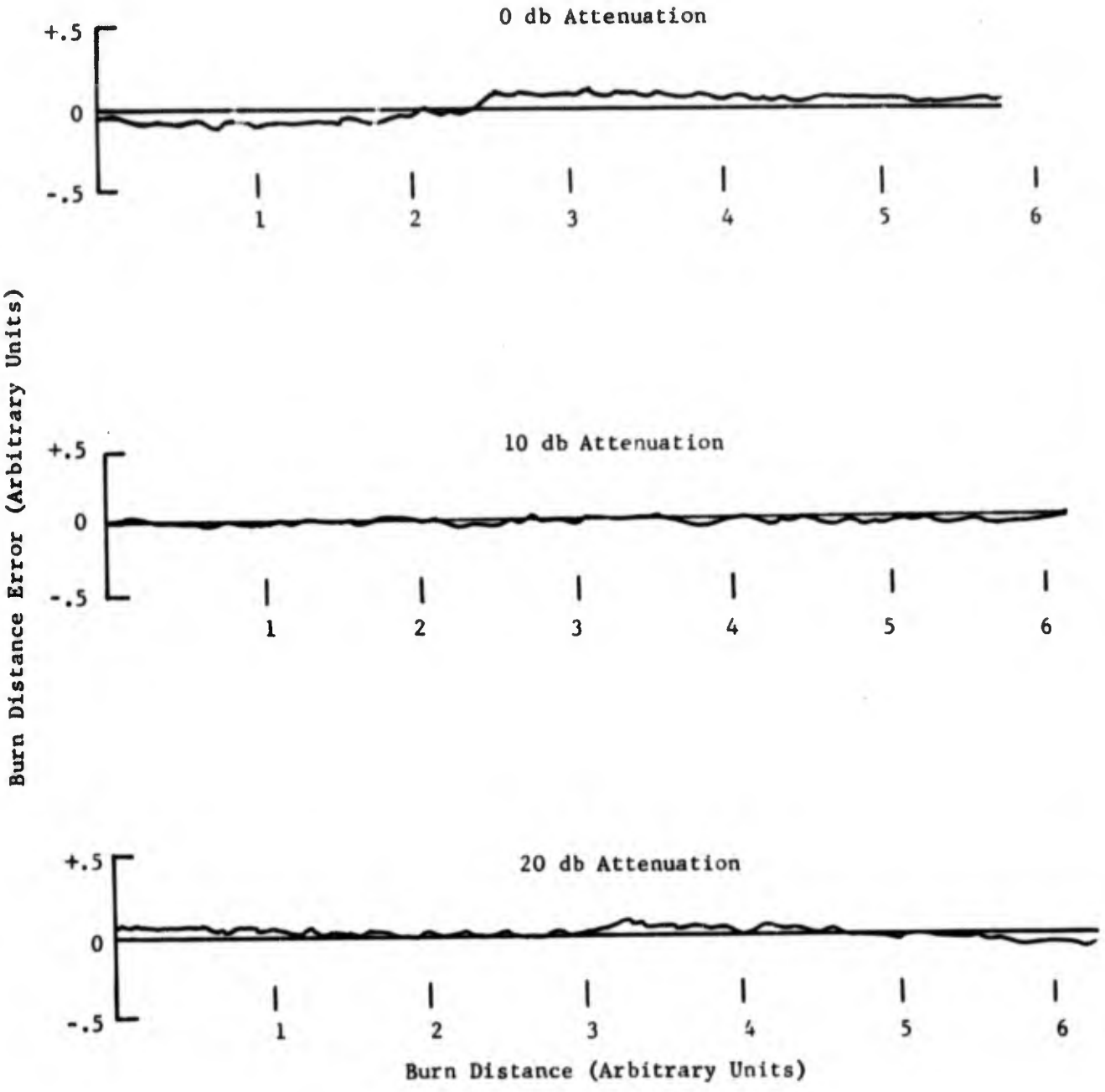

Figure 17. Performance of Hybrid Tee Breadboard Burn Rate System at Three Attenuation Levels without Microwave Window

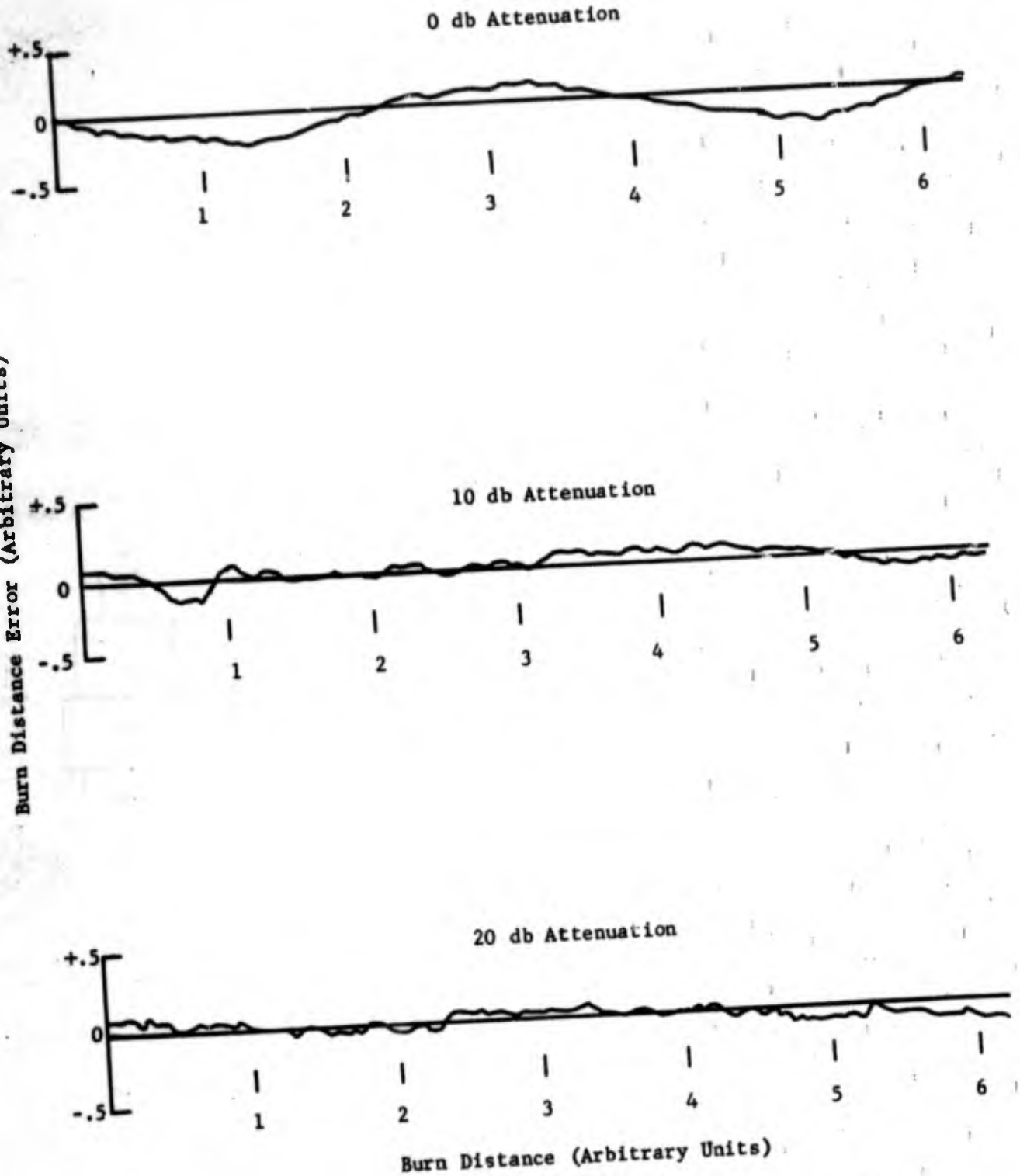

Figure 18. Performance of Twin Detector Burn Rate System at Three Attenuation Levels without Microwave Window

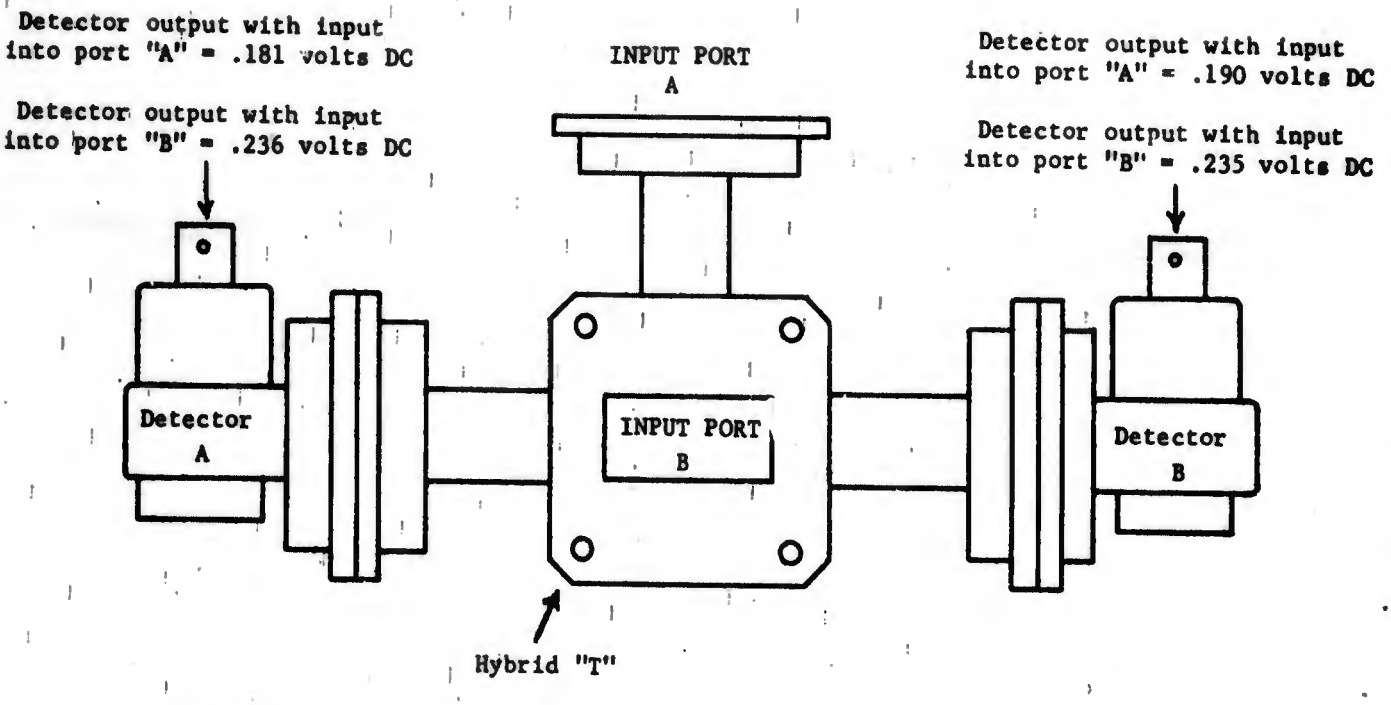

NOTE: The input level was the same when into port "A" or port "B." When one input port was receiving an input, the other was terminated.

Figure 19

Typical Test Results for a Hybrid "T" with Matched Detectors

Number 1 Hybrid Tee Performance

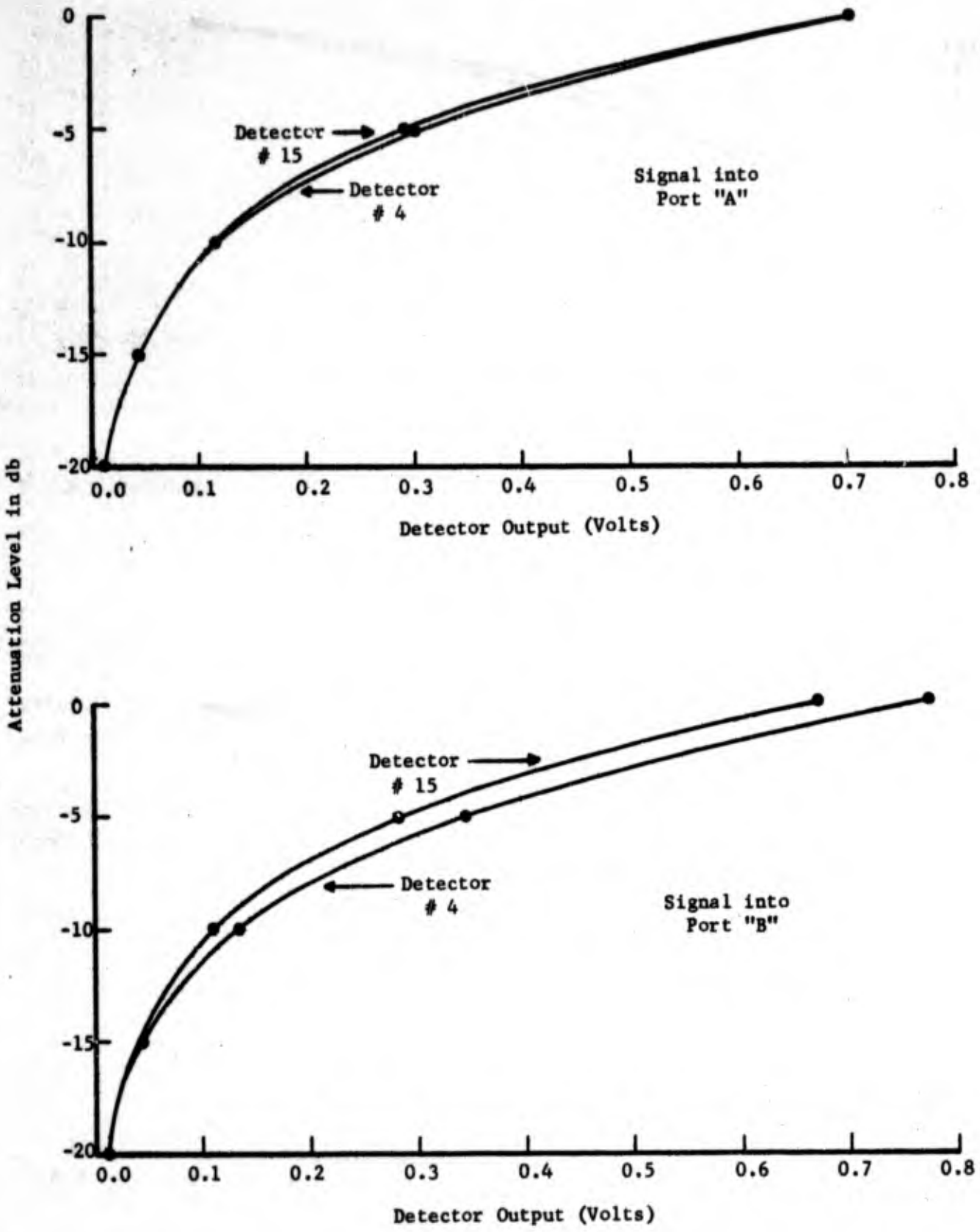

Figure 20

Number 2 Hybrid Tee Performance

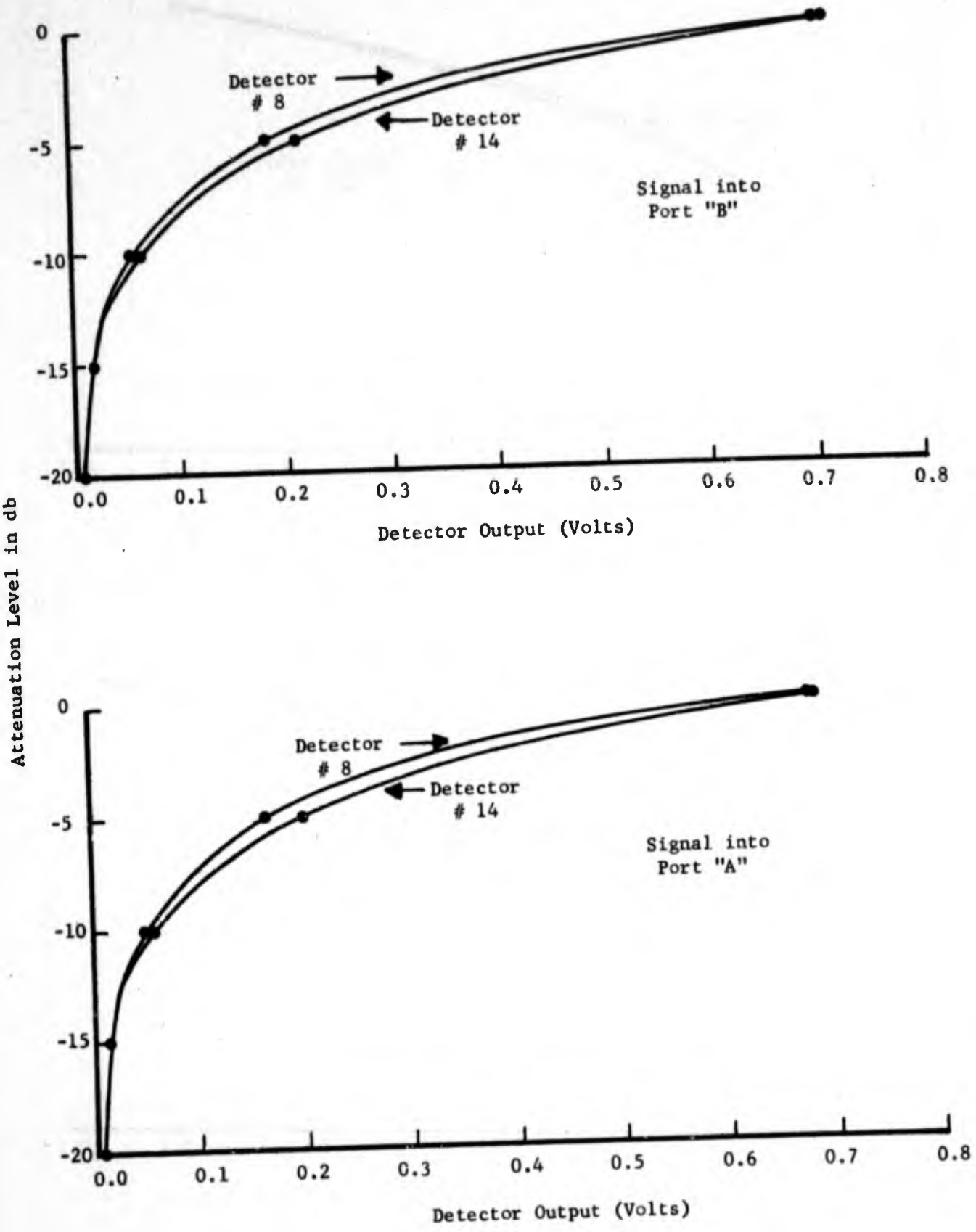

Figure 21

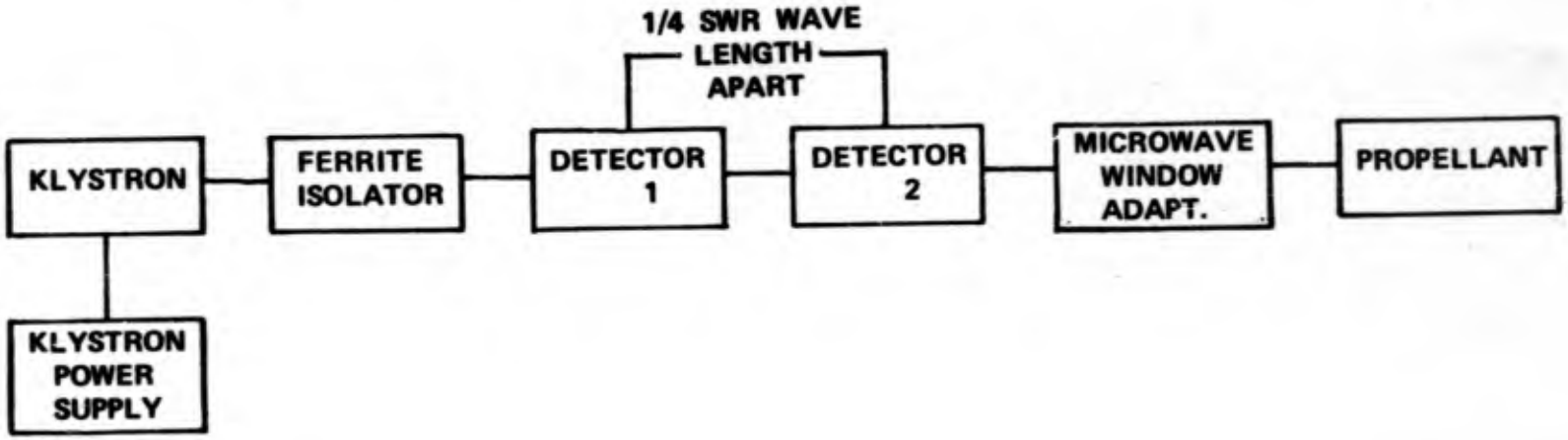

Figure 22. Schematic of Practical Embodiment of Twin Detector Burn Rate Apparatus

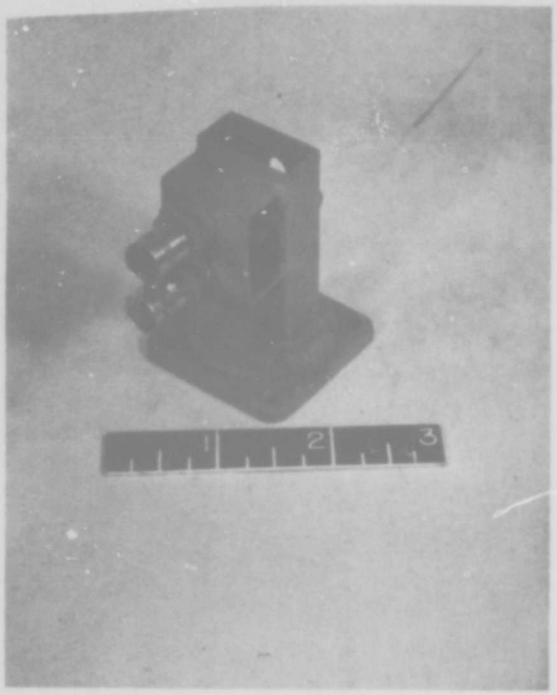

A

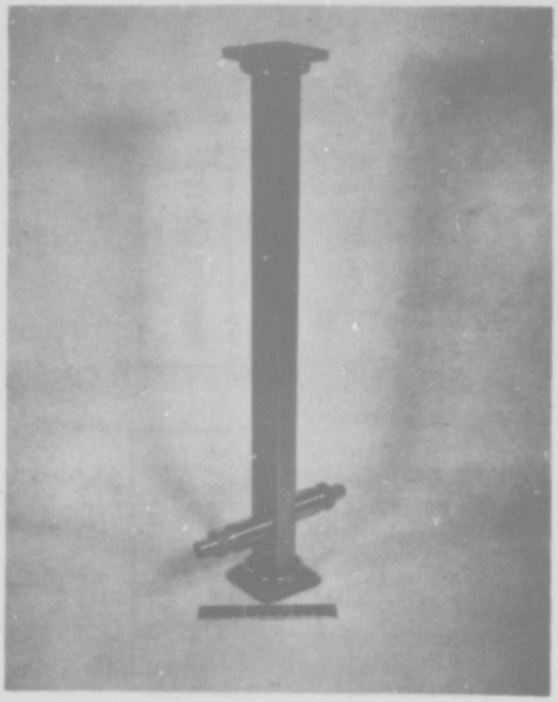

B

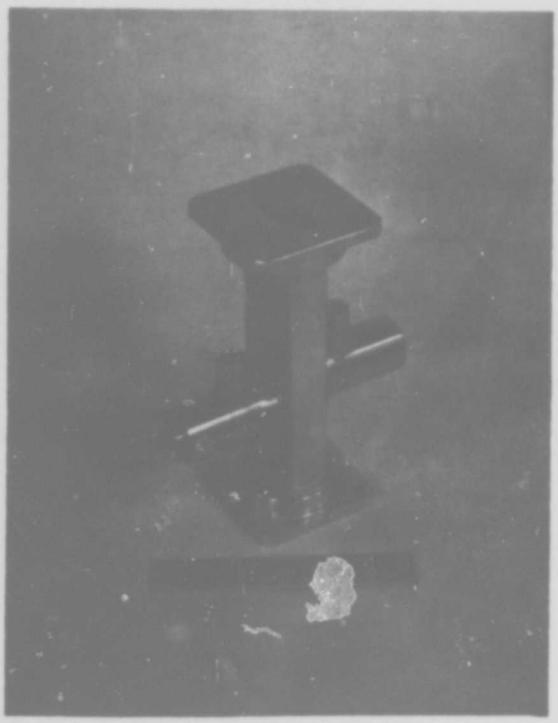

C

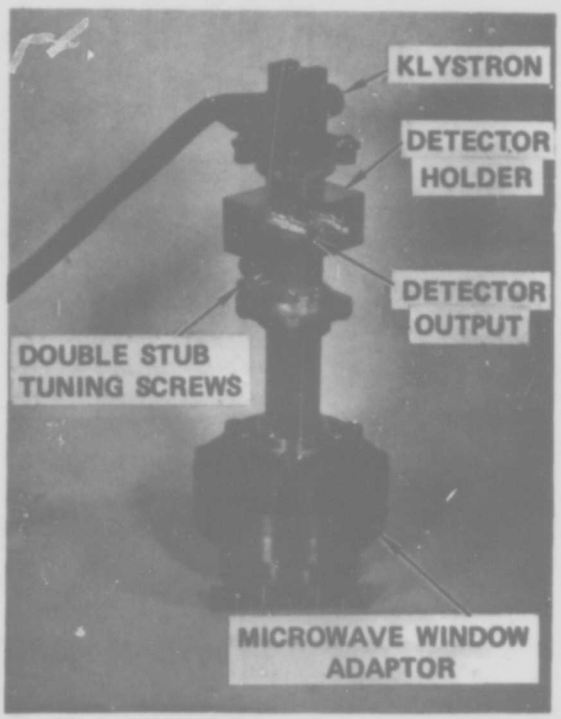

D

G-2782

Evolution of Twin Detector Burn Rate Apparatus

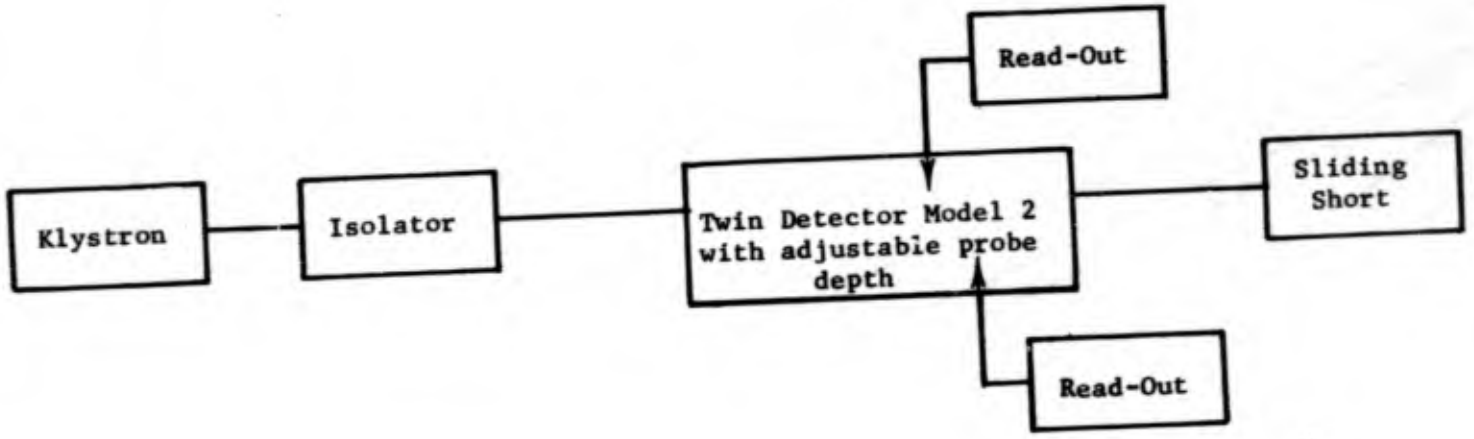

(A)

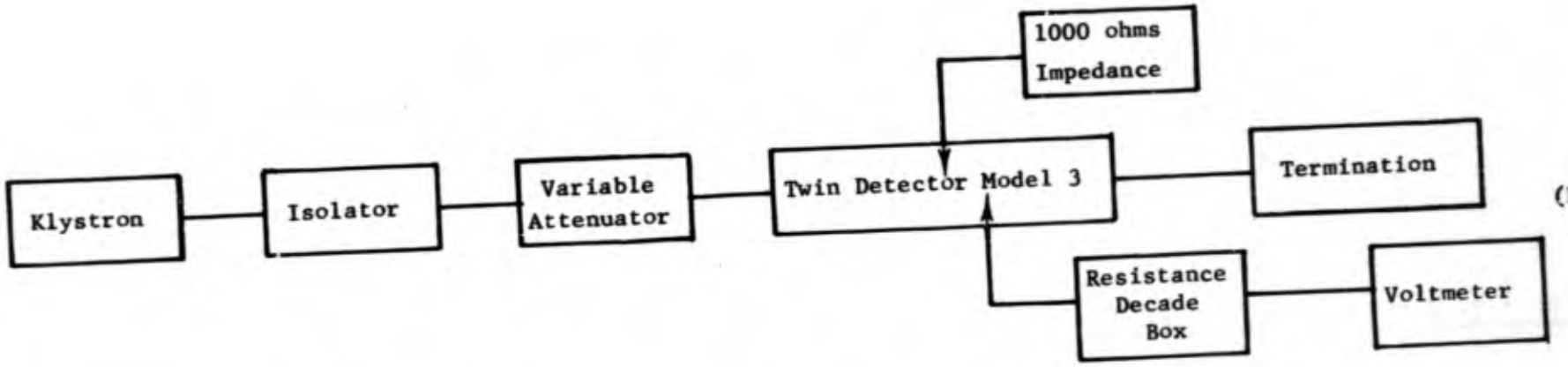

(B)

Figure 24a, b. Apparatus used for Optimizing Probe Depth and Output Impedance

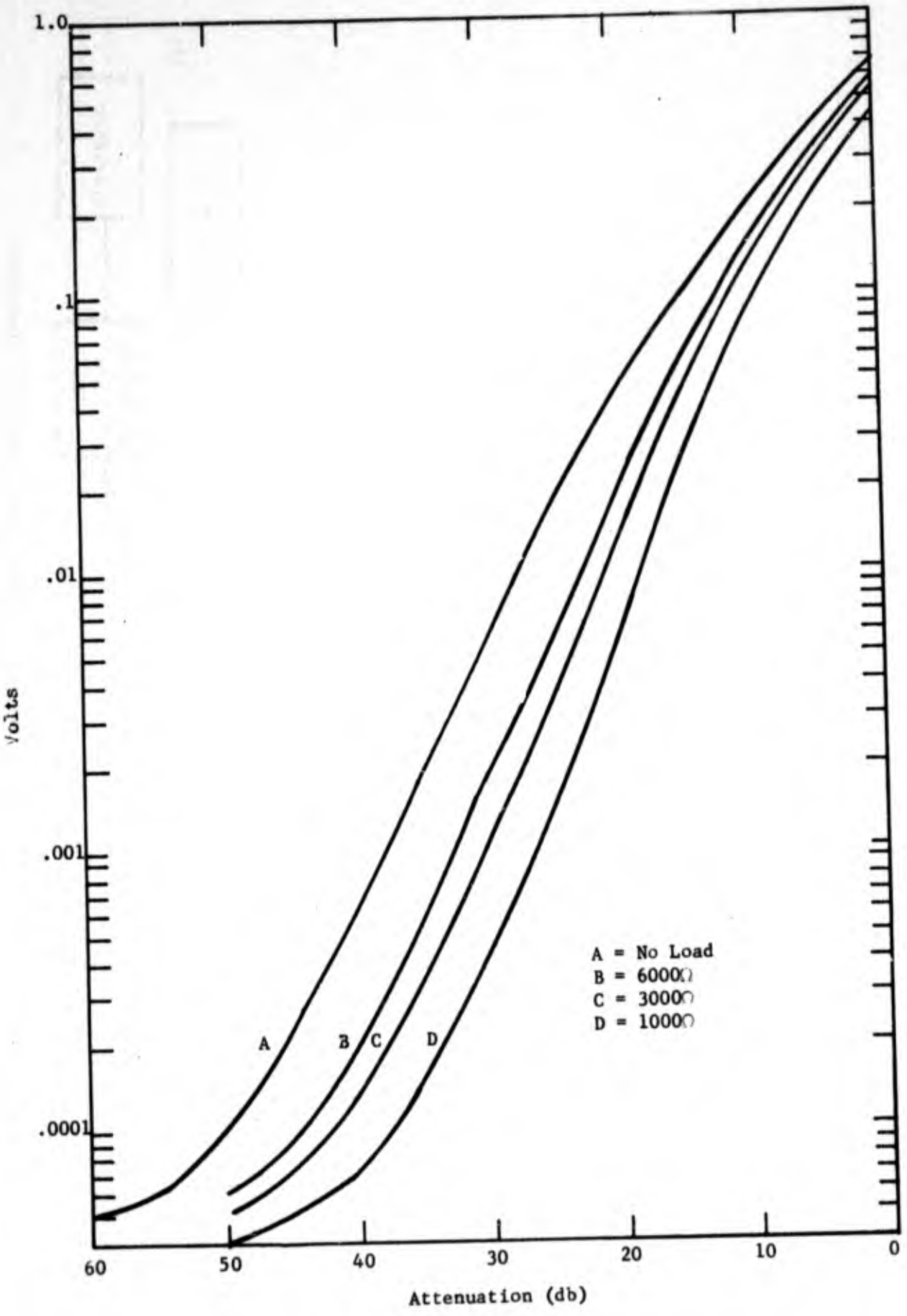

Figure 25. Detector Diode Output Versus Attenuation as a Function of Load Resistance

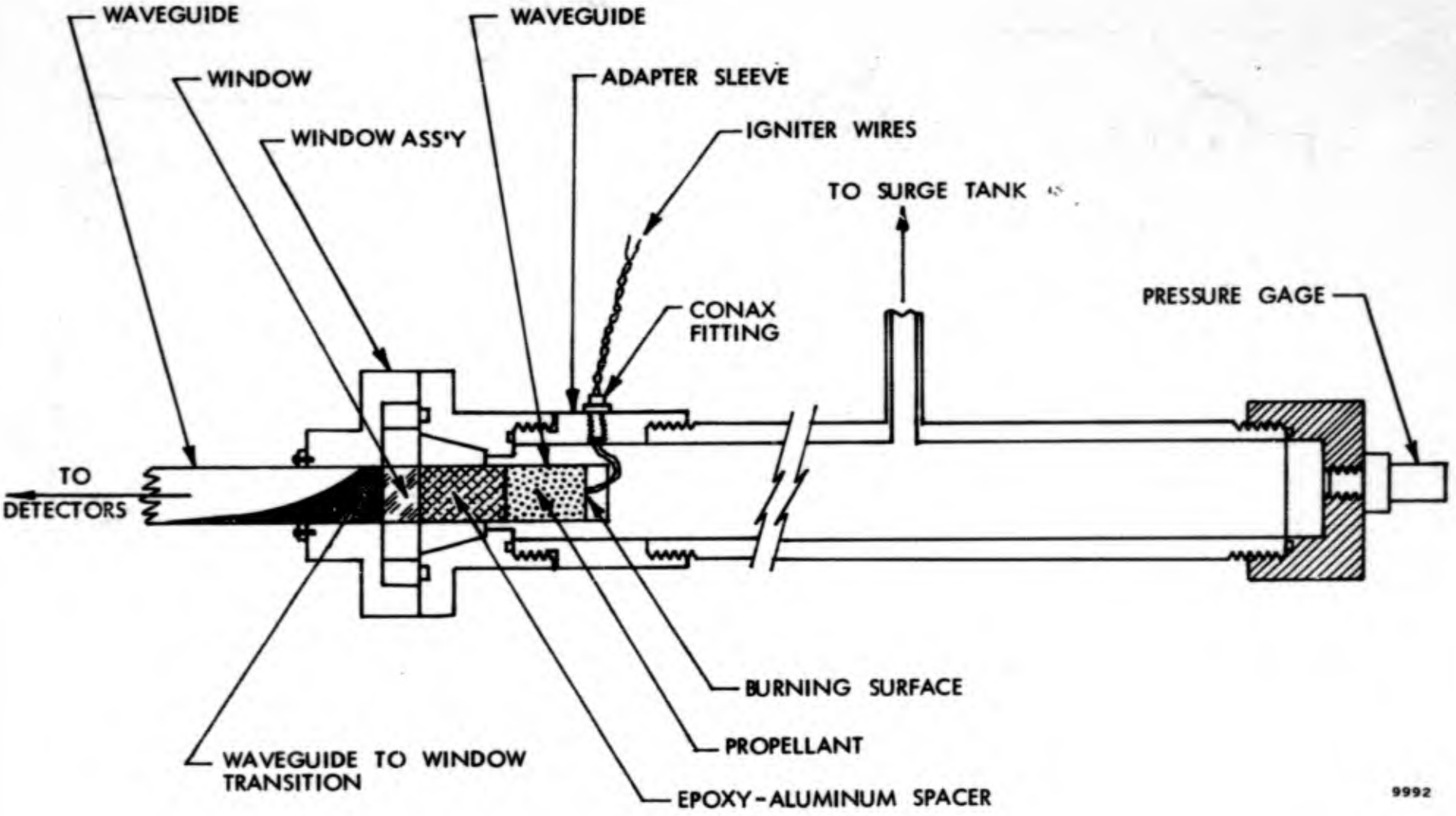

FIGURE 26
Small T-Burner Test Firing Setup

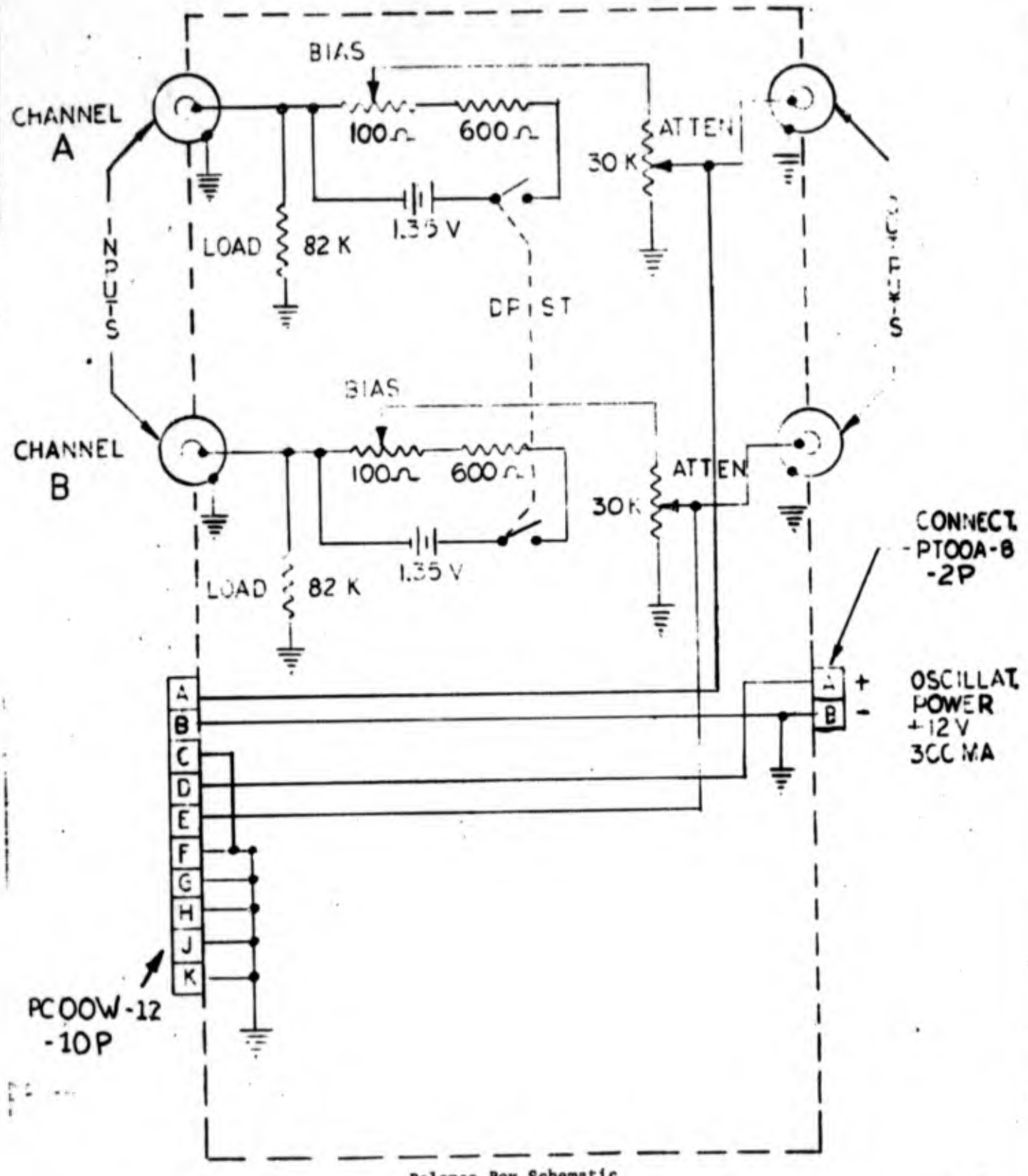

Balance Box Schematic

Figure 27

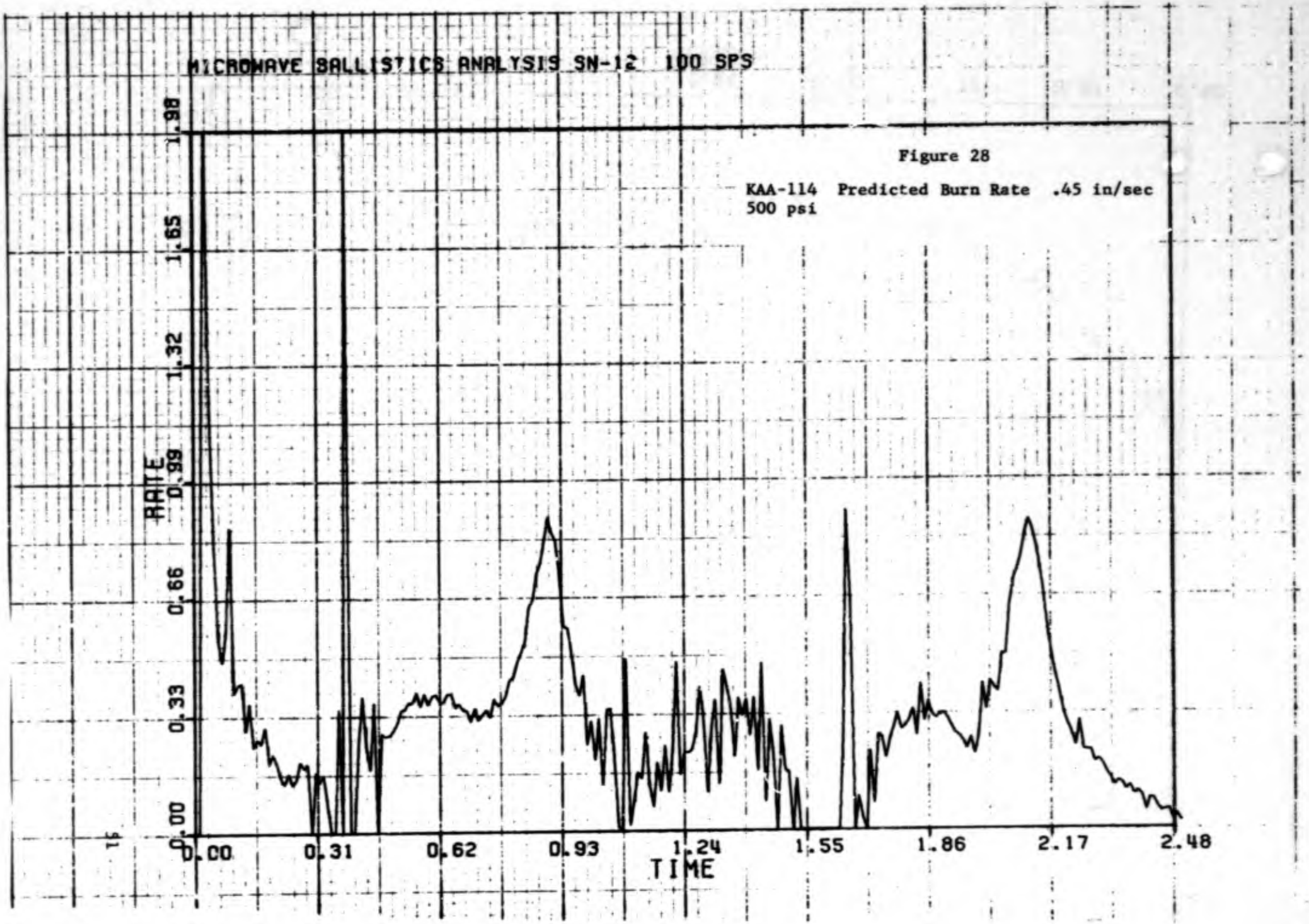

Figure 28

KAA-114 Predicted Burn Rate .45 in/sec
500 psi

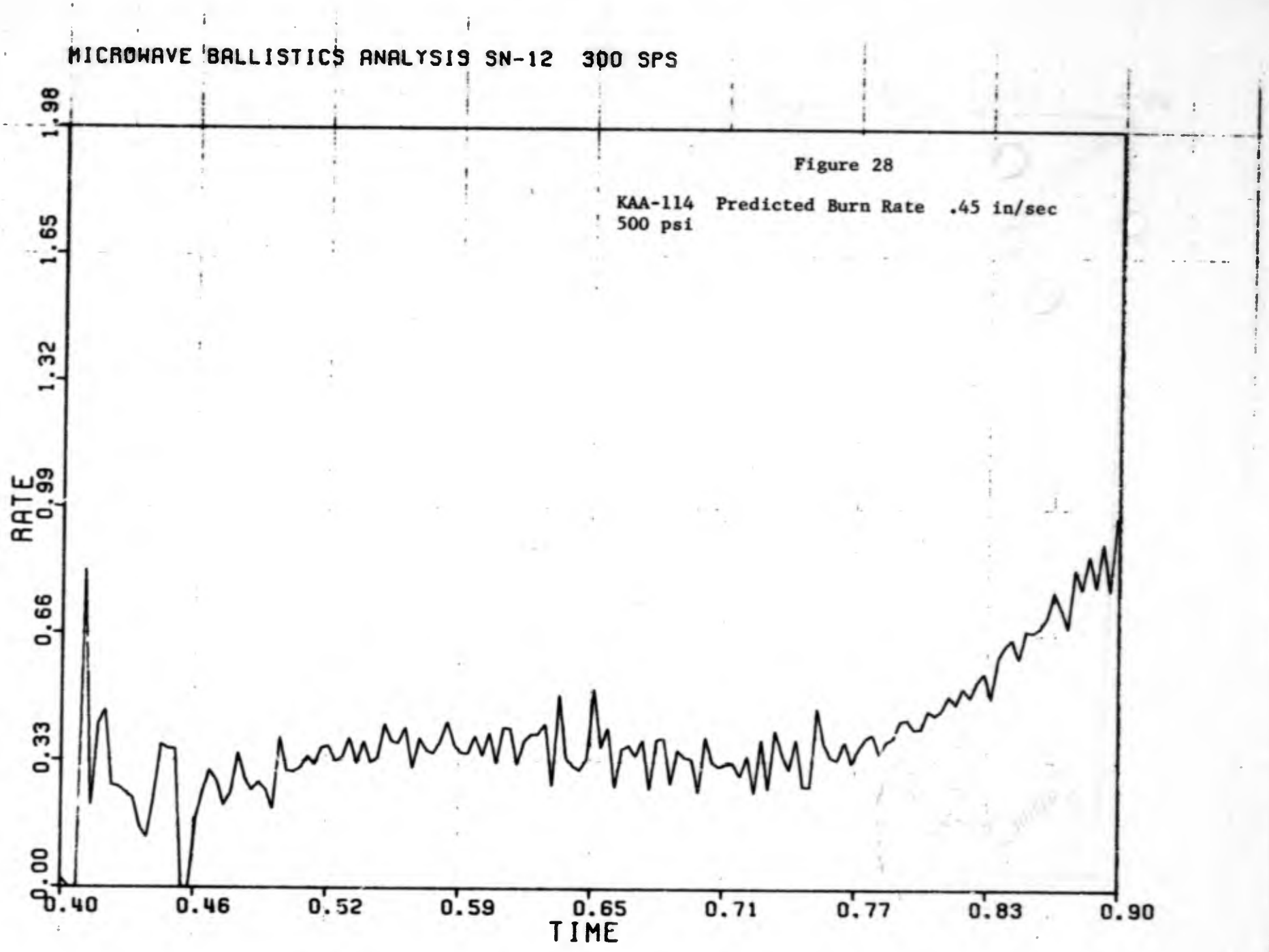

Figure 28

KAA-114 Predicted Burn Rate .45 in/sec
500 psi

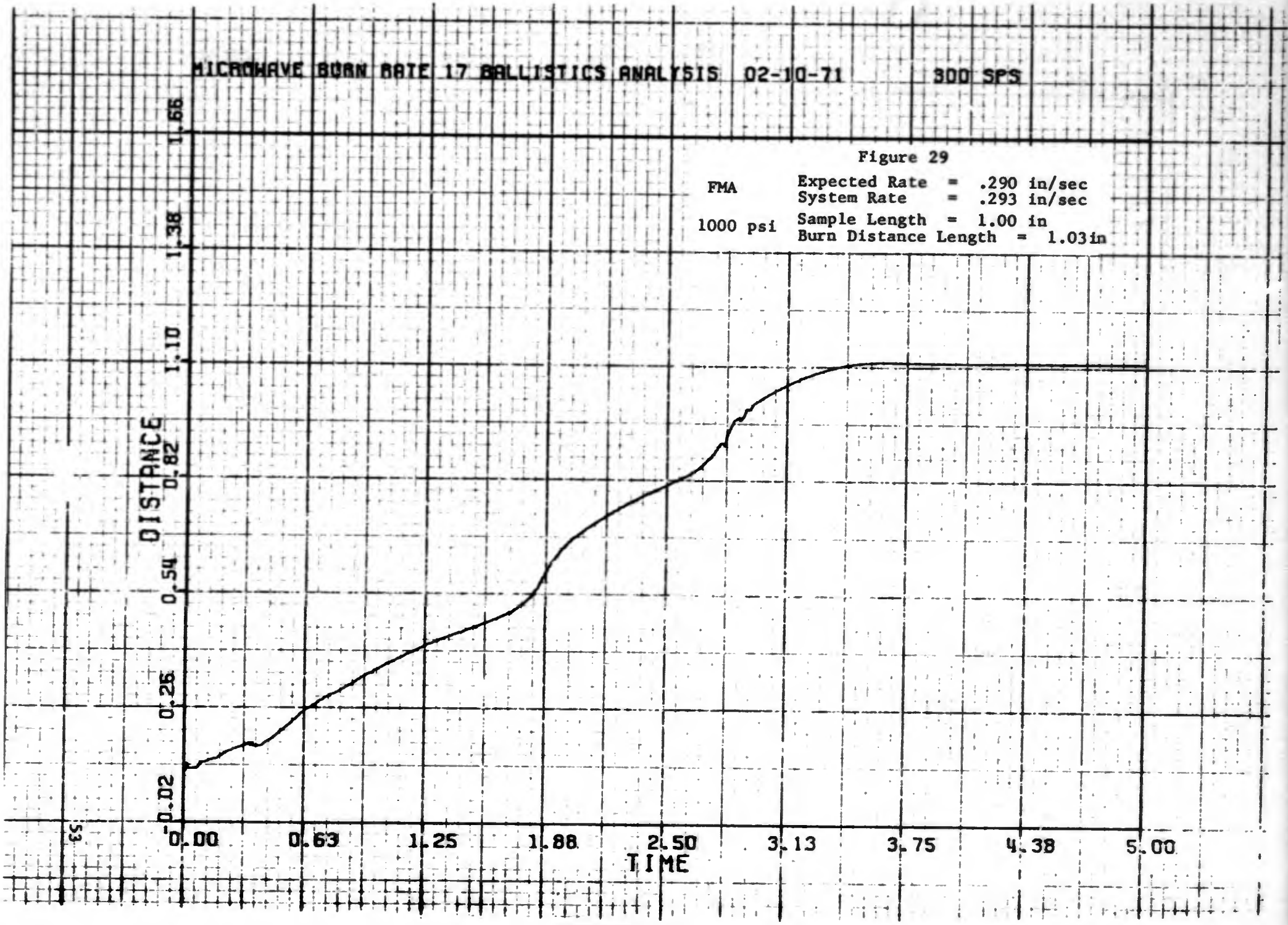

Figure 29

FMA

1000 psi

Expected Rate = .290 in/sec
System Rate = .293 in/sec
Sample Length = 1.00 in
Burn Distance Length = 1.03in

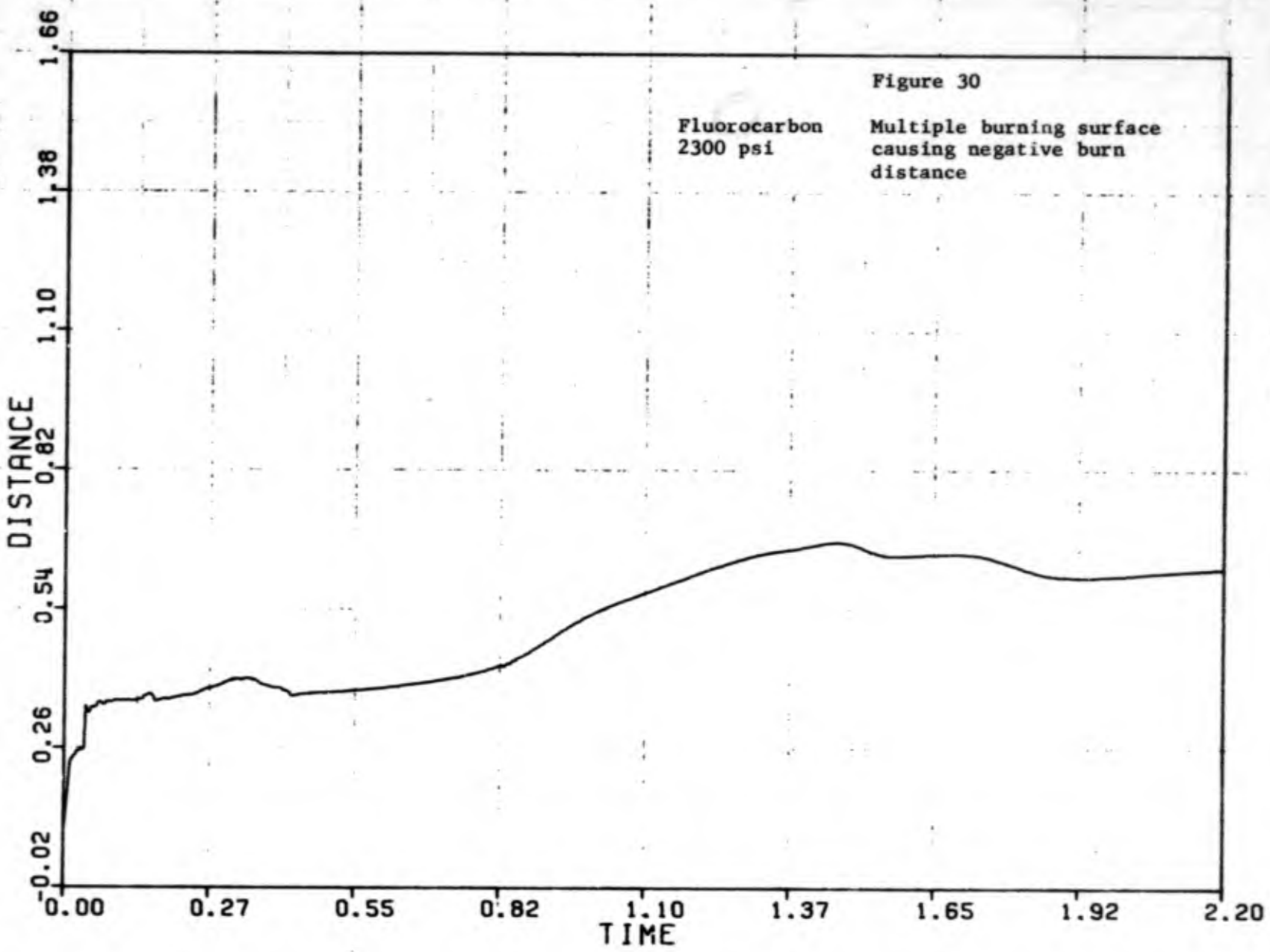

Figure 30

Fluorocarbon
2300 psi

Multiple burning surface causing negative burn distance

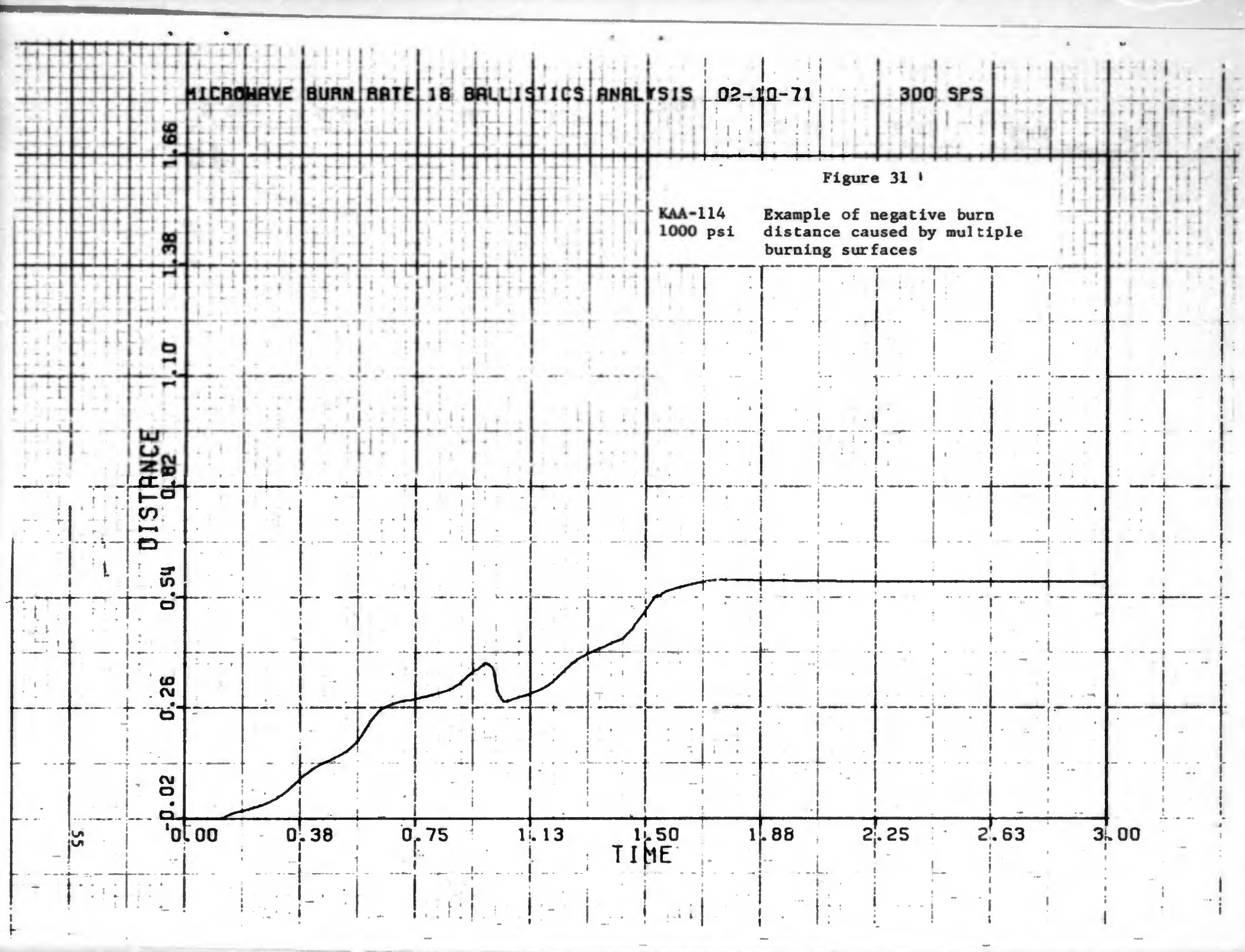

Figure 31

KAA-114
1000 psi

Example of negative burn distance caused by multiple burning surfaces

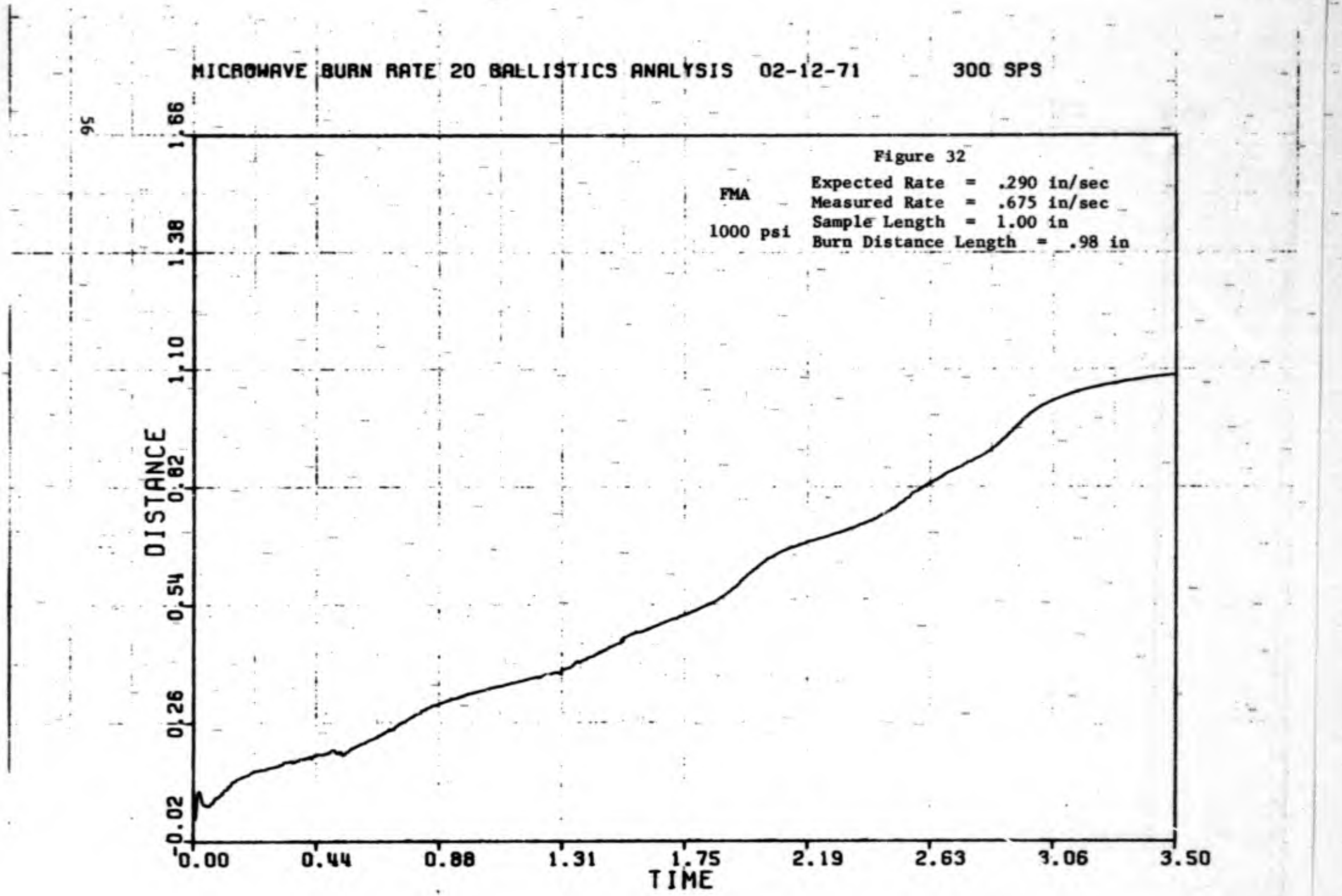
MICROWAVE BURN RATE 20 BALLISTICS ANALYSIS 02-12-71 300 SPS
Figure 32
FMA
1000 psi
Expected Rate = .290 in/sec
Measured Rate = .675 in/sec
Sample Length = 1.00 in
Burn Distance Length = .98 in
DISTANCE
-0.02
0.26
0.54
0.82
1.10
1.38
1.66
0.00
0.44
0.88
1.31
1.75
2.19
2.63
3.06
3.50
TIME

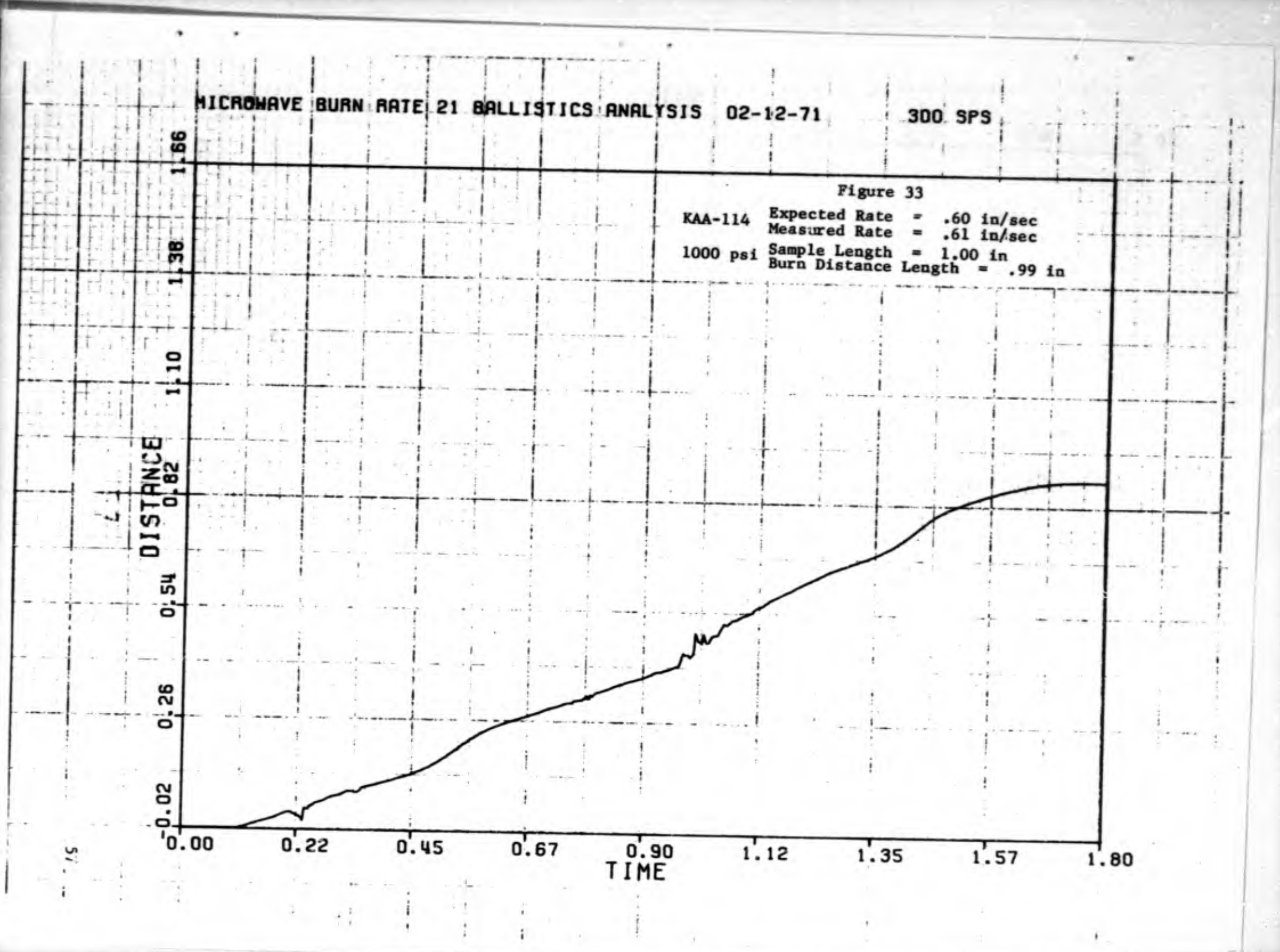
MICROWAVE BURN RATE 21 BALLISTICS ANALYSIS 02-12-71 300 SPS
Figure 33
KAA-114
1000 psi
Expected Rate = .60 in/sec
Measured Rate = .61 in/sec
Sample Length = 1.00 in
Burn Distance Length = .99 in
DISTANCE
-0.02
0.26
0.54
0.82
1.10
1.38
1.66
0.00
0.22
0.45
0.67
0.90
1.12
1.35
1.57
1.80
TIME

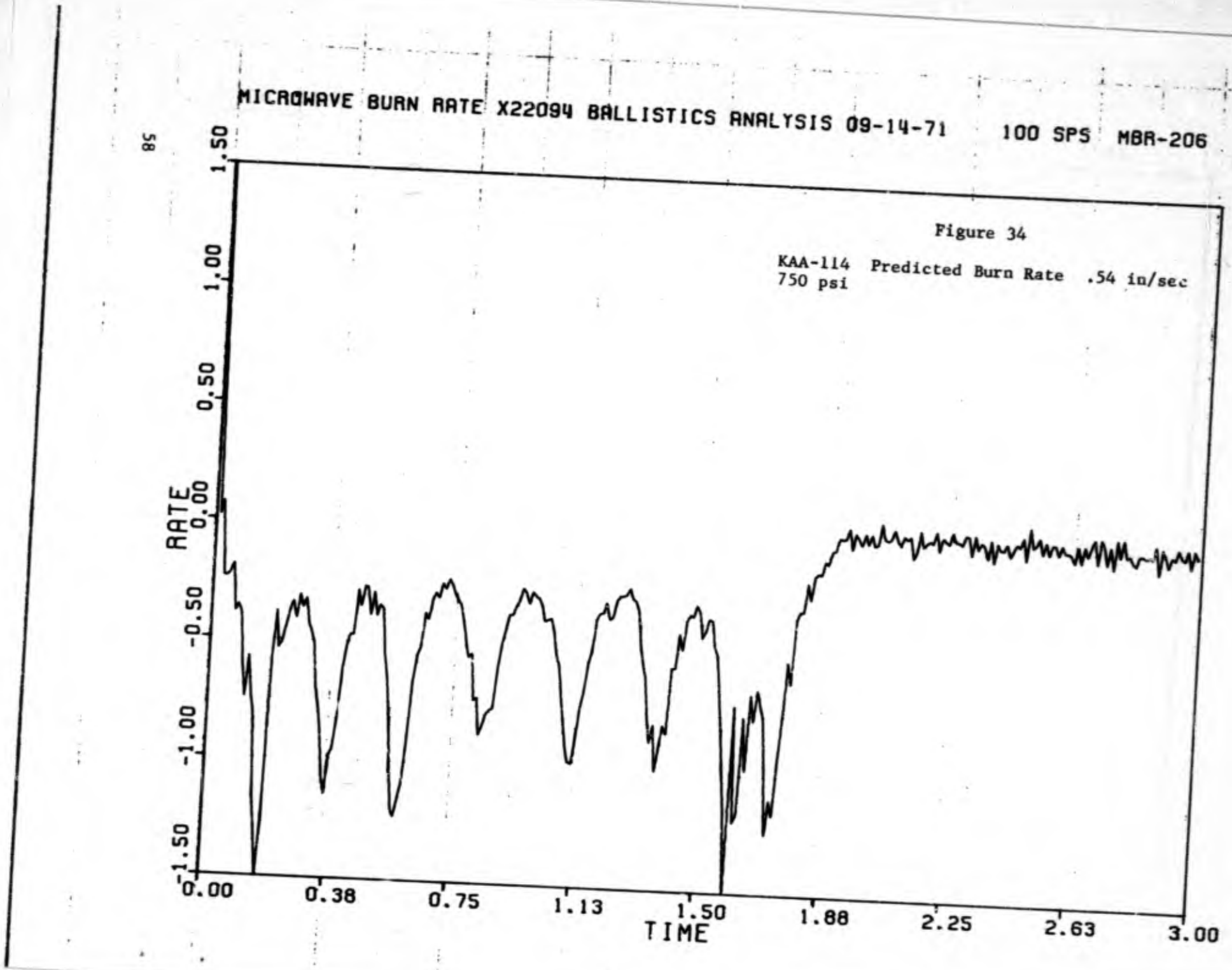

Figure 34

KAA-114 Predicted Burn Rate .54 in/sec
750 psi

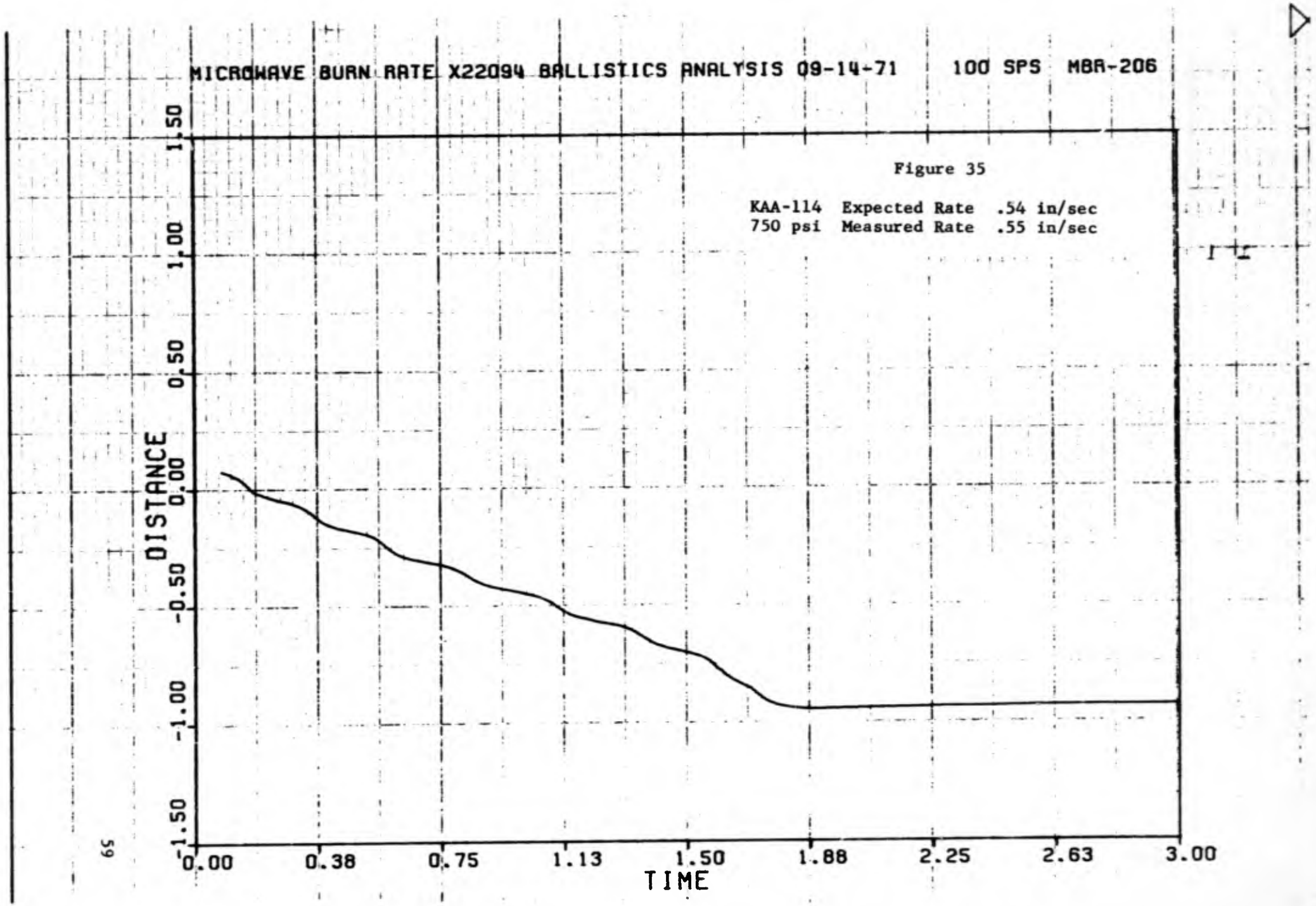
MICROWAVE BURN RATE X22094 BALLISTICS ANALYSIS 09-14-71 100 SPS MBR-206
Figure 35
KAA-114 Expected Rate .54 in/sec
750 psi Measured Rate .55 in/sec
DISTANCE
1.50
1.00
0.50
0.00
-0.50
-1.00
-1.50
0.00
0.38
0.75
1.13
1.50
1.88
2.25
2.63
3.00
TIME

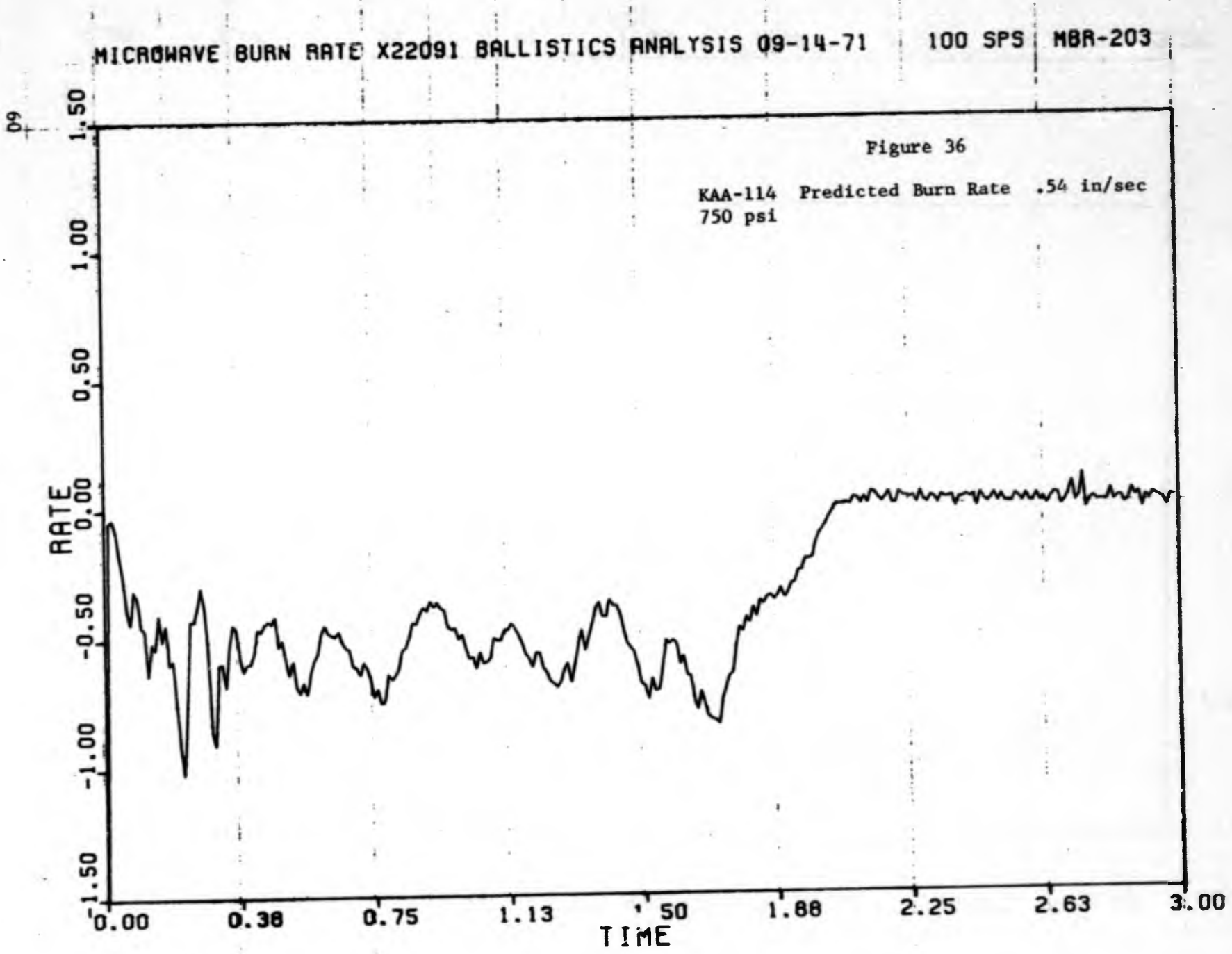
MICROWAVE BURN RATE X22091 BALLISTICS ANALYSIS 09-14-71 100 SPS MBR-203
09
Figure 36
KAA-114 Predicted Burn Rate .54 in/sec
750 psi
RATE
1.50
1.00
0.50
0.00
-0.50
-1.00
-1.50
0.00
0.38
0.75
1.13
1.50
1.88
2.25
2.63
3.00
TIME

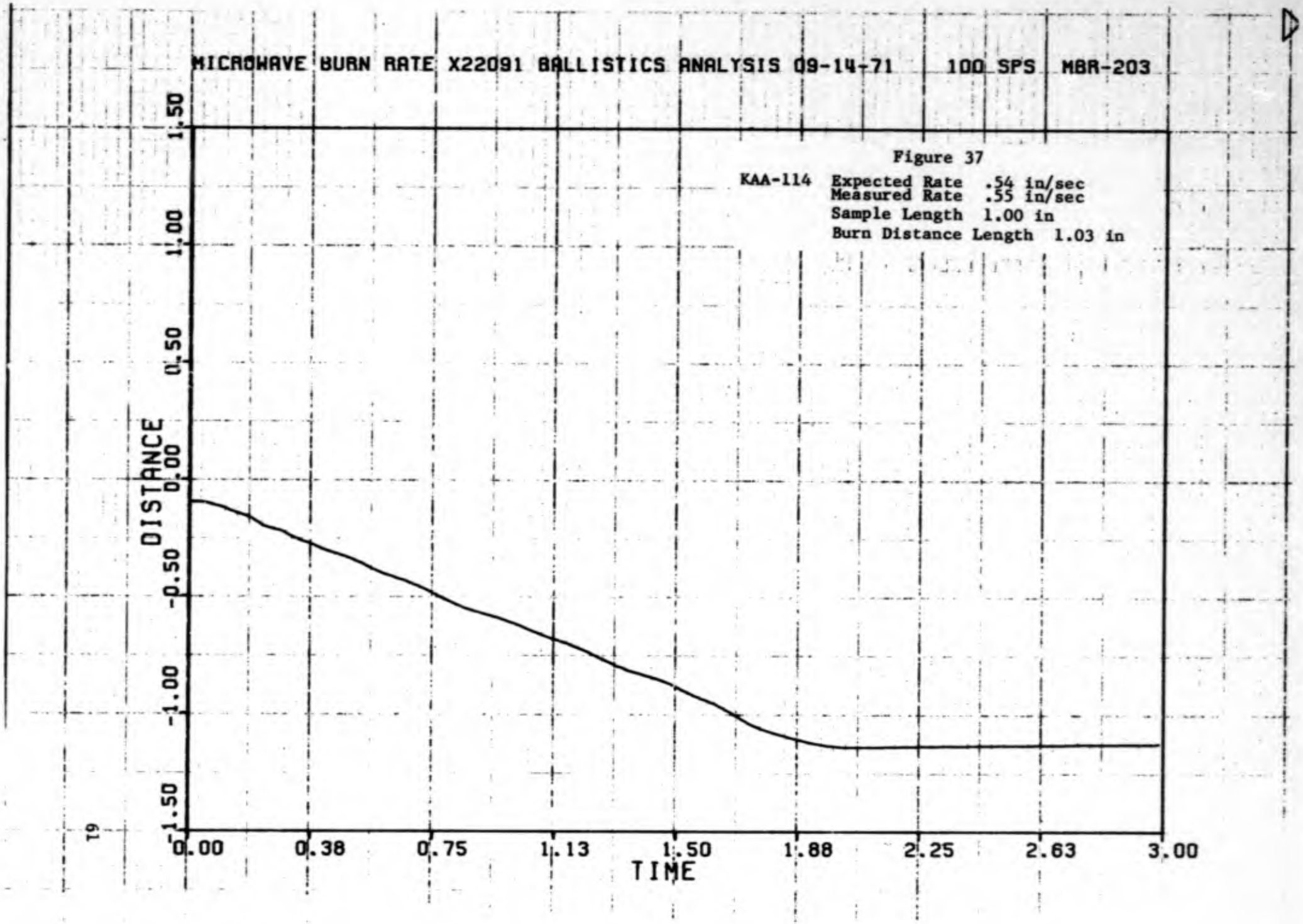
MICROWAVE BURN RATE X22091 BALLISTICS ANALYSIS 09-14-71 100 SPS MBR-203
Figure 37
KAA-114 Expected Rate .54 in/sec
Measured Rate .55 in/sec
Sample Length 1.00 in
Burn Distance Length 1.03 in
DISTANCE
1.50
1.00
0.50
0.00
-0.50
-1.00
-1.50
0.00
0.38
0.75
1.13
1.50
1.88
2.25
2.63
3.00
TIME

Appendix A

Test Plan

Contract F04611-70-C-0085

Test Plan

for

Microwave Burn Rate Detector

Effective Date _____

Prepared By _____ Date _____
L. S. Zajdel

Approved for Use by Hercules Incorporated

_____ _____ _____ _____

_____ _____ _____ _____

1. SCOPE

1.1 This document describes the materials, equipment, and procedure necessary to conduct static firing testing of the microwave burn rate detector apparatus in the small "T" Burner facility.

2. REQUIREMENTS

2.1 Operations shall be performed in the sequence listed unless otherwise specified.

2.2 All measuring devices that require calibration shall be inspected prior to an operation to verify that calibration intervals have not been exceeded.

3. APPLICABLE DOCUMENTS

Publications

None

4. MATERIALS AND EQUIPMENT

Materials	Description
Compound, Seam Sealing	Prestite 1118164X
Grease, Insulation	Silicone DC-33
O-rings	Parker 2-129 or equivalent
Rags	Clean
Spacers	Epoxy with 50% Aluminum content

Styrofoam	High density
Swabs	Cotton tipped
Tape	1 inch width masking
Waveguide	Flangeless X-gand

Equipment	Description
Microwave burn rate detector	X-band twin detector apparatus, ABL fabricated
Microwave window	High pressure small "T" burner end cap assembly
Microwave detector balance unit	Twin detector signal conditioning, ABL fabricated
Microwave Sliding Short	X-band
Microwave Termination	X-band
Pressure Transducer	Alinco Model C151 or equivalent
Small "T" burner facility	ABL Fabricated
Voltmeter	Digital, Dana Model 4430 or equivalent

5. SAFETY

5.1 All safety precautions and practices established in the General

Operating Procedure for the area in which this operation is performed shall be observed.

5.2 The compatibility of materials used in these operations, which may come in contact with propellant, shall be determined and approved prior to use.

5.3 At no time will any personnel expose their eyes to direct microwave radiation from the source. If visual inspection of the microwave burn rate apparatus waveguide is necessary, the source power supply voltage must be turned off.

NOTE: THIS OPERATION SHALL BE BROUGHT TO A SAFE, ORDERLY STOP AND TESTING SUPERVISION NOTIFIED IF THERE IS ANY UNUSUAL EVENT WHICH COULD AFFECT SAFETY, OR THE QUALITY OR COST OF THE DATA.

6. PRELIMINARY OPERATIONS

6.1 Operating personnel will be familiar with this document prior to commencing any test operation.

6.2 Connect the microwave apparatus as shown in Figure 1.

6.3 Turn the power supply voltage on and make sure 12 vdc is applied at the oscillator.

6.4 Connect each of the detector outputs to the D.V.M. to assure each is operating properly. At this point output A should be approximately equal to output B.

6.5 Connect respectively the twin detector outputs labeled "A" and "B" to

the inputs of the detector balance unit which are also labeled "A" and "B." Turn the balance unit on.

6.6 Set both controls on the balance unit marked "ATTENUATION" fully clockwise to the 10.00 position.

6.7 Connect the balance unit output marked "A OUTPUT" to the digital voltmeter and adjust the control marked "A-ZERO" for a zero volt reading on the voltmeter.

6.8 Repeat step 6.7 for the "B" channel.

6.9 Remove the termination from the preliminary microwave setup and install double stub tuner and window assembly as shown inFigure 3.

6.10 Separate the two halves of the microwave window by removing the eight 3/8-13 socket head cap screws from the window housing. Remove the split tapered waveguide clamps from the assembly.

6.11 Clean and grease the mating surfaces of the window assembly with silicone grease.

6.12 Locate the propellant transition section which consists of a tapered piece of KAA-114 propellant and 2.1 cm epoxy-aluminum spacer inside a 7 inch length of x-band waveguide.

6.13 Place the tapered clamps around the flangeless end of the transition section and insert this end into the window assembly. Reassemble the window housing and tighten the eight 3/8-13 socket head cap screws.

6.14 Place a termination on the flanged end of the transition section and adjust the double stub tuner until both balance unit outputs "A" and "B" read zero volts on the digital voltmeter. Lock the settings on the tuner.

6.15 Remove the termination and install a sliding short on the transition section.

6.16 Move the sliding short and observe the peak positive and negative balance unit outputs for both channels. The peak readings should be fairly symmetrical about the 0.0 volt level. If the symmetry is grossly off, repeat the tuning procedure.

6.17 From the information in step 6.16 determine which channel has the largest span and adjust that span to equal the span of the other channel. This is accomplished by turning the control on the balance unit marked "ATTENUATION" counterclockwise until the spans are equal as read by the digital voltmeter.

7. PROPELLANT LOADING

7.1 Select a flangeless piece of x-band waveguide about 1½ inches longer than the propellant sample length.

7.2 Taper the inner walls of the waveguide with a file to facilitate the insertion of the propellant sample.

CAUTION: Steps 7.3 to 7.8 are to carried out with the operator wearing conductive shoes and standing on a grounded plate on floor.

7.3 Measure the propellant sample length and record the length and type of propellant on the data sheet.

7.4 Apply a thin film of silicone grease to the sides of the propellant

sample and insert and push it into the waveguide until the front end of the propellant is about 1/2 inch from the end of the waveguide.

7.5 At the front end of the waveguide insert the 2.1 cm 50% aluminum epoxy spacer into the waveguide. Push the spacer in until it back face is flush with the waveguide edge and its front face is up against the propellant as shown in Figure 4.

7.6 Bend the igniter wires at a right angle to the igniter head and insert into the waveguide as shown in Figure 4. Place the waveguide into a vise which is grounded electrically.

7.7 Pour into the waveguide enough black powder to just cover the head of the igniter and push a 1/4 inch thick piece of styrofoam into the waveguide. This serves to hold the black powder and igniter up against the propellant surface as shown in Figure 4.

7.8 Wrap a few turns of masking tape around the outside of the waveguide to hold the igniter wires in place and serve as a strain relief.

8. INSTRUMENTATION AND RECORDING SYSTEM

8.1 Connect the instrumentation and recording equipment as shown in Figure 5.

8.2 Remove the transition section and sliding short from the microwave window by loosening the eight 3/8-13 socket head cap screws and pulling the transition section out of the window housing.

8.3 Insert an epoxy-aluminum spacer (identical in aluminum content and length to that used in step 7.5) into a piece of waveguide until just flush with the waveguide face. Attach a sliding short to the other end of the waveguide and insert the spacer end of the waveguide into the window housing and tighten enough socket head cap screws to hold the waveguide firmly in place.

8.4 While moving the sliding short back and forth, set the span on the digital recording system.

9. T-BURNER ASSEMBLY AND SAMPLE LOADING

9.1 Position all valves as designated in the "INITIAL" column of the Valve Position Check List, Figure 6.

9.2 Clean, grease, and fit a Parker 2-129 O-ring to a small "T" burner end cap. Screw on and tighten this end cap to one end of the small "T" burner chamber.

9.3 Screw the Alinco pressure gage into the head cap and connect instrumentation lead to the gage.

9.4 Loosen and remove the eight socket head cap screws in the microwave window housing and remove the waveguide and sliding short from the housing.

9.5 Load the sample to be fired (Figure 4) into the microwave window housing by inserting the sample waveguide end with the spacer up against the wingow and tighten the eight socket head cap screws.

9.6 Clean and lubricate the mating surfaces of the open end of the "T" Burner and "T" Burner adapter sleeve and fit with a Parker 2-129 O-ring.

9.7 Feed the igniter wires through the adapter sleeve and screw the adapter sleeve onto the microwave window housing.

9.8 Feed the igniter wires through the tapped hole on the side of the adapter sleeve. Wrap a single layer of teflon tape around the threads of the

igniter wire gland fitting. Feed the igniter wires through the gland fitting and then screw the fitting into the tapped hole in the adapter sleeve.

9.9 Unshort the igniter wires and slip the teflon gland over the igniter wires and into the gland holder, tapered end in first. Replace short on the igniter leads.

9.10 Assemble the remaining portion of the gland as per manufacturer's specifications.

9.11 Remove the window housing adapter sleeve and sample from the other microwave components by loosening and removing the four 10-32 screws which hold the stub tuner to the window housing.

9.12 Screw the window housing adapter sleeve combination onto the open end of the "T" Burner. Reconnect the other microwave components to the window housing by mating the stub tuner to the housing with four 10-32 screws.

9.13 Clear test bay and actuate the bay warning system.

9.14 Verify that all cables are connected as shown in Figure 5. Unshort the igniter leads and connect them to the firing line.

10. PRESSURIZATION AND TEST FIRING

10.1 Close the "T" Burner exhaust valve.

10.2 Open the surge tank valve. Pressure gage readings on the surge tank pressure gage and "T" Burner pressure gage should now be equal. If the desired pressure has been reached, neglect steps 10.3 and 10.4.

10.3 If the surge tank was not pressurized or pressurized below the desired firing pressure, it will be necessary to increase the "T" Burner-Surge Tank pressure by opening one of the Nitrogen supply valves until the pressure read by the "T" Burner pressure gage is at the desired level.

10.4 If the surge tank pressure was higher than the desired pressure level, it will be necessary to vent the surge tank-"T" Burner pressure by slowly opening the "T" Burner exhaust valve until the desired pressure level is reached as read by the "T" burner pressure gage.

10.5 At this point verify that all valves are in the positions designated by the column labeled "FIRE" on the Valve Position Checklist, Figure 6.

10.6 Record the firing pressure as read by the "T" burner pressure gage and bay temperature on the data sheet, Figure 2.

10.7 Rebalance P1.

10.8 Verify that all systems are ready and initiate the firing sequence.

10.9 When the visicorder beams indicate all transients have died out, shut off the recording equipment.

11. DEPRESSURIZATION AND FINAL OPERATIONS

11.1 Close the surge tank valve.

11.2 Open the "T" burner exhaust valve. "T" burner pressure gage should now read zero.

11.3 Verify that all valves are in the positions designated by the column labeled "DEPRESSURIZE" on the Valve Position Checklist, Figure 6.

11.4 Remove the double stub tuner from the microwave window housing by removing the four 10-32 retaining screws.

11.5 Unscrew the adapter sleeve window housing combination from the "T" burner and disconnect the remaining igniter wires from the firing line.

11.6 Disassemble the igniter wire gland and unscrew the adapter sleeve from the microwave window housing.

11.7 Disassemble the microwave window and carefully inspect the parts and window and record any applicable remarks on the data sheet.

11.8 If another firing is to take place refer back to section 6. Otherwise continue with step 11.9.

11.9 Turn off all recording and conditioning equipment.

11.10 Close both the surge tank shut-off valve and the nitrogen tank valves.

11.11 Clean up area.

Preliminary Microwave Setup

Figure 1

74

Code No._____ Workorder No._____ TEST DATA ACQUISITION SHEET Round No._____

Test Engr._____ Plant Ph._____ Home Ph._____ Date Tested_____

Date Requested_____ Time Tested_____

Project_____ Purpose_____ Barometer Press._____

Motor Design_____ Loading No._____ Temperature_____

Grain No._____ QA Accepted____ Rejected_____ Recording Time_____

TEMP. COND. Box	Temp.	Hrs. In Date	Time
		Out Date	Time

Test Arrg. Dwg._____

IRD's Used_____

PROPELLANT

Type_____

Wt._____

Lot_____

IGNITER

Number_____

Resistance_____

Firing Current_____

Firing Voltage_____

Type	Location BAY LINE	Location AMP	Max. Expected Value	Gage Size	Gage No.	Calib. Shunt MV/V	Channel	Tape Ch. DIG.
ALINCO	A2	5A6	*	1.		1st Step 1 mv/v	03-13	M19
MICROWAVE #1	A9	7A5				3 mv/v	03-15	M21
MICROWAVE #2	A10	7A6				3 mv/v	03-16	M22

* Δ psi or change in firing pressure after ignition

SAMPLE DATA SHEET

Figure 2

Microwave Test Firing Setup

Figure 3

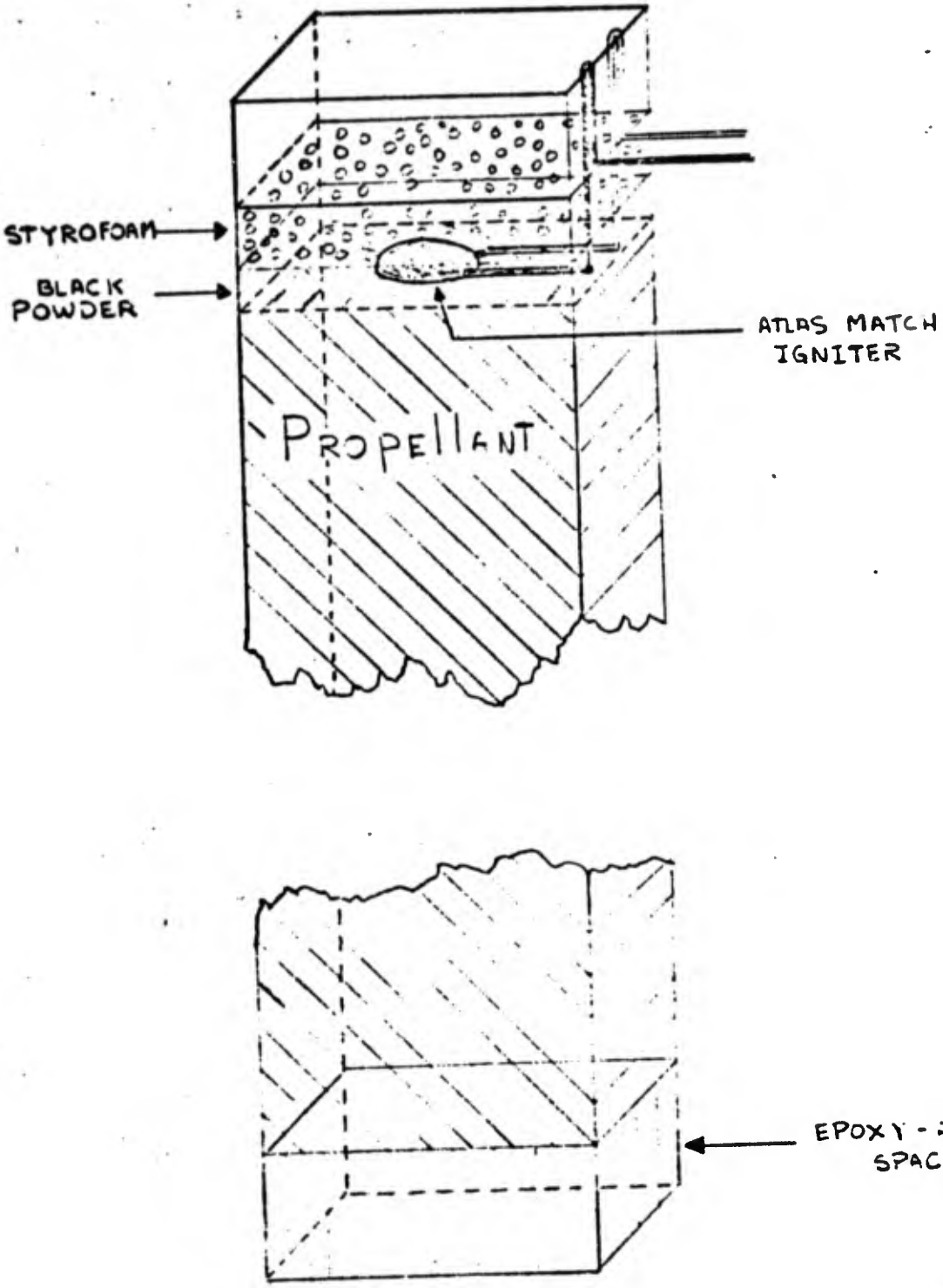

LOADED SAMPLE CONFIGURATION

Figure 4

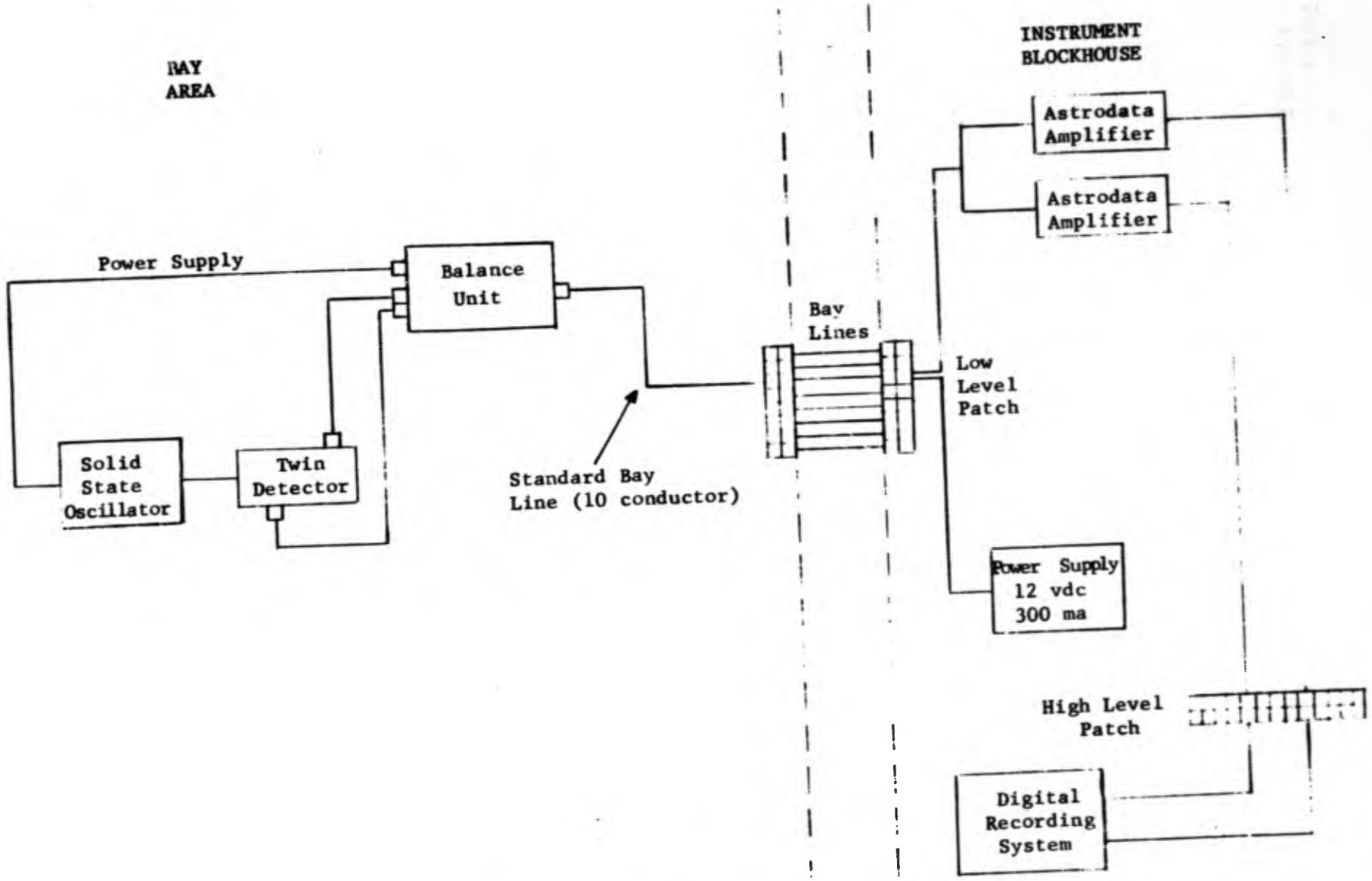

Microwave Instrumentation Recording Setup

Figure 5

Valve	Initial	Pressurize	Fire	Depressurize
Combustion Bomb Isolation Valve	Closed	Closed	Closed	Closed
T-Burner Exhaust Valve	OPEN	Closed	Closed	OPEN
Surge Tank Valve	Closed	OPEN	OPEN	Closed
Surge Tank Shut-Off Valve	OPEN	OPEN	OPEN	OPEN
T-Burner Isolation Valve	OPEN	OPEN	OPEN	OPEN
Nitrogen Supply Valves (2)	Closed	Regulate	Closed	Closed
Nitrogen Tank Valves (2)	OPEN	OPEN	OPEN	OPEN
Water Flush Isolation Valve	Closed	Closed	Closed	Closed
Water Flush Supply Valve	Closed	Closed	Closed	Closed

VALVE POSITION CHECK LIST

Figure 6

Appendix B

Computer Program Instructions

SUBJECT

PROGRAM REPORT: MICROWAVE BURNING RATE PROGRAM

(IBM 360/50 FORTRAN IV)

PURPOSE

This program is designed to reduce the data from the microwave burning rate system which is stored on a Hercules formatted floating data tape (FDT).

METHOD

The program reads the FDT and calls frequency control subroutine, then the burning rate is computed and printed for each acceptable time slice. If either time, x, or y is no data, the time slice is skipped. Time, burn distance and burn rate are saved in an array to make the CalComp plot. The program can pick the plot scales. If the plot scales are input, the program restricts the plotted data to the plot boundaries.

EQUATIONS

$$F1_n = X_n \cos(F5_{n-1}) + Y_n \sin(F5_{n-1})$$

$$F2_n = -X_n \sin(F5_{n-1}) + Y_n \cos(F5_{n-1})$$

$$F3_n = \tan^{-1} \frac{|F2_n|}{|F1_n|}$$

$$F4_n = F3_n \quad \text{if } F1_n > 0 \text{ and } F2_n \geq 0$$

$$= \pi - F3_n \quad \text{if } F1_n \leq 0 \text{ and } F2_n > 0$$

$$= -F3_n \quad \text{if } F1_n \geq 0 \text{ and } F2_n < 0$$

$$= F3_n - \pi \quad \text{if } F1_n < 0 \text{ and } F2_n \leq 0$$

$$F5_n = F4_n + F5_{n-1}$$

$$F6_n = (X_n^2 + Y_n^2)^{\frac{1}{2}}$$

$$F7_n = \frac{1}{2\alpha} \ln(F6_n)$$

EQUATIONS (Continued)

$$D_n = \frac{1}{2\beta} F5_n$$

$$S = \frac{1}{time_n - time_{n-1}}$$

$$R_n = S \frac{1}{2\beta} F4_n$$

$$F8_n = S (F7_n - F7_{n-1})$$

where:

n is the current time slice.

n - 1 is the last time slice accepted by frequence control.

X and Y are the two channels of synchronized digital data from the test firing recorded every time slice.

α is the propellant attenuation factor.

β is the propellant phase factor.

D is the burning surface position.

R is the propellant burn rate.

S is the sampling rate.

Initial values are:

$F5_o = 0$

$F7_o = 0$

S at $time_o$ = input sampling rate.

SUBJECT
PROGRAM REPORT: MICROWAVE BURNING RATE PROGRAM

SUBROUTINES

Function	Call Name	Program Number
Read FDT header	FDTRID	47001
Read FDT data	FDTREA	47001
Close the FDT	FDTCLS	47001
Frequency control	FREQ2	47003
CalComp plot	HIPLOT	75718

INPUT

The input to this program consists of a Hercules formatted FDT and four input cards. Multiple cases may be input with each run.

Card	Column	Format	Field Description
1	1-80	10A8	An 80 character title to be printed on the first page of the output listing and drawn on the plot. Col. 1-8 cannot be all blanks.
2	1-8	A8	The FDT Channel name of the X-parameter output from the microwave burning rate system. *
	11-18	A8	The FDT Channel name of the Y-parameter output from the microwave burning rate system. *
	21-30	E10.0	α - The propellant attenuation factor. Default value = 1.
	31-40	E10.0	β - The propellant phase factor. Default value = 1.
	41-50	E10.0	Sampling rate. Default value = 305.
3	1-10	E10.0	Start time for output.
	11-20	E10.0	Stop time for output.
	21-30	E10.0	Delta time for output. If this value is positive, it is considered to be a delta time. If this value is negative, every ith point will be accepted (i.e. -1.0 accepts every point, -2.0 accepts every other point, etc.).

* These names must match exactly with the names on the FDT. Left adjust.

INPUT (Continued)

Card	Column	Format	Field Description
3	31-40	E10.0	Second start, stop, delta as described above, if needed. These two frequency control increments cannot overlap.
	41-50	E10.0	
	51-60	E10.0	
4	1-10	E10.0	First value on plot for time scale.
	11-20	E10.0	Delta units per inch on plot for time scale.*
	21-30	E10.0	First value on plot for distance scale.
	31-40	E10.0	Delta units per inch on plot for distance scale. *
	41-50	E10.0	First value on plot for rate scale.
	51-60	E10.0	Delta units per inch on plot for rate scale.*
n			A blank card terminates the run.

Note: For multiple cases using the same FDT, repeat cards 1 thru 4 in groups. Then a blank card ends the run.

* - When scaling plots, consider the x-axis to be eight inches long and the y-axis to be six inches long. The program will automatically pick a scale for any or all of the parameters if the "delta units per inch" field is blank.

RESTRICTIONS

1. Multiple cases are run using the same FDT.
2. If the data exceeds the input plot scale, it is restricted to the plot boundary.
3. The data plotted will be thinned, if necessary, so the total number of points is less than 2000.

OUTPUT

The output consists of a listing with one line per time slice accepted by the frequency control. The listing contains five parameters: Time, X, Y, distance, and rate. Two plots are created for each run: Burn distance vs. time and burn rate vs. time.

USAGE

Machine Requirements

The program is designed to operate on the IBM 360/50 computer. It requires 96K bytes of core storage including subroutines.

Timing

This program runs less than one minute for a 4 second FDT.

SUBJECT: PROGRAM REPORT: MICROWAVE BURNING RATE PROGRAM
APPENDIX A: PARAMETER KEY SHEET

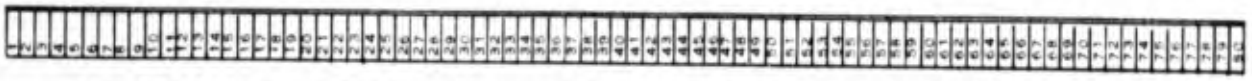

Any 80 character title. (Col. 1-8 cannot be all blanks). 1

XNAME	YNAME	ALPHA	BETA	SAMP RATE				2
START1	STOP1	DELTA1	START2	STOP2	DELTA2	(freq. control card)		3
FVALUE T	DETLA T	FVALUE D	DELTA D	FVALUE R	DELTA R	(plot scales card)		4

5

Note: To run multiple cases on the same FDT, repeat cards 1-4 as a group. 6

The blank card ends the run. 7

8 9 10 11 12 13 14 15 16 17 18 19 20 21 22 23 24 25 26

SUBJECT
PROGRAM REPORT: MICROWAVE BURNING RATE PROGRAM
APPENDIX B: SAMPLE INPUT

```
TEST CASE MBR-6
MHMS01    MHMS02    2.        11.1      305.
-.1       3.0       -1.
     blank card lets program pick plot scales
     blank card ends run
```

MICROWAVE BURNING RATE PROGRAM 48103 JUN 02/11/71

TEST CASE MBR-8

X= MHMS01
Y= MHMS02
ATTENUATION FACTOR= 2.000
PHASE FACTOR= 8.880
FREQ= 0.0 3.0000 -1.0000 3.0001 4.0000 -2.0000

TIME	X	Y	DISTANCE, INCHES	RATE, INCHES/SEC
0.0	-0.437650 03	0.475000 02	0.170400 00	0.520000 02
0.0033	-0.324710 03	-0.285000 02	0.181920 00	0.334630 01
0.0065	-0.451760 03	0.0	0.176990 00	-0.150620 01
0.0098	-0.394120 03	0.190000 02	0.174730 00	-0.461240 00
0.0131	-0.240000 03	0.475000 02	0.165300 00	-0.270040 01
0.0164	-0.296470 03	-0.380000 02	0.194070 00	0.555440 01
0.0196	-0.127060 03	0.133000 03	0.131360 00	-0.140690 02
0.0229	-0.352940 03	0.285000 02	0.172350 00	0.125170 02
0.0262	-0.211760 03	0.190000 02	0.171950 00	-0.153250 00
0.0295	-0.127040 03	0.570000 02	0.153150 00	-0.571570 01
0.0327	-0.367060 03	-0.570000 02	0.185570 00	0.990570 01
0.0360	-0.197650 03	0.950000 01	0.174130 00	-0.347060 01
0.0393	-0.211760 03	-0.760000 02	0.136280 00	0.675460 01
0.0425	-0.352940 03	-0.570000 02	0.185410 00	-0.317350 01
0.0458	-0.112940 03	0.133000 03	0.128090 00	-0.176570 02
0.0491	-0.296470 03	-0.133000 03	0.200440 00	0.221690 02
0.0524	-0.381180 03	-0.950000 01	0.178270 00	-0.642650 01
0.0556	-0.480000 03	0.380000 02	0.172440 00	-0.174730 01
0.0589	-0.578820 03	0.190000 02	0.175040 00	0.736660 00
0.0622	-0.480000 03	0.380000 02	0.172440 00	-0.736660 00
0.0655	-0.381180 03	0.190000 02	0.174000 00	0.502330 00
0.0687	-0.494120 03	0.665000 02	0.169360 00	-0.144440 01
0.0720	-0.310540 03	-0.285000 02	0.182040 00	0.397600 01
0.0753	-0.242350 03	0.104500 03	0.156230 00	-0.747230 01
0.0785	-0.381180 03	0.570000 02	0.164530 00	0.354440 01
0.0818	-0.268240 03	0.190000 02	0.172010 00	0.133720 01
0.0851	-0.197650 03	0.475000 02	0.163610 00	-0.284120 01
0.0884	-0.352940 03	-0.190000 02	0.179020 00	0.475310 01
0.0916	-0.367040 03	0.950000 01	0.175430 00	-0.137030 01
0.0949	-0.254120 03	-0.570000 02	0.180320 00	0.434150 01
0.0982	-0.155290 03	-0.141500 03	0.222220 00	0.190330 02
0.1015	-0.268240 03	-0.190000 02	0.140470 00	-0.126320 02
0.1047	-0.352940 03	-0.665000 02	0.187390 00	0.133750 01
0.1080	-0.282350 03	-0.142500 03	0.233210 00	0.484720 01
0.1113	-0.169410 03	0.760000 02	0.145150 00	-0.152870 02
0.1145	-0.296470 03	-0.950000 02	0.194450 00	0.125500 02
0.1178	-0.268240 03	-0.190000 02	0.196050 00	0.521010 00
0.1211	-0.338230 03	0.475000 02	0.179150 00	-0.771370 01
0.1244	-0.353530 03	-0.475000 02	0.161740 00	0.354410 01
0.1276	-0.5923-0 03	0.235000 02	0.174100 00	-0.230000 01
0.1309	-0.508240 03	-0.950000 01	0.177440 00	0.114700 01
0.1342	-0.423530 03	0.340000 02	0.171450 00	-0.194110 01
0.1375	-0.296470 03	0.950000 01	0.176010 00	-0.238410 00
0.1407	-0.451760 03	-0.470000 02	0.152360 00	0.271050 01
0.1440	-0.141180 03	-0.570000 02	0.184000 00	0.644270 01
0.1473	-0.240000 03	0.665000 02	0.141470 00	-0.112530 02

SUBJECT
PROGRAM REPORT: MICROWAVE BURNING RATE PROGRAM
APPENDIX D: SAMPLE JCL

```
//JOBNAME  JOB CARD
//MWAVE    EXEC FORTGLG,REGION.GO=96K
//LKED.LOADDS  DD DSN=SCI.LOADDS,DISP=SHR
//LKED.SYSIN   DD *
  INCLUDE LOADDS(P4810300)
  ENTRY MAIN
/*
//GO.FT06F001 DD SYSOUT=T,DCB=(LRECL=133,BLKSIZE=1330,RECFM=FBA)
//GO.FDT   DD DSN=FDT,UNIT=TAPE,DISP=(OLD,KEEP),VOL=SER=XXXXXX
//GO.PLOTTAPE DD DSN=P48103.CALCOMP,UNIT=(TAPE,,DEFER),DISP=(NEW,KEEP),
//          VOL=PRIVATE,DCB=DEN=2
//GO.SYSIN  DD *
        .
        .
     DATA
        .
        .
/*
```

Microwave Burn Rate

Computer Program

```
//S010500  JOB (9,
// 48103,10467,2),529528900,CLASS=B,MSGLEVEL=1,PRTY=7
// EXEC FORTHCL,PARM.LKED=(XREF,LIST,LET,NCAL)
//COMP.SYSIN DD *
      IMPLICIT REAL*8 (A-H,O-Z)
      REAL DAT *4(2) , NAMES*8(3)/0.,0.,0./
      REAL*4 ATIT(40),TITLP(20),TIME(2003),DIST(2003),RATE(2003),
     1       A(10)/8.,1.,1.5,6.,1.,1.25,1.,.14,0./
      REAL*4 TOP,    TSC(3),DSC(3),RSC(3)
      DIMENSION TS(3),TITLE(10)
      DIMENSION FBLK(9), IFLAG(4)
      DIMENSION AXT(3),DTIT(20)
      DATA PI,FBLK /3.1415927,9*0.0/
      DATA   TS/3*0.0/,     BAD/'7FFFFFFF00000000'/
      DATA AXT  /'          ','RATE      ','DISTANCE'/, DTIT/'TIME      '/
      EQUIVALENCE (TSC(3),TIME(1)),(DSC(3),DIST(1)),(RSC(3),RATE(1))
      EQUIVALENCE(TITLE(1),TITLP(1)),(ATIT(1),DTIT(1))
      EQUIVALENCE(NFLAG   ,IFLAG(1))
      CALL SRETRN(NERR)
      IF(NERR.EQ.0) GO TO 10
    1 CONTINUE
      WRITE(6,6003)
 6003 FORMAT('0END OF PGM 48103')
      CALL HCPLOT(TIME,RATE,-999 ,0,1)
      CALL SDUMP(NERR)
   10 CONTINUE
      CALL DATE(DAT )
      MA=0
      INDEX=0
      NFLAG=1
      KCU=46
      F5=0.
      F7=0.
      TSAVE=BAD
      DO 15 I=2,20
   15 DTIT(I)=AXT(1)
C.....READ INPUT CARDS
      READ (5,5001) TITLE
 5001 FORMAT(10A8)
      IF(TITLE(1).EQ.AXT(1)) GO TO 1
      READ (5,5002)(NAMES(I),I=1,2),ALPHA,BETA ,SRATE
 5002 FORMAT(A8,2X,A8,2X,6F10.0)
       IF(ALPHA.EQ.0.0) ALPHA=1.
       IF( BETA.EQ.0.0)  BETA=1.
      IF(SRATE.EQ.0.0) SRATE=305.
      READ(5,5003) (FBLK(I),I=1,6)
      READ(5,5003) TSC(1),TSC(2),DSC(1),DSC(2),RSC(1),RSC(2)
 5003 FORMAT (8E10.0)
      TMAXP=8.*TSC(2)+TSC(1)
      INC=0
C.... FIGURE PLOT INCREMENT(NUB).
      NSAMP=0
      DO 35 I=3,6,3
      IF(FBLK(I)) 20,35,25
   20 MUD=-FBLK(I)
      NSS=SRATE/MUD
      GO TO 34
   25 CONTINUE
```

```
      IF(FBLK(I)-.0025)33,30,30
   30 NSS=1./FBLK(I)
      GO TO 34
   33 NSS=SRATE
   34 NSEC=(FBLK(I-1)-FBLK(I-2))
      NSAMP=NSEC*NSS+NSAMP
   35 CONTINUE
      NUB=NSAMP/2000 + 1
C.....SKIP TO NEXT PAGE & WRITE INPUT & TITLE
      WRITE(6,6001) DAT ,TITLE,  (NAMES(I),I=1,2),ALPHA,BETA
     1 ,(FBLK(I),I=1,6)
 6001 FORMAT('1',T30,'MICROWAVE BURNING RATE PROGRAM 48103',T87,
     1'RUN ',2A4// T20,10A8/// T43,'     X=  ',A8
     2                       / T43,'     Y=  ',A8
     3                       / T30,'ATTENUATION FACTOR= ',F12.3
     4                       / T36,'PHASE FACTOR= ',F12.3
     5                       / T44,'FREQ= ',6F12.4/)
      IF(NUB.EQ.1) GO TO  39
      WRITE(6,6006) NUB
 6006 FORMAT('+', T30,'     EVERY',I3,' DATA POINT TO BE PLOTTED')
   39 CONTINUE
      CALL FDTRID(NAMES)
      GO TO 45
   40 CONTINUE
      MA=1
      KOU=58
   45 CONTINUE
C.....SKIP TO NEXT PAGE & WRITE COLUMN HEADINGS
      WRITE(6,6002) MA
 6002 FORMAT(I1,T7,'TIME',T25,'X',T45,'Y',
     1 T56,'DISTANCE,INCHES', T76,'RATE,INCHES/SEC'/)
      KOT=0
   50 CONTINUE
C.....READ A DATA RECORD
      CALL FDTREA(TS,&90)
      CALL FREQ2(TS(1),FBLK,IFLAG,CONT)
      GO TO (50,52,50,110) ,NFLAG
   52 CONTINUE
      IF(TS(2).EQ.0.0.AND.TS(3).EQ.0.0) GO TO 50
      DO 55 I=1,3
      IF(DABS(TS(I)).GT.BAD) GO TO 50
   55 CONTINUE
C.....DO THE CALCULATIONS ......
      F1=TS(3)*DSIN(F5)+TS(2)*DCOS(F5)
      F2=TS(3)*DCOS(F5)-TS(2)*DSIN(F5)
      F3=DATAN(DABS(F2)/DABS(F1))
      IF(F1.GT.0.AND.F2.GE.0) F4=F3
      IF(F1.LE.0.AND.F2.GT.0) F4=PI-F3
      IF(F1.GE.0.AND.F2.LT.0) F4=-F3
      IF(F1.LT.0.AND.F2.LE.0) F4=F3-PI
      F5=F4+F5
      F6=DSQRT(TS(2)**2+TS(3)**2)
      F7SAVE=F7
      F7=(.5D0/ALPHA)* DLOG(F6)
      D=(.5D0/BETA)*F5
      S=1.D0/(TS(1)-TSAVE)
      IF(TSAVE.EQ.BAD) S=SRATE
      R=S*(.5/BETA)*F4
```

```
      F8=S*(F7-F7SAVE)
      TSAVE=TS(1)
C.....WRITE A LINE OF RESULTS
      WRITE(6,6004) (TS(I),I=1,3),      D,R
 6004 FORMAT(' ',F10.4,8E20.5)
C..... SAVE THE DATA FOR A PLOT
      IF(TS(1).LT.TSC(1) .OR. TS(1).GT.TMAXP) GO TO 70
      INC=INC+1
      IF(NUB.NE.INC) GO TO 70
      INC=0
      INDEX=INDEX+1
      TIME(INDEX)=TS(1)
      DIST(INDEX)=D
      RATE(INDEX)=R
   70 CONTINUE
      KCT=KCT+1
      IF(KCT.EQ.KOU) GO TO 40
      GO TO 50
C.....MESSAGES
   90 CONTINUE
      WRITE(6,6007)
 6007 FORMAT('0TRIED TO READ PAST END OF FDT. MAKE A PLOT AND END PGM.')
  110 CONTINUE
      CALL FDTRWD
      WRITE(6,6008)
 6008 FORMAT('1')
      IF(TSC(2).NE.0.) GO TO 130
      A(2)=INDEX
      IT=3
      GO TO 135
  130 CONTINUE
      A(2)=1.
      IT=1
  135 CONTINUE
      IF(DSC(2).NE.0.) GO TO 140
      A(5)=INDEX
      ID=3
      GO TO 155
  140 CONTINUE
      ID=1
      A(5)=1.
      TOP=(DSC(2)*6.) + DSC(1)
      DO 145 I=1,INDEX
      IF(DIST(I).GT.TOP)  DIST(I)=TOP
      IF(DIST(I).LT.DSC(1)) DIST(I)=DSC(1)
  145 CONTINUE
  155 CONTINUE
      DTIT(11)=AXT(3)
      CALL HIPLOT(TSC(IT),DSC(ID),A,AT(I)
      CALL SYMBOL(0.,6.5,.105,TITLP,0.0,80)
      CALL HCPLOT(TIME,DIST,INDEX,0,1)
      CALL HCPLOT(TIME,DIST,-998 ,0,1)
      IF(RSC(2).NE.0.) GO TO 160
      A(5)=INDEX
      IR=3
      GO TO 165
  160 CONTINUE
      A(5)=1.
```

```
      IR=1
      TOP=RSC(1) + RSC(2)*6.
      DO 162 I=1,INDEX
      IF(RATE(I).GT.TOP)  RATE(I)=TOP
      IF(RATE(I).LT.RSC(1)) RATE(I)=RSC(1)
  162 CONTINUE
  165 CONTINUE
      DTIT(11)=AXT(2)
      CALL HIPLOT(TSC(IT),RSC(IR),A,ATIT)
      CALL SYMBOL(0.,6.5,.105,TITLE,0.0,80)
      CALL HOPLOT(TIME,RATE,INDEX,0,1)
      CALL HCPLOT(TIME,RATE,-998 ,0,1)
      GO TO 10
      END
/*
//LKED.SYSLMOD  DD DSN=SCI.LOADDS,DISP=SHR
//LKED.SYSIN DD *
  NAME P4810300(R)
/*
//MWAVE  EXEC  FORTGLG,REGION.GO=96K
//LKED.LOADDS DD DSN=SCI.LOADDS,DISP=SHR
//LKED.SYSIN DD *
  INCLUDE LOADDS(P4810300)
  ENTRY MAIN
/*
//GO.FDT DD DSNAME=FDT,UNIT=TAPE,DISP=(OLD,KEEP),VOL=SER=004965
//GO.PLOTTAPE DD DSN=P48103.CALCOMP,UNIT=(TAPE,,DEFER),DISP=(NEW,KEEP),
//     VOL=PRIVATE,DCB=(DEN=2)
//GO.SYSUDUMP DD SYSOUT=A
//GO.SYSIN DD *
TEST CASE    MBR-8
MHMSC1     MHMSD2    2.          9.88
0.         2.          -2.


/*
```

```
INPUT DESCRIPTION.....
CARD 1:
          AN 80 CHARACTER TITLE. COLS 1-8 CANNOT BE ALL BLANKS.
CARD 2:
          COL  1-8  FDT NAME OF X-PARAMETER (LEFT ADJUST)
          COL 11-18 FDT NAME OF Y-PARAMETER (LEFT ADJUST)
          COL 21-30 ALPHA - PROPELLANT ATTENUATION FACTOR(FLOAT)
          COL 31-40 BETA  - PROPELLANT PHASE FACTOR(FLOAT)
          COL 41-50 SAMPLING RATE.  DEFAULT=305.. (FLOAT)
CARD 3:
          FREQUENCY IN 10 COL FIELDS.  START,STOP,DELTA.
          IF DELTA=-1.  EVERY POINT IS ACCEPTED BETWEEN START AND STOP TIME.
CARD 4:
          PLOT SCALES.
          LEAVE ANY PAIR BLANK AND THE PGM PICKS SCALE FOR THAT PARAMETER.
          COL  1-10  TIME FIRST VALUE
          COL 11-20  TIME UNITS PER INCH
          COL 21-30  DIST FIRST VALUE
          COL 31-40  DIST UNITS PER INCH
```

COL 41-50 RATE FIRST VALUE
COL 51-60 RATE UNITS PER INCH

CARD N+1 BLANK CARD

NOTE: TO RUN MULTIPLE CASES USING THE SAME INPUT TAPE, REPEAT CARDS 1 THRU 4 IN GROUPS OF 4. A BLANK CARD TERMINATES THE RUN.

```
/*
//
00240
```

References

1. Handbook of Microwave Measurements, Vol. II, Third Edition (1963), Polytechnic Press of the Polytechnic Institute of Brooklyn, A Division of John Wiley & Sons

2. Hercules Propellant Properties Manual, Section VII-5

3. High Density, High Temperature Binder for Solid Propellants, AFRPL-TR-69-175, p. 176

4. Combustion Mechanism of Low Burning Rate Propellant, AFRPL-69-130, pp. 158, 159